5-2018

Connected Vehicle Data-Based Tools for Work Zone Active Traffic Management

Michelle Mekker
Purdue University

CONNECTED VEHICLE DATA-BASED TOOLS FOR WORK ZONE ACTIVE TRAFFIC MANAGEMENT

by

Michelle Mekker

A Dissertation

Submitted to the Faculty of Purdue University

In Partial Fulfillment of the Requirements for the degree of

Doctor of Philosophy

Lyles School of Civil Engineering

West Lafayette, Indiana

May 2018

THE PURDUE UNIVERSITY GRADUATE SCHOOL
STATEMENT OF COMMITTEE APPROVAL

Dr. Darcy Bullock, Chair

Lyles School of Civil Engineering

Dr. Jon Fricker

Lyles School of Civil Engineering

Dr. Andrew Tarko

Lyles School of Civil Engineering

Dr. Heidi Diefes-Dux

School of Engineering Education

Approved by:

Dr. Dulcy Abraham

Head of the Graduate Program

For my husband,
who believed in me
even when I didn't.

ACKNOWLEDGMENTS

First, many thanks to my advisor, Darcy Bullock, whose endless support has taken me to heights I never thought I could reach. His passion for his work and his students is unmatched. Through him, I learned many important lessons: how to say “yes”, how to say “no”, and how to conduct meaningful research.

The chapter on the application of LiDAR in work zones would not exist if not for the collaboration with Dr. Ayman Habib and his students. Tamer Shamseldin and Magdy Elbahnasawy stuck it out with me on multiple field runs, though they gave me plenty of ribbing for the late nights and early mornings. Yun-Jou “Rose” Lin processed most, if not all, of the data for me and learned quite a bite about transportation along the way.

I would also like to thank the Joint Transportation Research Board team (Bridget Brunton, Katie Hendryx, Debbie Horton, Howell Li, and Kym Pelfree) for their support in everything from research to scheduling to planning events. Thank you to colleagues at INDOT, too. Ed Cox, Jim Sturdevant, Steve Harney, and Mischa Kachler have always been very enthusiastic about my work. I sincerely hope that my work documented here is used for the benefit of INDOT and the traveling public.

To Maggie McNamara, thank you for commiserating with me and understanding the anxiety. To Jijo Mathew, thank you for constantly reminding me that I have nothing to worry about and that I’m doing great, even if I didn’t believe you. Thank you both for the great times both in and out of the lab!

Finally, I want to thank my family, especially my parents, Sue and Chris. When I doubted my abilities and my qualifications, they always reminded me how I had the same doubts in a dozen other situations but ended up succeeding with flying colors in the end anyway.

TABLE OF CONTENTS

LIST OF TABLES

LIST OF FIGURES

LIST OF SYMBOLS AND ABBREVIATIONS

AADT	Annual average daily traffic
BOQ	Back-of-queue
DOT	Department of Transportation
F	Fatal (crash severity)
FHWA	Federal Highway Administration
ft	Feet
HCM	Highway Capacity Manual
HSM	Highway Safety Manual
INDOT	Indiana Department of Transportation
LiDAR	Light detection and ranging
MH	Mile-hour
MM	Mile marker
MOT	Maintenance of traffic
MP	Mile post
MPH	Miles per hour
MUTCD	Manual on Uniform Traffic Control Devices
NCHRP	National Cooperative Highway Research Program
non-WZ	Non-work zone
PDO	Property damage only (crash severity)
PI	Personal injury (crash severity)
vphpl	Vehicles per hour per lane
veh-hr	Vehicle-hour
WZ	Work zone

ABSTRACT

Author: Mekker, Michelle, M. Ph.D.
Institution: Purdue University
Degree Received: May 2018
Title: Connected Vehicle Data-Based Tools for Work Zone Active Traffic Management
Major Professor: Darcy Bullock

Work zones present challenges to safety and mobility that require agencies to balance limited resources with vital traffic management activities. It is important to obtain operational feedback for successful active traffic management in work zones. Extensive literature exists regarding the impact of congestion and recommendations for work zone design to provide safe and efficient traffic operations. However, it is often infeasible or unsafe to inspect every work zone within an agency's jurisdiction. This dissertation outlines the use of connected vehicle data, crash data, and geometric data from mobile light detection and ranging (LiDAR) technology for active traffic management in work zones.

Back-of-queue crashes on high-speed roads are often severe and present an early opportunity for leveraging connected vehicle data to mitigate queueing. The connected vehicle data presented in this dissertation provides compelling evidence that there are significant opportunities to reduce back-of-queue crashes by warning drivers of unexpected congestion ahead. In 2014 and 2015, approximately 1% of the total mile-hours of Indiana interstates were operating below 45 MPH and were considered congested. Congested conditions were observable in the connected vehicle data prior to 18.5% of all interstate crashes. The congested crash rate was found to be 20.6-24.0 times greater than the uncongested crash rate.

A real-time queue alert system was developed to detect queues and notify INDOT personnel via email. When average speeds drop below 45 MPH, queue monitoring algorithms are triggered, and an alert is sent to selected individuals. Still camera images, work schedules, and crash reports were used to ground-truth the alert system. The notification model could be easily extended to in-car notification.

A weekly work zone report was developed for use by the Indiana Department of Transportation (INDOT) for the purpose of assessing and improving both mobility and safety in work zones. The report includes a number of graphs, figures, and statistics to present a comprehensive picture of performance. This weekly report provided a mechanism for INDOT staff to maintain situational awareness of which work zones were most challenging for queues and during what periods those were likely to occur. These weekly reports provided the foundation for objective dialog with contractors and project managers to identify mechanisms to minimize queueing and allocate public safety resources.

Lastly, this dissertation discusses the integration of LiDAR-generated geometric data with connected vehicle speed data to evaluate the impact of work zone geometry on traffic operations. A LiDAR-mounted vehicle was deployed to a variety of work zones where recurring bottlenecks were identified to collect geometric data. The advantages and disadvantages of the technology are discussed. A number of case studies demonstrate versatility of the technology in transportation applications.

1. INTRODUCTION

The purpose of the work presented in this dissertation is to improve mobility and safety in freeway work zones by producing a suite of tools and performance measures for use by traffic managers and decision-makers. The safety problem associated with congestion was quantified and served as the motivation for the development and use of work zone traffic monitoring tools. It is intended for these tools to be used in real-time, short-term, and long-term capacities to improve mobility and safety in work zones.

1.1 Background

As much of the 1970s interstate-era construction ages and requires rehabilitation, interstate work zones are challenges that require agencies to balance construction worker safety, motorist safety, and mobility. Modern work zones employ advance signs, temporary shoulders, and barriers to separate workers from traffic. However, work zones frequently cause a reduction in capacity either due to removing a lane from service and/or narrowing of lanes. Thus, it is not uncommon for interstate queueing (Figure 1) to occur in advance of a work zone, and back of queue crashes are a concern to all agencies.

Maintenance of traffic (MOT) plans are an integral part of any roadway construction, maintenance, or rehabilitation project. The design of an MOT plan often occurs late in the design phase of a project (Figure 2). For longer and more complex projects, the process typically involves modeling to predict queue lengths and other impacts on mobility and safety. For smaller projects, the experience of the project engineer or contractor may be relied upon. Most agencies with substantial interstate volumes have strict policies regarding the restriction of traffic on interstates to minimize queueing. Lane closures are often only allowed during certain hours or days with lower traffic volumes to minimize the formation of queues. The MOT plan implemented during construction (Figure 2) often involves multiple stages depending on the schedule of work activities. Ideally, traffic management personnel would monitor traffic and use the observed impacts to calibrate the queue models and/or make dynamic changes to the

MOT plan as needed. However, with dozens of construction projects underway at any given time, monitoring work zones via in-person visits or asset deployment can consume significant and limited resources. Furthermore, construction work zones have subtle changes on a near daily basis that can significantly impact work zone queueing.

(a) I-70 E at mile post 8

(b) I-65 N at Exit 172

Figure 1 Photos of queues on interstates in Indiana

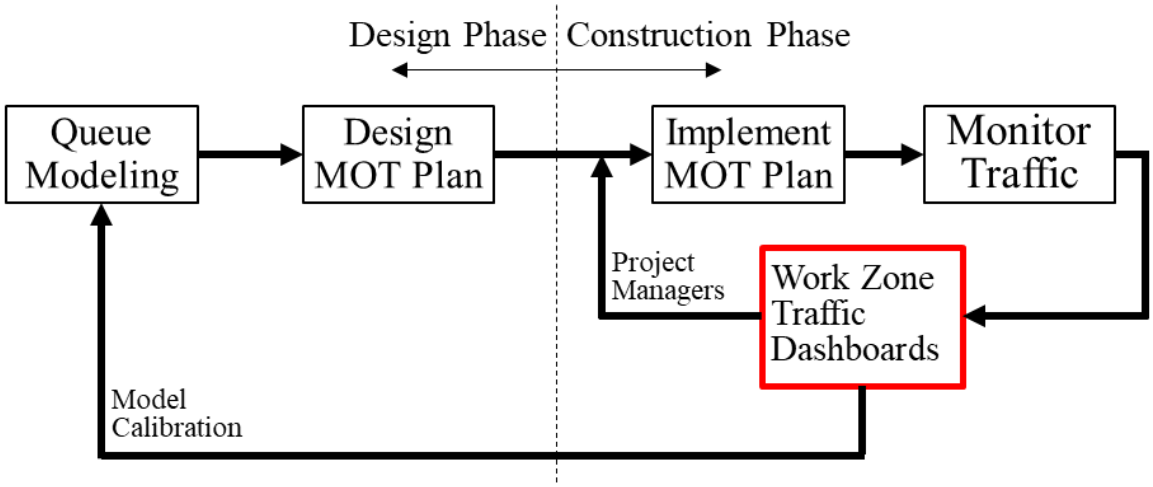

Figure 2 Work zone maintenance of traffic plan development flow chart

Monitoring traffic and maintaining roadway capacity is an important task for transportation agencies. Congestion, caused by insufficient capacity to meet demand, impacts both safety and mobility on the roadway. In work zones on high-speed facilities, queueing can be unexpected to drivers. It is important to minimize and mitigate queueing when possible. However, active monitoring and assessment of work zones can be difficult for agencies with limited resources.

1.2 Research Objectives

The four main elements of this dissertation unfolded organically with the intention of evolving work zone traffic management strategy. Based on the discussion above, the objectives of this research and dissertation were to:

- Quantify the impact of congestion on interstate safety in Indiana.
- Develop a system for the detection of queues in real-time and subsequent notification of traffic management personnel.
- Develop a method of monitoring and reporting work zone traffic performance that allows for dynamic, informed decision-making by traffic management personnel.
- Develop a methodology for deployment of mobile LiDAR technology for inspection of work zones and diagnosis of congestion and crashes.

The first objective, quantification of the impact of congestion on safety, was intended as the motivational backbone for the research. Quantifiable evidence of need is important for decision- and policy-makers. Based on the discovered safety impacts, the second and third objectives were developed. A real-time queue detection and alert tool would allow traffic managers to mitigate queues as they occur while a dynamic reporting tool would allow traffic managers to assess performance over time. Collaboration opportunities arose and the use mobile LiDAR technology for work zone assessment evolved. Used in conjunction, these tools could improve mobility and safety in both current and future projects with quantifiable performance measures.

1.3 Dissertation Organization

The dissertation is organized in the following manner:

Chapter 2 presents a review of the existing literature relevant to this dissertation. The history of and current practices in work zone traffic management are discussed. A review of work zone capacity studies demonstrates the underlying impact of work zones on mobility. Relevant crash studies, especially those focused on the effect of congestion and queueing are presented. A review of emerging queue detection programs is discussed. Finally, an introductory review of the uses of light detection and ranging (LiDAR) technology shows the growing applicability to transportation engineering.

Chapter 3 provides an overview of the four data sources used for this research. Information regarding the work zones selected for this study are presented first. Connected vehicle data were the backbone of this study. Crash data were used for safety analyses. LiDAR was used to collect geometric data within selected work zones.

Chapter 4 presents a statewide analysis of the impact of congestion on safety, which is a significant motivation behind this work. A six-year study of fatal back-of-queue crashes is followed by a two-year study of all interstate crashes related to congestion.

Chapter 5 presents a queue detection system and algorithm developed for use by traffic managers. This system monitors real-time connected vehicle data and sends targeted alerts to traffic management personnel.

Chapter 6 presents a weekly work zone report and dashboards developed for traffic management personnel. The report and dashboards present the connected vehicle data in a variety of ways to provide insight into the weekly traffic operations within work zones. The report generation process is discussed as well as common examples of interpretation.

Chapter 7 presents the deployment process and use of mobile LiDAR in work zones for diagnosis of congestion and crashes observed in the work zone reports. The usefulness and utility of this technology is discussed. A number of case studies demonstrate how the LiDAR data can be integrated with the connected vehicle data presented in the work zone reports.

Chapter 8 concludes the dissertation with a summary of the research findings and reiteration of the work's significance. The contributions and current implementations of this work are also summarized. Finally, possible future research and applications are briefly discussed.

2. LITERATURE REVIEW

This chapter covers a literature review of topics relevant to this research: work zone traffic management, work zone capacity, safety studies, queue detection, and geometric measurement. Each section is presented as an introduction to and demonstration of the importance of the topic in relation to this dissertation. A brief overview of common or best practices and specific studies relevant to this dissertation are included.

2.1 Work Zone Traffic Management

The Federal Highway Administration (FHWA) published the *Final Rule on Work Zone Safety and Mobility* [1] in September of 2004. In short, this rule states that any roadway project receiving federal funds must have a maintenance of traffic (MOT) plan. In response, many state and local agencies developed guidelines, policies, or programs for oversight of traffic management plans. The New York State Department of Transportation outlined clear contractual requirements, accident reporting, quality assurance/quality control procedures, etc. in its construction safety and health program [2]. The Virginia Department of Transportation developed its own *Transportation Management Plan Requirements* [3] based on recommendations published in 2005 [4]. These requirements apply to all projects within state right-of-way, regardless of funding source. In Washington, DC, a *Citywide Transportation Management Plan* was deployed to coordinate and analyze work zones and special events [5]. The Indiana Department of Transportation (INDOT) frequently updates its *Interstate Highways Congestion Policy*, which defines acceptable impacts on traffic, lane closure policy, etc. [6]. The purpose of these policies is to maintain capacity and reduce congestion due to work zones.

Evaluation and enforcement are critical in ensuring these policies are upheld and updated. Rouphail, Yang, and Fazio found significant “discrepancies between standards and practice” in their study of short- and long-term work zones [7]. In the work zones with such discrepancies, there were higher speed variations between vehicles. Gambatese

and Johnson found that traffic management plans were of higher quality and had improved implementation when construction personnel were involved in the design phase and constructability was prioritized [8]. To manage compliance and quality, some agencies have developed quality assurance programs and inspection procedures [9]. Development and approval of maintenance of traffic plans often involve simulation [10] to assess mobility and safety impacts so effective work zone MOT plans can be designed. The Ohio Department of Transportation uses measured flow data to evaluate and calibrate their queue simulation programs [11].

Performance measures are an integral part of the monitoring and assessment of the impacts of MOT plans. Queue length, travel time, and delay are common performance measures [12], [13]. Bourne et. al. [14] summarize some of the best practices in work zone assessment, data collection, and performance evaluation. The State of Virginia has its own performance assessment process [15]. Another study considered the effects of quantitative performance measures on the revision of the work zone decision-making process [16]. A common theme in all of these initiatives is that actively monitoring work zones and conducting after-action assessment is important for continued improvement of traffic management and maintenance of traffic plans in the future.

While post-project assessment is important for future decision-making, active monitoring and dynamic management during the course of a work zone can reveal opportunities for improvement in mobility and safety. Real-time measurement of travel time delay can assist motorists in their decision to divert and avoid congestion and could be utilized for contracts with innovative travel time reliability clauses [17]. For example, the citywide work zone management and monitoring system developed for Washington, DC, included a suite of web-based tools [5]. Work zone monitoring tools are valuable to agencies for the dynamic management of traffic in and around work zones.

2.2 Work Zone Capacity

When planning work zones and anticipating congestion, it is necessary to understand how work zones affect capacity. There are many different methods and models available for estimating work zone capacity. Figure 3 shows capacity estimation results for 10 different freeway scenarios. Figure 3 represents only a subset of the literature. Four editions of the *Highway Capacity Manual* [18], [19], [20], [21] (HCM) were referenced to demonstrate the change in capacity estimation over the last few decades. Between 1985 and 2000, the base capacity for high-speed facilities changed from 2000 vehicles per hour per lane (vphpl) to 2400 vphpl. Until the 2000 edition, the *Highway Capacity Manual*s did not include lane width as a variable in work zone capacity estimation. Other models have been developed for specific scenarios or locations. Jiang [22] determined average capacities for work zones in Indiana. Weng and Meng [23] developed a decision tree with 16 variables to estimate work zone capacity. Yeom et. al. [24] used nationwide data to develop and validate a new model to be incorporated in the next release of the *Highway Capacity Manual*, as part of NCHRP Project 3-107.

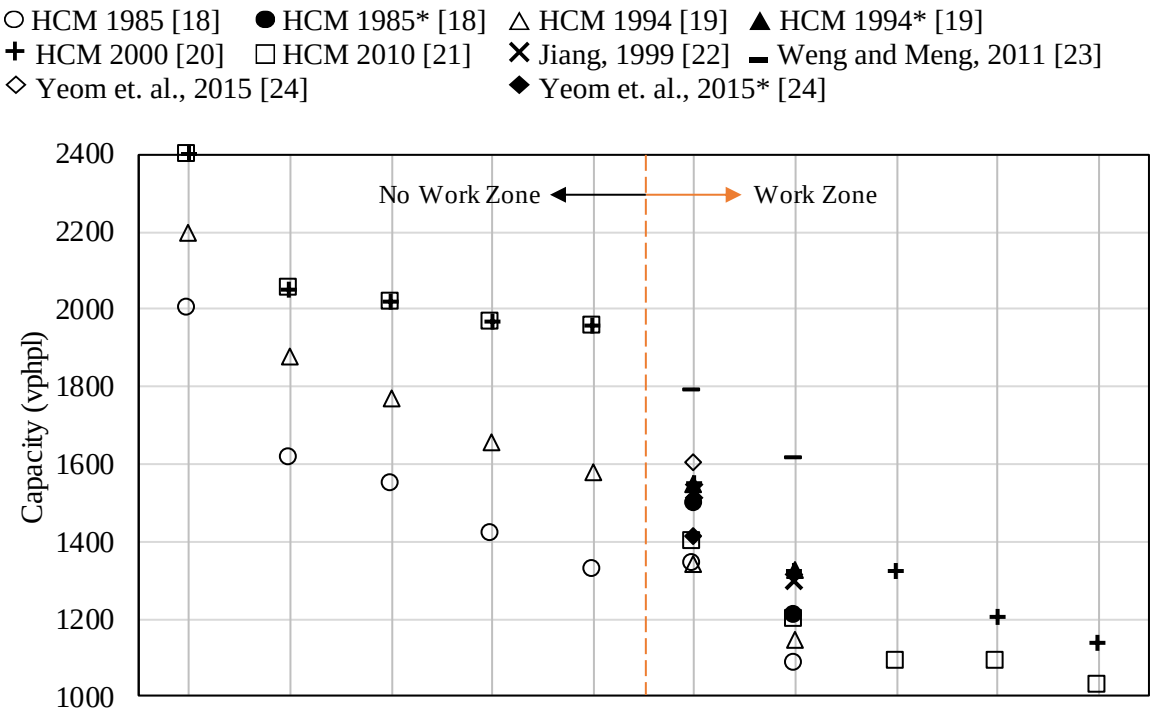

Lane Width (ft)	12	12	11	10	10	12	12	11	10	9
Shoulder Width (ft)	6	6	4	2	0	N/A	N/A	N/A	N/A	N/A
Percent Trucks (%)	0	34	34	34	34	0	34	34	34	34

*Concrete barriers present.

Figure 3 Summary of freeway capacity estimation for different scenarios

The capacity models discussed above include variables such as lane width, work intensity, number of open/closed lanes, driver composition, etc. Variables of particular interest, for case studies discussed in this dissertation, are lane width (Figure 3) and taper length. A taper refers to the lateral shift of traffic over a longitudinal distance. A merging taper is used when two lanes are merged into one. There have been few studies on the effect of taper length on work zone capacity. In 1979, Sharp and Harwood [25] published their study of work zone taper lengths and design speeds. A study of reduced taper lengths was conducted on lower-speed urban arterials by Theiss, Finley, and Ullman [26]. Many agencies and designers refer to the *Manual on Uniform Traffic Control Devices* (MUTCD) [27] recommendations for taper length. INDOT publishes work zone traffic

control guidelines [28], which include required taper lengths. The INDOT values are based on the MUTCD values but are rounded up depending on the number of skip lines. Table 1 shows both the MUTCD and INDOT values for merging taper lengths at different speeds.

Table 1 Merging Taper Length Recommendations

	Merging Taper Length (ft)	
Speed (MPH)	MUTCD [27]	INDOT [28]
45	540	560
50	600	600
55	660	680
60	720	720
65	780	800
70	840	840

2.3 Safety Studies

Agencies are concerned with the effect of roadway and traffic conditions on safety since these are factors that can potentially be impacted by infrastructure improvements and changes. When safety is a concern, crash rates are the most common performance measure used by agencies and researchers. The *Highway Safety Manual* [29] (HSM) defines crash frequency as the number of crashes over a period of time, usually one year. Crash rate is defined as the crash frequency over a period of time divided by the exposure in that same time period. Exposure is the measure of all opportunities for a crash to occur, whether or not a crash actually occurs. The HSM refers to exposure as a measure of volume but, over the years, researchers have used a number of different ways to measure exposure, such as induced exposure or density. Safety studies concerned with the effect of congestion and queueing are the most relevant to the research presented in this dissertation.

Volume or volume-based measures are the most common basis for exposure. Some studies use traffic counts recorded by infrastructure technology. Other studies use annual average daily traffic (AADT). Mensah and Hauer [30] advise caution when using AADT as a measure of exposure. AADT is an aggregate measure and is not appropriate when considering non-normal traffic conditions at the time of a crash. Specifically, when

studying the effect of congestion on safety, an average measure of volume does not adequately represent the traffic conditions.

One study the effect of hourly flow on crash rates for different levels of severity, finding that property damage only (PDO) and injury crash rates were highest when traffic was lightest [31]. Another study used AADT-based hourly volumes to estimate the potential for conflicts [32]. A third study modeled crash severity using flow as a variable in addition to speed and delay caused by congestion [33].

Vehicle-miles traveled (VMT) is also a widely accepted and often used measure of exposure when calculating crash rates [34], [35], [36]. In a study by University of California-Berkeley's Transportation Research and Education Center [37] [38], four different traffic states were considered. The four traffic states were based on speeds upstream and downstream of a crash and used 50 MPH as a threshold for congestion, using VMT and vehicle-hours traveled (VHT) as exposure. In this study, the researchers found that crash rates for the three different congestion states were about 5 times greater than the crash rate for the free flow state.

Density (vehicles per mile) is frequently used in safety studies directly concerned with the effects of congestion on crash rates [39], [40], [41], [42]. A common finding amongst safety studies using density as exposure is the parabolic, or U-shaped, relationship between density and crash rates, where the highest crash rates occur at low densities (mostly single vehicle crashes) and high densities (mostly multi-vehicle crashes). Some less common but no less viable measures of exposure are the standard deviation of speed between vehicles [43] and the volume-to-capacity ratio at the time of the crash [44].

There is substantial literature on safety in work zones. Negative binomial models were developed to predict the expected number of crashes in rural interstate work zones in Indiana [45]. Further studies in Indiana have produced models that account for police enforcement [46] and work zone design and traffic management features [47]. Other studies have also included different work zone configurations in developing safety performance functions [48] and analyzing crash severity [49]. In Singapore, rear-end

crash risk models were developed using work zone traffic data [50]. It was found that rear-end crash risk increases with the percentage of heavy vehicles and flow.

2.4 Queue Detection

Queue detection refers to locating, in real-time, the back of a queue. The back of a queue is a type of shockwave. “Shockwaves are defined as boundary conditions in the time-space domain that demark a discontinuity in flow-density conditions” [51, p. 205].

As real-time, high-resolution traffic data becomes more available and reliable, queue detection and alert systems are becoming more common. These systems use a variety of different data sources and detection algorithms. One detection system developed for high-crash locations used average speed, density, headway variability, acceleration noise, etc. to calculate crash likelihood in real time [52]. The detection system succeeded in detecting 58% of crashes during the study. A vehicle queue length detection methodology was developed for signalized intersections using an array of low-angle cameras [53]. Tiaprasert et. al. used connected vehicle technology to estimate queue length for adaptive signal control [54]. An incident management integration tool developed by Khattak, Wang, and Zhang uses roadway inventory and traffic incident data to predict incident durations, secondary incident occurrence, and delay [55]. In Indiana [56] and France [57], connected vehicle data was used for real-time shockwave detection on freeways. The Indiana system was developed for the Indiana Department of Transportation (INDOT) and covers the statewide interstate system. If the speed of an upstream segment is significantly higher than the speed of the immediate downstream segment, an alert is made visible to dispatchers and emergency responders.

There have been several studies focused on warning drivers about queues. Wiles et. al. provided an overview of practices for advance warning of motorists [58]. One study in Texas estimated that a system of radar speed sensors and portable message signs reduced back-of-queue crashes 44% [59]. In San Francisco, the use of in-vehicle auditory alerts to warn drivers that they were approaching slowed or stopped traffic was investigated [60]. Another study used simulations to explore the effects of advanced driver-assistance systems with queue warning on traffic flow [61].

2.5 Geometric Measurement

Light detection and ranging (LiDAR) systems onboard terrestrial mobile platforms have emerged as a prominent tool for collecting high density point clouds along object surfaces relative to a global reference frame [62], [63]. In short, LiDAR is a surveying tool used to collect data on the precise location of surrounding surfaces and objects. The use of LiDAR in the context of transportation is a quickly expanding topic in literature. In 2013, NCHRP Report 748 was published, which included guidelines for using mobile LiDAR in transportation applications [64]. Chang et. al. also published guidance on how agencies could practically use and deploy LiDAR in 2014 [65]. Change et. al. discuss common transportation applications and acquisition options of LiDAR. For example, the authors recommend the mobile LiDAR platform for applications such as construction clearance measurement, corridor mapping, safety assessments, and traffic operations. A great deal of research has been developed regarding the use of LiDAR for the recognition of objects along roadways [66], [67], improvement of road safety [68], automated driving [69], and risk management [70].

2.6 Opportunities

The following chapters introduce emerging connected vehicle probe data sources and show how this new data can be integrated with the above data sources to develop improved performance measure and warning systems that will allow agencies to design and operate safer work zones.

3. DATA SOURCES

This work utilized four data sources: work zone data, connected vehicle data, crash data, and geometric data from mobile LiDAR. The following sections will detail the nature and use of each data source in this research.

3.1 Work Zone Data

For this research, 18 work zones across the State of Indiana were selected (Figure 4). They ranged from 1 to 24 miles in length and included a variety of construction activities. These work zones were selected by INDOT personnel based on expected congestion, publicity, and duration. Location details for each of the work zones, by direction, are listed in Table 2. The selected work zones are divided by INDOT district, route, direction, and start/end mile posts. For seven of the work zones, the exact mile post location of the advance warning signs was known. The final column, "Label," defines the shorthand label used for each work zone in Figure 4 and throughout the rest of this dissertation. The first letter corresponds to the district. The number corresponds to the work zone's arbitrary order within that district. The last letter corresponds to the direction of travel. For example, the work zone labeled "C3S" corresponds to the southbound direction of the third work zone in the Crawfordsville district, which is on I-65 between mile posts 197 and 207.

Six work zones in the sample could not have congestion extend upstream of the work zone. For F2S and G4N, the beginning of the work zone and the interstate coincide. Any congestion extending past these work zones would be on non-interstate roadways. For L1S, L2N, S1S, and S2N, a different work zone is immediately upstream of and overlaps with that work zone. Therefore, any congestion extending upstream of these four work zones would be counted as congestion in the adjacent work zones.

Figure 4 Map of selected work zones

Table 2 Summary of Selected Work Zones

INDOT District	Route	Project Description	Dir.	Advance Warning Sign Mile Post Location	Start Mile Post	End Mile Post	Label
Crawfordsville	I-65	HMA overlay/bridge deck replacement	N	140.0	141	165	C1N
			S	166.1	165	141	C1S
	I-65	Added travel lane/bridge widening	N	166.1	167	176	C2N
			S	177.7	176	167	C2S
	I-65	HMA overlay/bridge deck overlay	N	195.3	197	207	C3N
			S	208.9	207	197	C3S
	I-70	Bridge deck replacement and widening	E	4.5	6.8	12	C4E
			W	13.0	12	6.8	C4W
Fort Wayne	I-69	Concrete pavement restoration & bridge rehabs	N		325	334	F1N
			S		334	325	F1S
	I-469	HMA overlay/bridge deck patching	N		16	31	F2N
			S		31	16	F2S
Greenfield	I-65	Replace superstructure	N	104	105.5	106.5	G1N
			S	107.2	106.5	105.5	G1S
	I-65	Concrete pavement restoration	N		110	112	G2N
			S		112	110	G2S
	I-465	Concrete pavement restoration	IL		43	53	G3IL
			OL		53	43	G3OL
	I-69	HMA overlay/preventative maintenance	N		200	201	G4N
			S		201	200	G4S
	I-69	Added travel lanes/bridge widening/interchange	N		205	220	G5N
			S		220	205	G5S
	I-465	Added travel lanes	IL	26.4	26.3	27.3	G6IL
			OL	27.1	27.3	26.3	G6OL
La Porte	I-65	Added travel lane/bridge deck overlay	N	232.5	234	253	L1N
			S		253	229	L1S
	I-65	Added travel lane/concrete pavement restoration	N		252	260	L2N
			S		260	252	L2S
	I-94	Concrete pavement restoration	E		3	11	L3E
			W		11	3	L3W
	I-94	HMA overlay/bridge deck replacement	E		19	27	L4E
			W		27	19	L4W
Seymour	I-65	Concrete pavement restoration	N		1.3	8.4	S1N
			S		8.4	1.3	S1S
	I-65	Added travel lane/replace superstructure	N		8	16.5	S2N
			S		16.5	8	S2S

3.2 Connected Vehicle Data

Connected vehicle speed data were collected from GPS devices, cellular phones, freight data, or vehicle telematics. These data came from 1-2% of vehicles on interstates in Indiana. Individual vehicle trajectory data were aggregated as minute-by-minute space mean speeds for predefined road segments to preserve driver anonymity. The average road segment length was 0.88 miles. In Indiana, there were approximately 2600 segments covering all of the 2250 directional miles of interstate. Each data point had a timestamp, location, speed, and confidence level.

Figure 5 shows a sample of the vehicle trajectory data from work zone C4W before it is aggregated. Each line represents an individual vehicle trajectory and is colored according to the vehicle's speed. This time-space diagram represents vehicles passing through a section of I-65 N on October 22, 2016, before, during, and after a back-of-queue crash (Figure 6). A queue initially formed at approximately 10:30 in a work zone at mile post 16 (callout 'i' in Figure 5). At 14:00, a back-of-queue crash occurred at mile post 19 (callout 'ii' in Figure 5). Due to the severity of the crash, I-70 W was closed (callout 'iii' in Figure 5) and traffic was detoured at Exit 23 (callout 'iv' in Figure 5). After approximately 3 hours, the left lane of I-70 W was reopened (callout 'v' in Figure 5). The roadway did not return to free-flow conditions until midnight, over 12 hours after the queue initially formed. Figure 7 depicts the same queue as in Figure 5 with the aggregated connected vehicle speed data. The average speed of each segment between mile posts 10 and 30 are represented by the appropriate speed bin color over time. Segment speeds greater than 45 MPH are not represented in Figure 7. The light-yellow shading and dashed orange line represent the work zone area and work zone boundary, respectively.

Using these data, performance measures have been created that visually depict the performance of an entire roadway over a period of time. These data have been used for performance measures in Indiana in the *Indiana Mobility Report* [71], [72], [73], [74] and nationwide in the *Urban Mobility Scorecard* [75]. In Indiana, performance measures for decision-makers were developed using these data [76], [77].These data have also been used for real-time traffic monitoring [56], in which there is a 3-5 minute lag.

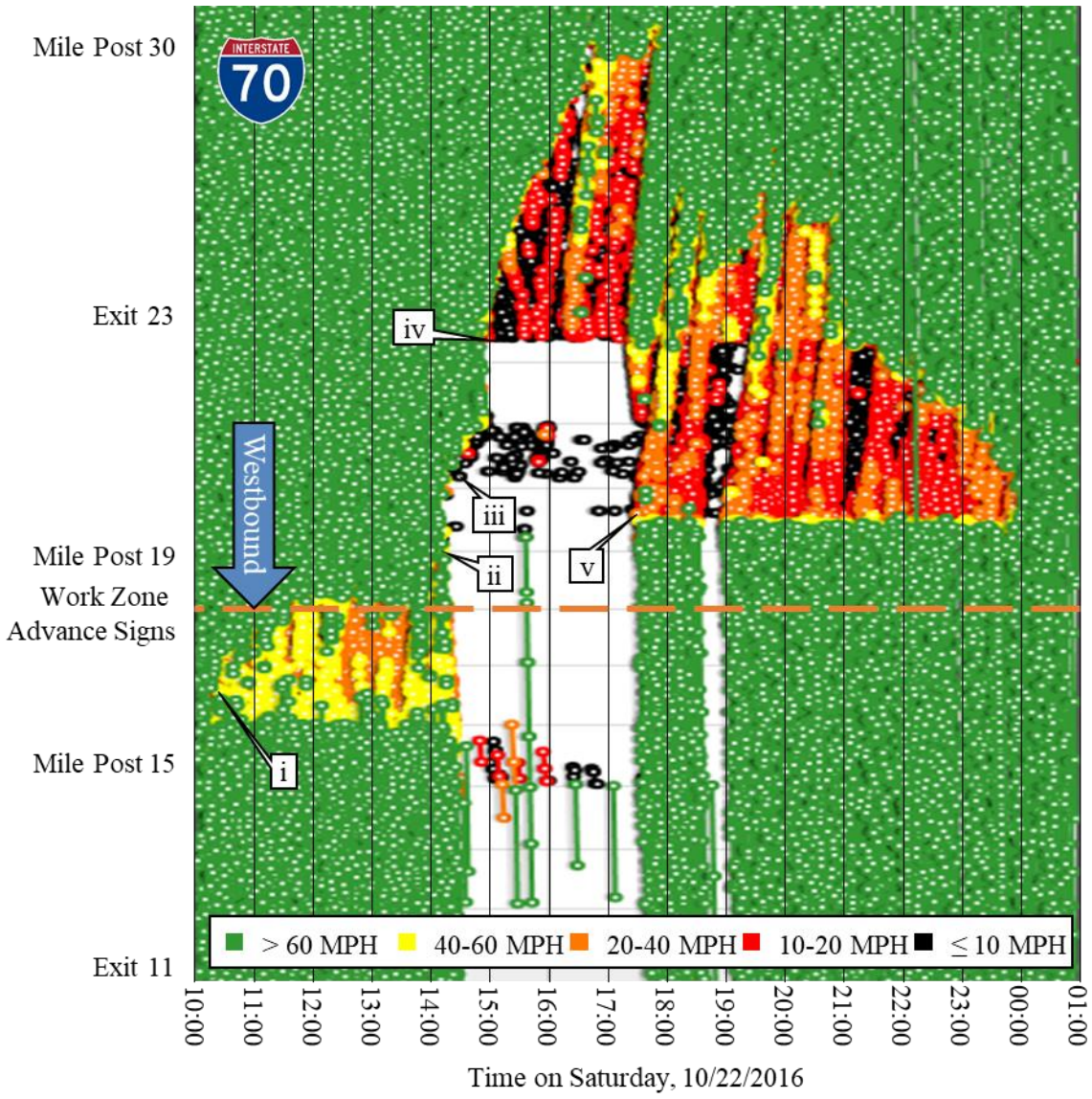

Figure 5 Time-space diagram with individual vehicle trajectories (C4W)

Figure 6 Photo of aftermath of back-of-queue crash on October 22, 2016

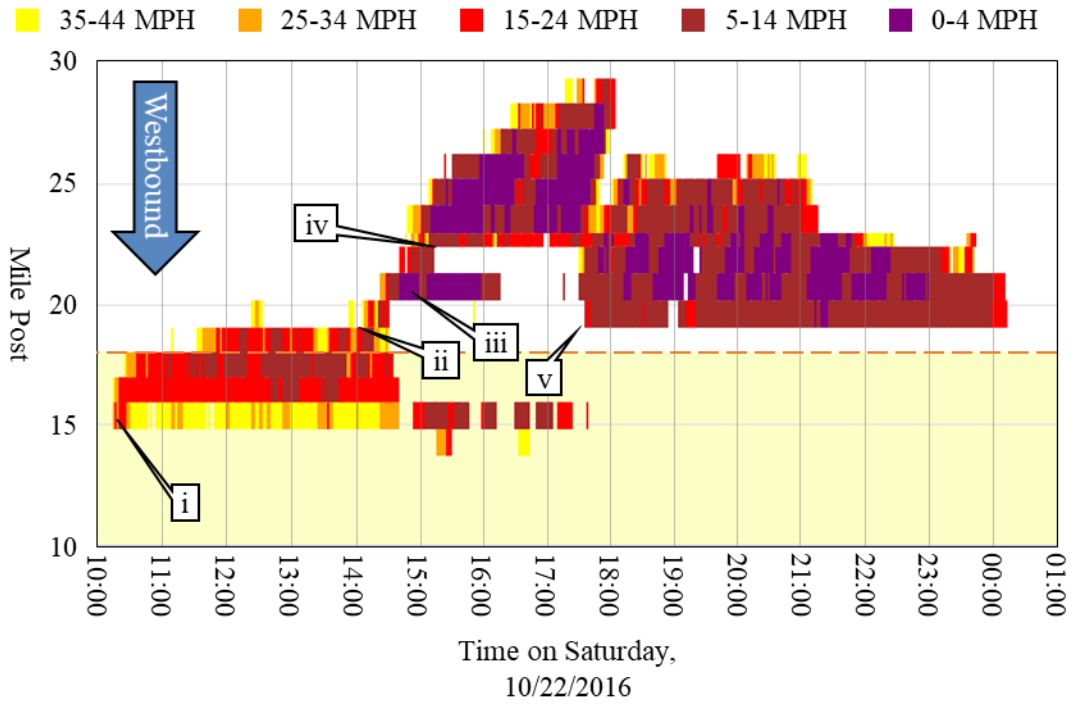

Figure 7 Queue heat map with aggregated connected vehicle speed data

3.3 Crash Data

Crash data were retrieved from the state crash database. Only crashes that occurred on an interstate in Indiana were used in this study. Personal information about the crash participants and investigating officers, such as names and license plate numbers, were not included in these data. These data did include the following relevant information for each crash:

- Date and time
- Location (route, direction, and mile post)
- Number/types of vehicles and trailers involved
- Number of injuries and fatalities
- Primary factor and manner of collision
- Construction indicator
- Officer's narrative
- Crash diagram

Before being used in this research, the raw interstate crash data were further refined. Any crash with an unknown or unreliable location was eliminated from the study data. Any crash that occurred, in its entirety, on a ramp or at an intersection was eliminated. Only crashes that occurred on the travel lanes of the interstate were included.

3.4 Geometric Data from LiDAR

A LiDAR system includes a laser ranging and scanning unit, which measures the GPS coordinates and reflectivity of points on nearby surfaces. For the laser ranging, the LiDAR system emits a pulse to estimate the distance from the unit based on the transmission time between the firing point and its footprint. Moreover, every pulse has an intensity defined by the return strength of the laser pulse. The intensity can indicate the reflectivity of an object hit by the laser pulse. For the scanning mechanism, laser scanners can be mainly classified into two categories: single laser scanners steered by a mirror (used for static scanning) and rotating multi-beam laser scanners (used for terrestrial

mobile mapping). A typical, directly geo-referenced LiDAR system consists of a laser scanner, Global Navigation Satellite System (GNSS), and Inertial Navigation System (INS), which can provide the accurate position and orientation of the vehicle platform.

A directly geo-referenced LiDAR system comprises three coordinate systems (mapping frame, *m*, GNSS/INS body frame, *b*, and laser unit frame, *Lu*) as illustrated in Figure 8. These coordinate systems and their spatial/rotational relationships are used to define the mapping coordinates (callout 'i') of a given point, *P*, acquired from a mobile LiDAR mapping system, as given in Equation 1. The coordinates of point *P* relative to the laser unit coordinate system can be defined as $r_P^{Lu}(t)$ (callout 'ii') by Equation 2, where α is the vertical angle determined by the fired laser beam ID; β is the horizontal angle, which depends on the rotation of the laser unit; ρ is the range defined by the distance from firing point to the footprint of the laser beam; and *t* is the time. The lever arm angle, r_{Lu}^b, and boresight angle, R_{Lu}^b, (callout 'iii') between the laser unit and body frame coordinate systems are time-independent since the laser scanner and body frame are rigidly fixed relative to each other. The lever arm and boresight angles can be derived from a system calibration using conjugate targets in multiple drive runs [78], [79], [80]. The GNSS/INS integration provides the time-dependent position, $r_b^m(t)$, and orientation, $R_b^m(t)$, (callout 'iv') relating the mapping frame to the body frame. In short, these equations take the coordinates of the data points, relative to the LiDAR unit, and convert them to GPS coordinates, which can be easily displayed and referenced in relation to existing road maps.

$$r_P^m = r_b^m(t) + R_b^m(t)\, r_{Lu}^b + R_b^m(t)\, R_{Lu}^b\, r_P^{Lu}(t) \tag{1}$$

$$r_P^{Lu}(t) = \begin{pmatrix} x \\ y \\ z \end{pmatrix} = \begin{pmatrix} \rho(t)\cos\beta(t)\cos\alpha(t) \\ \rho(t)\cos\beta(t)\sin\alpha(t) \\ \rho(t)\ \sin\beta(t) \end{pmatrix} \tag{2}$$

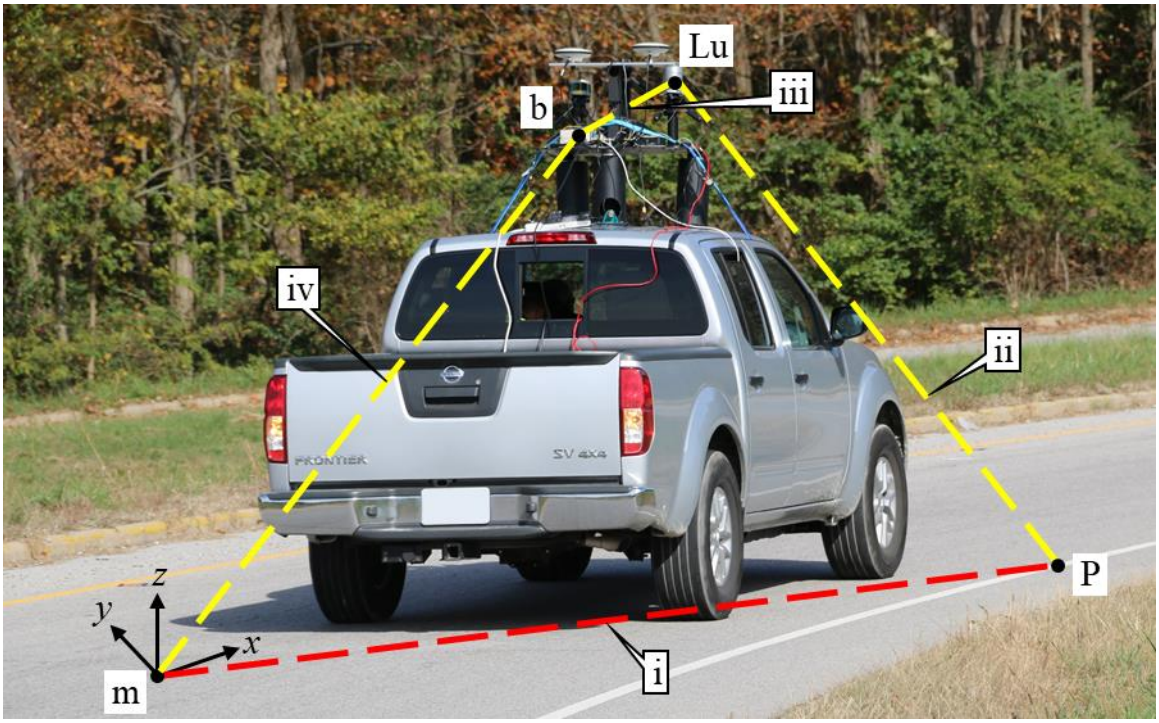

Figure 8 Illustration of point positioning of a directly geo-referenced LiDAR system

After reconstructing the geo-referenced point cloud, features of interest can be identified and extracted automatically. Objects that are highly reflective can be identified using the intensity data in a given point cloud. Figure 9 shows some features of interest in the I-70 work zone (C4W) in three different images. Figure 9a shows the vehicle with the mobile LiDAR unit and surrounding features of interest. Figure 9b shows a camera image from the LiDAR system at the same location. In Figure 9c, the point cloud consists of a black background with data points colored according to reflective intensity (unitless), with white being the most reflective. For the majority of the LiDAR data used in this study, data points with a reflective intensity less than 30 were removed to reduce noise in the data. Callout ‘i’ refers to a Type 3 barricade. Callout ‘ii’ is a channelizing drum. Callout ‘iii’ is a reflective marker atop a concrete barrier. Callouts ‘iv’ and ‘v’ are the dashed centerline and edgeline markings, respectively. Callouts ‘vi’ and ‘vii’ in Figure 9a correspond to the on-board camera and the LiDAR unit. With mobile LiDAR technology, precise data regarding the location and reflectivity of surfaces around the system can be collected. These data can be used for measurement of features along the roadway.

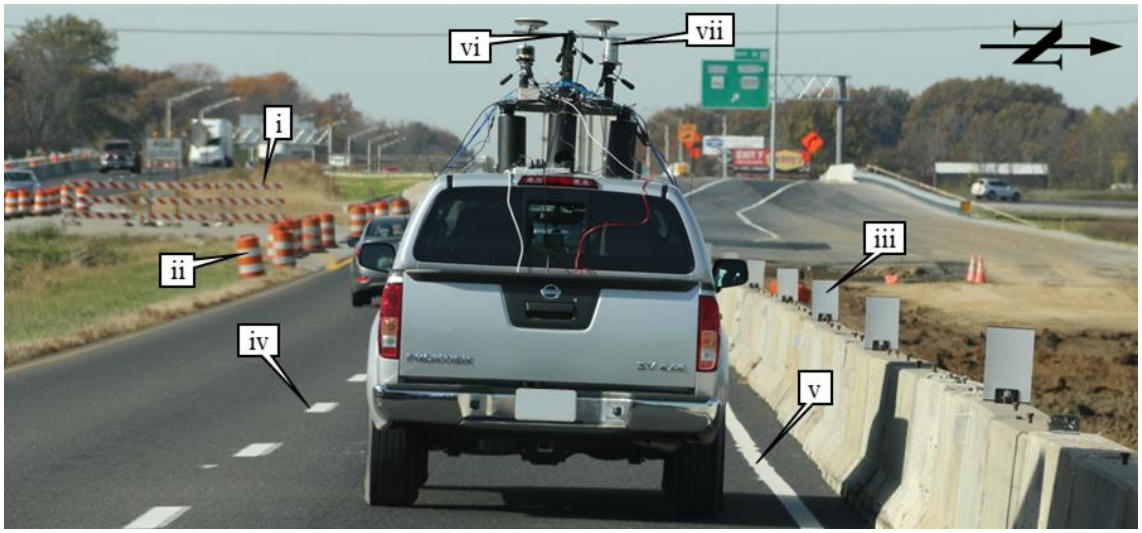

(a) Picture of LiDAR-mounted vehicle

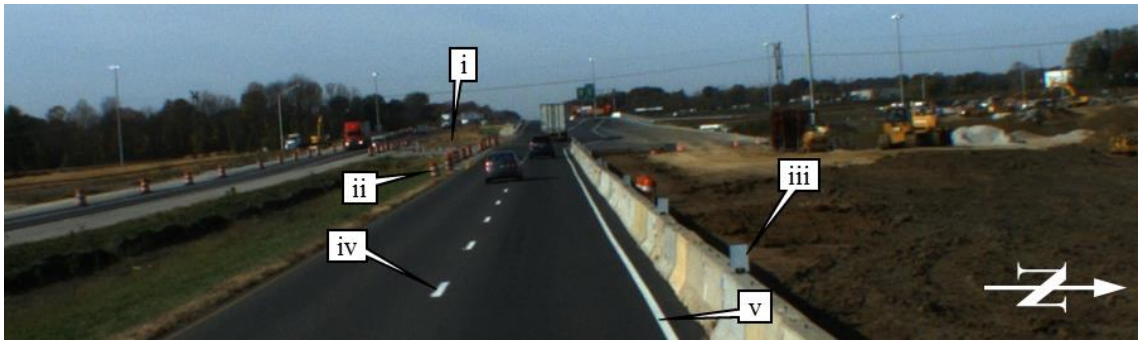

(b) Camera-view from LiDAR-mounted vehicle

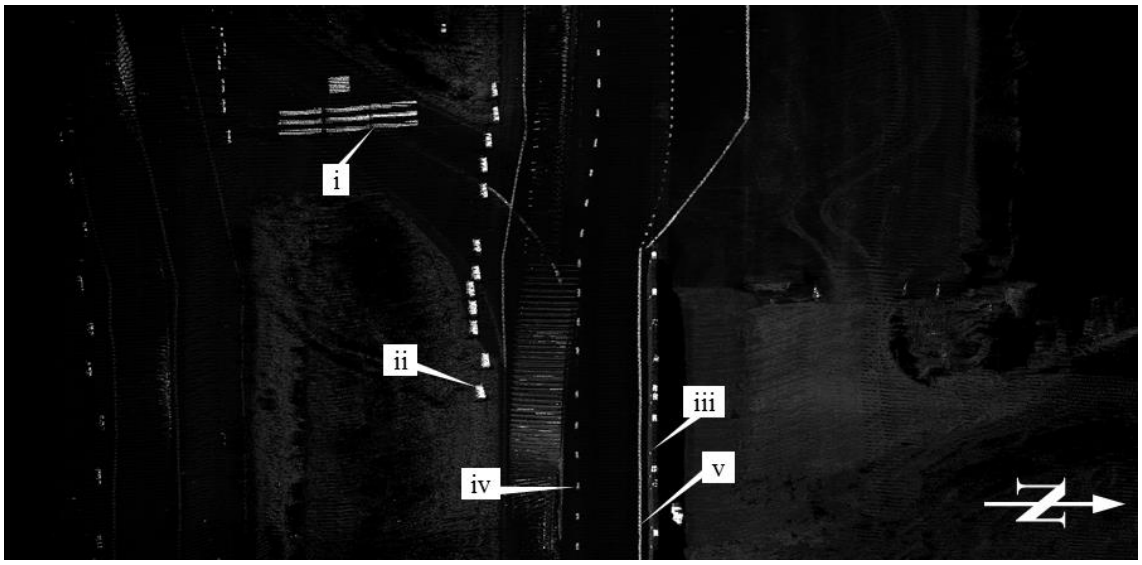

(c) Point cloud from LiDAR at vehicle location

Figure 9 Example LiDAR data near mile post 11.5 in C4W work zone

4. QUANITIFYING THE IMPACT OF CONGESTION ON SAFETY

The initial part of this study was devoted to quantifying the impact of congestion on safety on interstates. It is important for decision-makers to understand how congestion affects safety and where there are opportunities for improvement. Six years of statewide, interstate crash data were used. The following three sections discuss the analysis of these data. First, definitions are provided for terms used throughout the chapter and the rest of the dissertation. Second, a detailed analysis of fatal back-of-queue crashes is discussed. Third, a large-scale analysis of crashes of all severities was conducted.

4.1 Definitions

Congestion or congested conditions were defined in this study by a speed threshold of 45 MPH. Any interstate segments with an average speed less than 45 MPH were considered to be congested. This threshold was previously used in the *Indiana Mobility Report* [71], [72], [73], [74]. Conversely, uncongested conditions were defined by speeds greater than or equal to 45 MPH. Agencies may have different perspectives on the most appropriate speed threshold, but the most commonly used speed threshold in Indiana to screen for congestion is 45 MPH, although other thresholds, such as 15 or 30 MPH, may be appropriate.

A back-of-queue (BOQ) crash was defined in this study as a crash that occurred at the back of a queue, or at a shockwave boundary between high- and low-speed traffic. The time and location of the crash was compared to the times and locations of shockwaves in the speed data. For example, the boundary between the colored (low-speed) segments and the non-colored (high-speed) segments in Figure 7, such as at callout ‘ii’, is considered a shockwave. Due to the variability in crash reporting accuracy and the aggregate nature of the speed data, the crash narratives were used when it was unclear if the crash occurred at the back of a queue. A common indicator of a back-of-queue crash in the report narrative is a driver/s stating that traffic slowed or stopped suddenly.

A congested or congestion crash is defined in this study as a crash that occurs during congested conditions. This encompasses crashes that occur either within a queue or at the boundary of a queue (i.e. back-of-queue crashes). The number of congested crashes is always greater than or equal to the number of back-of-queue crashes. Conversely, an uncongested crash is defined in this study as a crash that occurs during uncongested conditions.

4.2 Fatal Back-of-Queue Crashes

There was a total of 456 fatal crashes on interstates in Indiana from January 1, 2012, through December 31, 2017. For each fatal crash, the connected vehicle speed data prior to and upstream of the crash were analyzed to ascertain whether or not the crash occurred at the back of a queue. The speed data were augmented by the crash report narratives. Using this method, 53 of the 456 fatal crashes were determined to be back-of-queue crashes. Figure 10 shows the total fatal crashes and fatal back-of-queue crashes by year. The highest percentage and number of fatal back-of-queue crashes occurred in 2014.

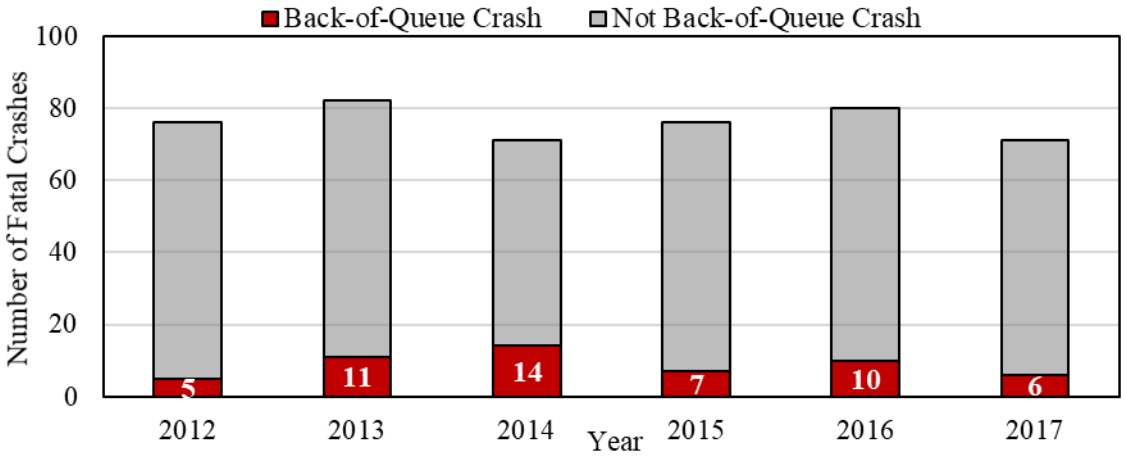

Figure 10 Number of fatal crashes on Indiana interstate by year

Figure 11 shows the number of fatal crashes by interstate for the six-year period. Of the interstates in Indiana, I-65 and I-70 have the highest numbers of both fatal crashes and fatal back-of-queue crashes. Note that in this plot, the results, crash frequencies, were

not normalized by length of the roadway. Normalized crash rates were calculated in the next study, discussed in the next section.

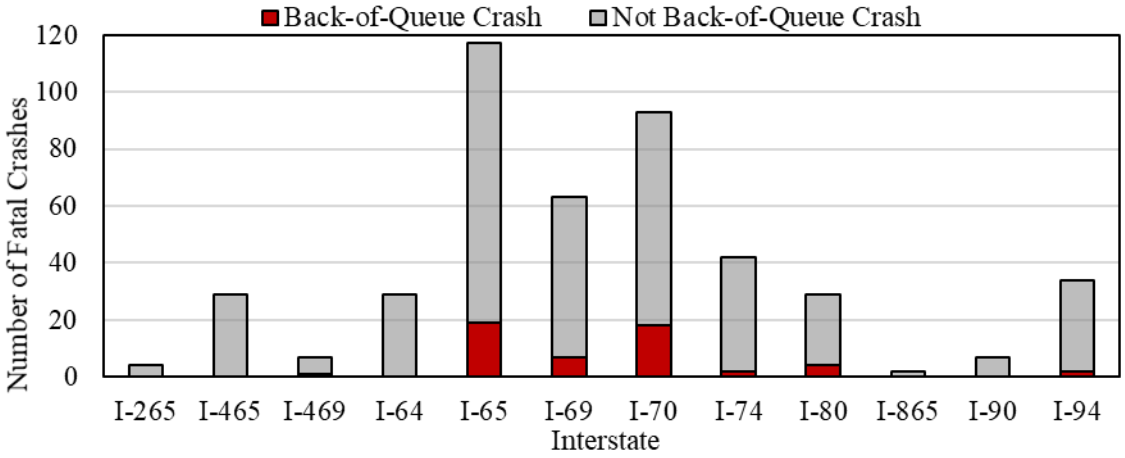

Figure 11 Number of fatal crashes on Indiana interstates by interstate, 2012-2017

In this part of the study, different possible trends in back-of-queue fatal crashes were considered and evaluated. A significant trend found in fatal back-of-queue crashes is the involvement of one or more trucks with trailers (Figure 12). Out of all fatal back-of queue crashes over the six-year period, 90.6% involved at least one truck. In comparison, only 33.3% of the non-back-of-queue fatal crashes involved at least one truck.

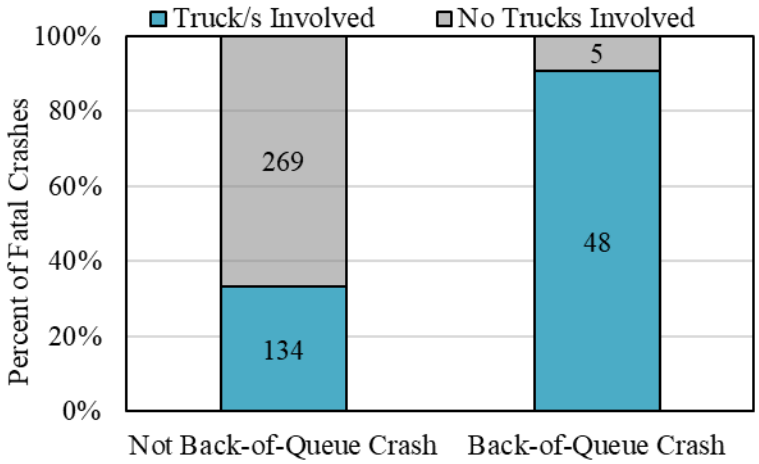

Figure 12 Percent of fatal crashes that involved truck/s, 2012-2017

A larger percentage of back-of-queue crashes than non-back-of-queue crashes were associated with construction (Figure 13). This trend is most likely influenced by the fact that work zones cause queueing more so than non-work zones.

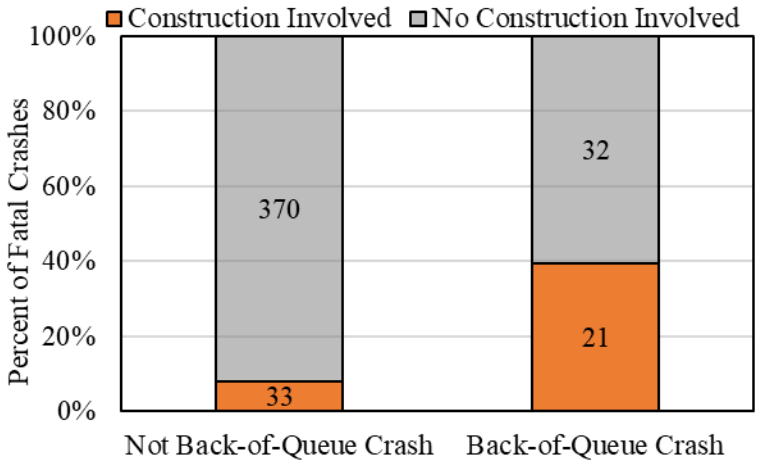

Figure 13 Percent of fatal crashes that involved construction, 2012-2017

Figure 14 shows a Pareto chart of the durations of queues observed in the connected vehicle data before each of the 53 fatal, back-of-queue crashes. The maximum observed duration of queueing prior to a fatal back-of-queue crashes was over 6 hours. For four fatal back-of-queue crashes, the queue was not visible in the connected vehicle data prior to the crash. The four crashes occurred during a time period when the data source was relatively new and was based on longer roadway segments, which muted the impact of queueing. The chart also shows which back-of-queue crashes were associated with construction. For 83% of these crashes, the queue was visible in the connected vehicle data for at least 30 minutes prior to the crash occurrence.

Figure 14 Duration of queue in connected vehicle data prior to fatal BOQ crash

4.3 Congestion Crash Rate

Following the study of fatal crashes, crashes of all severities were analyzed. Crash rates in congested and uncongested traffic conditions were the focus. As discussed in the literature review, the vast majority of crash rates use a volume-based unit of exposure. Many safety studies use AADT to derive volume. However, an aggregate measure of volume would be insufficient is this case since congested conditions are not adequately represented by average measures.

For this study, a new measure of congestion and exposure was developed: the mile-hour. This measure is both spatially and temporally weighted and is the product of the duration of time that a specified condition persists in a segment and the length of that segment. All parts of Figure 15 display data on I-70 between mile post 0 and 18 (C4) on April 14, 2017. In Figure 15a and Figure 15b, the vertical gray lines represent the boundaries between segments on I-70 E and I-70 W, respectively. The height of each column between the segment boundaries represents the duration of time in which that segment had an average speed less than 45 MPH, with speed bins represented by color.

Figure 15c displays the summation of mile-hours by hour of the day. Figure 15d is the total mile-hours of congestion on I-70 between mile post 0 and 18 on April 14, 2017.

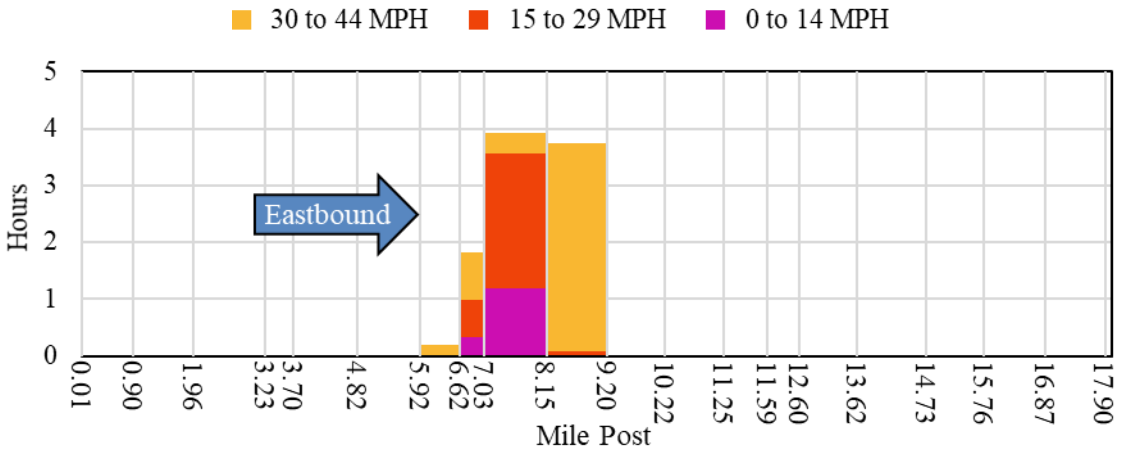

(a) I-70 E speed profile

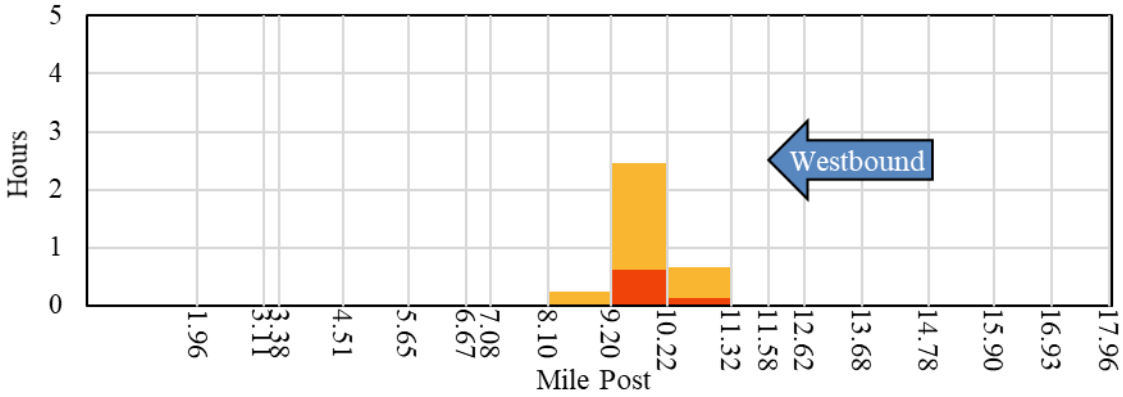

(b) I-70 W speed profile

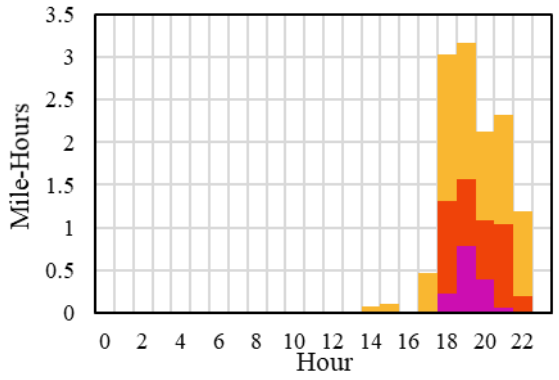

(c) Mile-hours by speed bin by hour of day

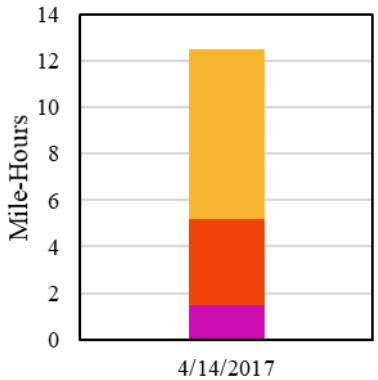

(d) Mile-hours by speed bin

Figure 15 Mile-hours of congestion on I-70 on April 14, 2017 (C4)

The areas under the curves in Figure 15a and Figure 15b are the total mile-hours, which can be calculated using Equation 3

$$MH_{<45} = \sum_{i=1}^{n} (L_i \times t_i) \quad (3)$$

Where:

$MH_{<45}$ = total mile-hours of operation < 45 MPH
n = total number of segments
L_i = length of segment i in miles
t_i = duration of time in hours where segment i has an average speed < 45 MPH

A sample calculation for the 45 MPH threshold is shown below.

Example Calculation:

Time Range: 4/14/2017 00:00 EDT – 4/14/2017 23:59 EDT
Location: I-70, mile post 0 to 18
I-70 E (Figure 15a):

$$MH_{<45,E} = (0.90mi \times 0.00hr) + (1.06mi \times 0.00hr) + (1.26mi \times 0.00hr) + (0.47mi \times 0.00hr) + (1.12mi \times 0.00hr) + (1.10mi \times 0.00hr) + (0.70mi \times 0.20hr) + (0.41mi \times 1.82hr) + (1.12mi \times 3.92hr) + (1.05mi \times 3.73hr) + (1.02mi \times 0.00hr) + (1.11mi \times 0.00hr) + (1.03mi \times 0.00hr) + (1.11mi \times 0.00hr) + (1.03mi \times 0.00hr) + (1.04mi \times 0.00hr) = 9.19 \text{ mile-hours}$$

I-70 W (Figure 15b):

$$MH_{<45,W} = (1.15mi \times 0.00hr) + (0.27mi \times 0.00hr) + (1.12mi \times 0.00hr) + (1.14mi \times 0.02hr) + (1.02mi \times 0.00hr) + (0.41mi \times 0.00hr) + (1.02mi \times 0.00hr) + (1.10mi \times 0.25hr) + (1.02mi \times 2.45hr) + (1.10mi \times 0.67hr) + (0.27mi \times 0.02hr) + (1.04mi \times 0.00hr) + (1.06mi \times 0.00hr) + (1.10mi \times 0.00hr) + (1.12mi \times 0.00hr) + (1.03mi \times 0.00hr) + (1.03mi \times 0.00hr) = 3.53 \text{ mile-hours}$$

Total (Figure 15d): $MH_{45} = MH_{45,W} + MH_{45,E} = 12.72$ mile-hours

Figure 16a and Figure 16b show the percentage of congested conditions out of the total possible mile-hours of operation for all Indiana interstates in 2014 and 2015, respectively. In 2014, interstates statewide were congested for only 1.1% of the time. In 2015, interstates statewide were congested for only 0.8% of the time. Congestion is a relatively rare occurrence on Indiana interstates.

In 2014 and 2015, a total of 30,159 crashes occurred in the main lanes of travel on interstates in Indiana. Each crash was compared with the connected vehicle speed data to

determine if it occurred during congested conditions. Of these crashes, 5,592 crashes were designated as congested crashes. Figure 16c and Figure 16d show the percentage of congested and uncongested crashes in 2014 and 2015, respectively.

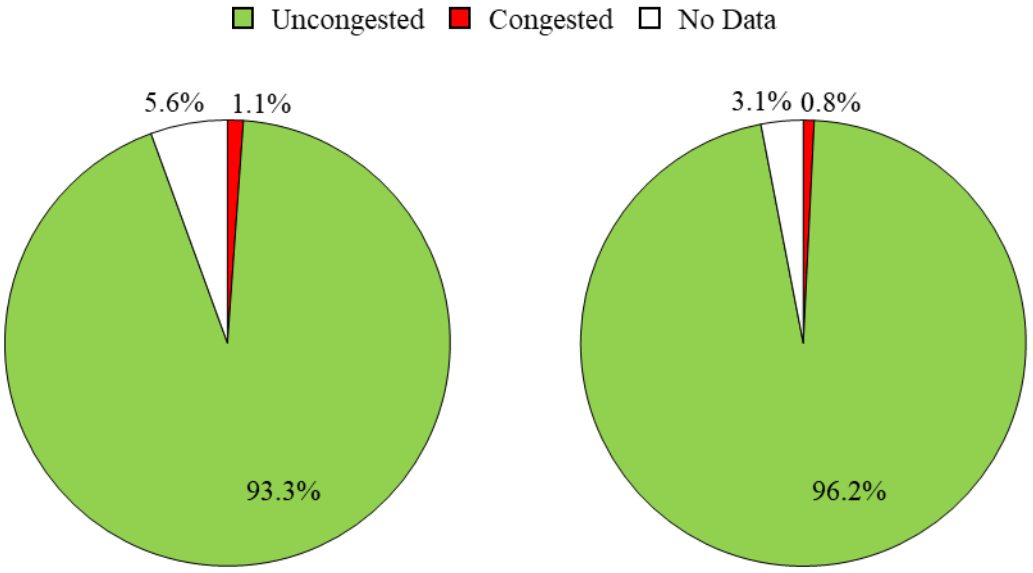

(a) 2014 statewide interstate mile-hours (b) 2015 statewide interstate mile-hours

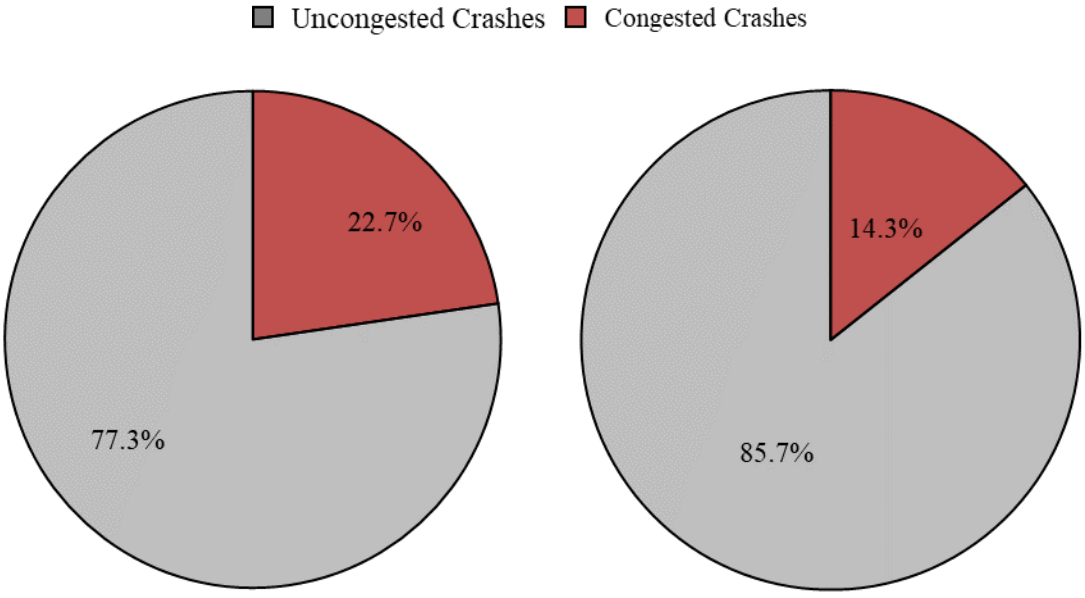

(c) 2014 statewide interstate crashes (d) 2015 statewide interstate crashes

Figure 16 Statewide congestion and crashes by year

Figure 16 shows that the percentage of crashes occurring during congestion is larger than the percentage of mile-hours of operation that are congested. In this study, the crash rate is defined by the number of crashes that occurred during a specified traffic condition (uncongested or congested) and the mile-hours of exposure to that condition. In this case, the uncongested crash rate (Equation 4) uses mile-hours of uncongested conditions and the congested crash rate (Equation 5) uses mile-hours of congested conditions.

$$Uncongested\ crash\ rate = \frac{Number\ of\ uncongested\ crashes}{MH_{\geq 45}} \quad (4)$$

$$Congested\ crash\ rate = \frac{Number\ of\ congested\ crashes}{MH_{<45}} \quad (5)$$

The impact of congestion on safety is demonstrated in Figure 17, which are plots of congested and uncongested crash rates by interstate for 2014 and 2015. Note that the units for the y-axis are crashes per 100 mile-hours. The uncongested crash rates are barely visible compared to the congested crash rates in these plots.

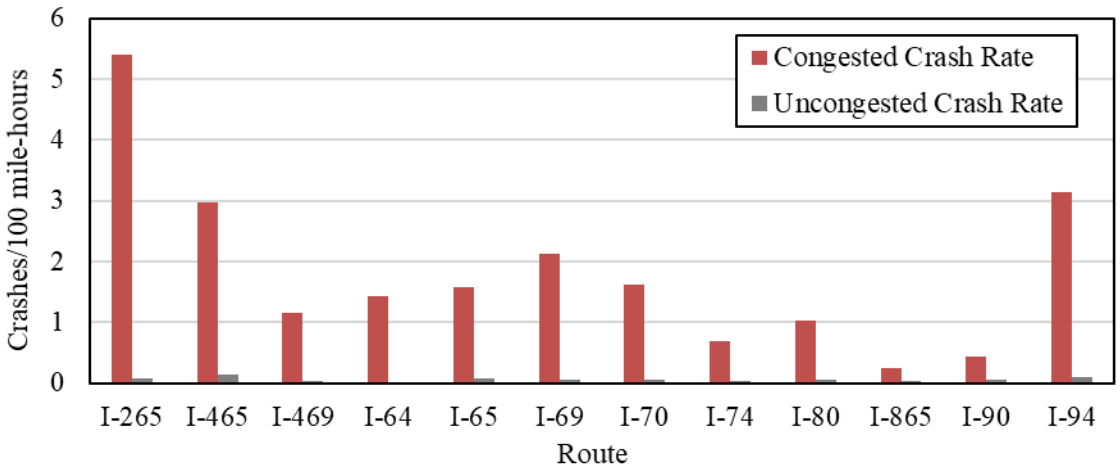

(a) 2014

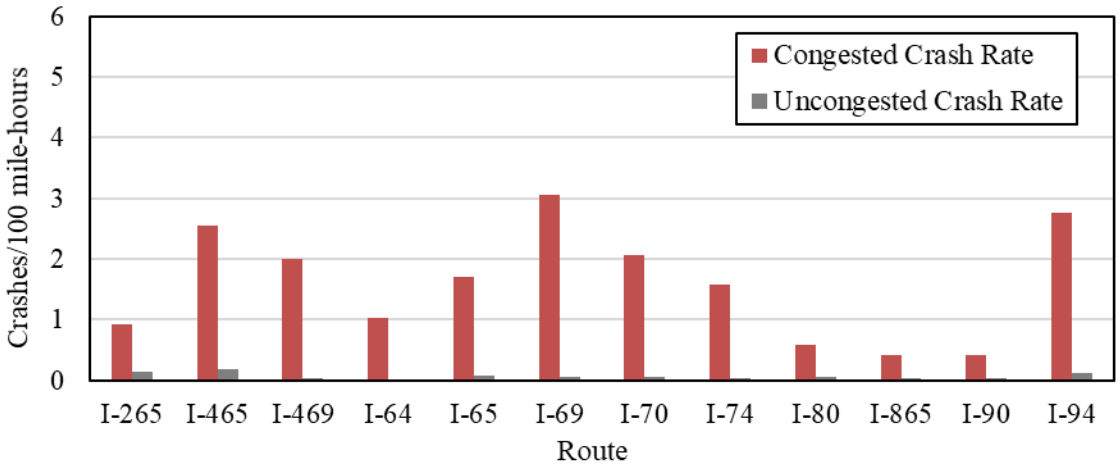

(b) 2015

Figure 17 Congested and uncongested crash rates by interstate

The ratios between the uncongested and congested crash rates are significant. The crash rate ratio is defined as the congested crash rate divided by the uncongested crash rate. Figure 18 shows the crash rate ratios for each interstate in 2014 and 2015. Overall, the congested crash rate is 24.0 and 20.6 times greater than the uncongested crash rate (shown by the dashed lines) in 2014 and 2015, respectively.

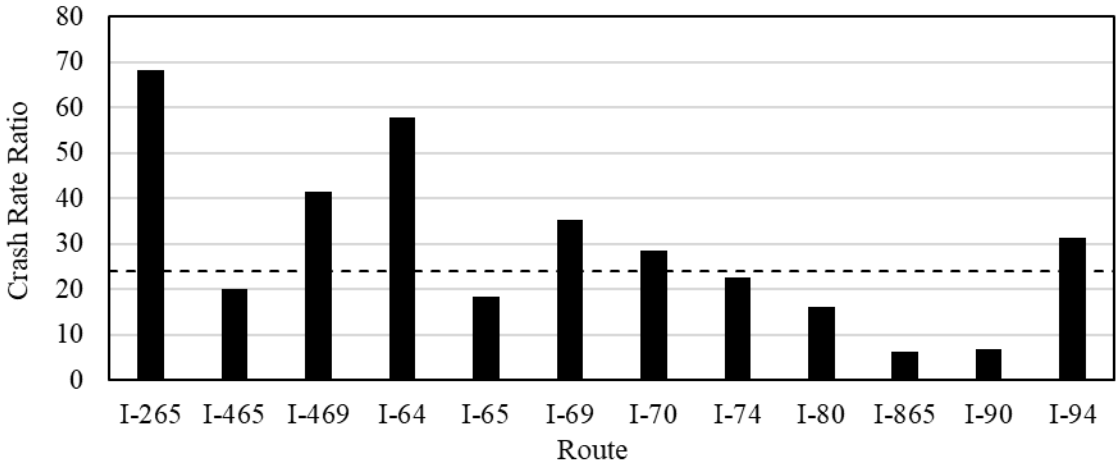

(a) 2014

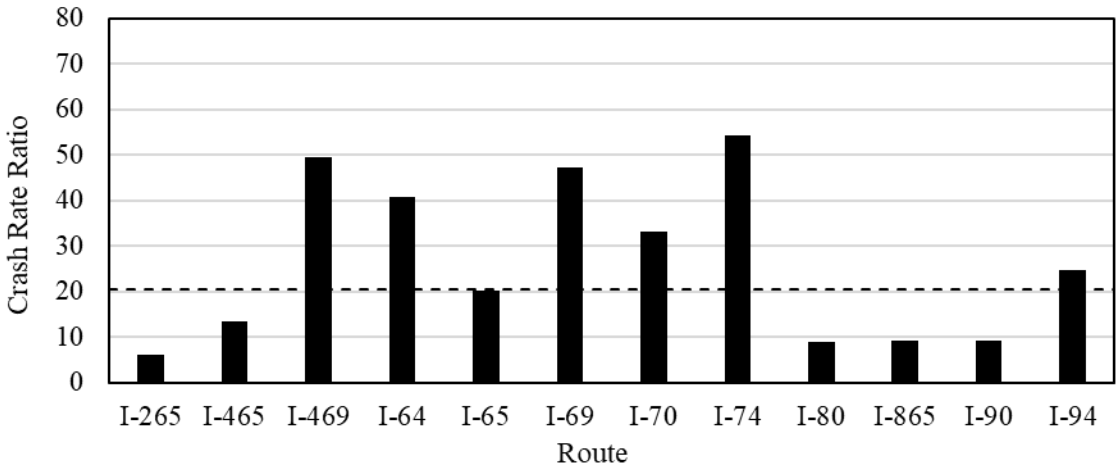

(b) 2015

Figure 18 Crash rate ratios by interstate

These findings are somewhat different from those of Potts et. al. [36] and Kononov et. al. [41], where the different crash rates were not found to be so drastically different. The measure of exposure used in this study, mile-hours of congestion, is different from the measures of exposure (vehicle-miles traveled and density) used by these researchers. However, the mile-hour measure of exposure is applicable in situations where connected vehicle data is available and volume data is not.

When the severity and involved vehicle types of these crashes are considered, another trend emerges. For property damage only (Figure 19a) and injury (Figure 19b) crashes, the percentage of crashes involving large trucks (FHWA vehicle class 6 and up)

are approximately the same between uncongested and congested crashes. However, the percentage of fatal congested crashes involving trucks is significantly higher than the percentage of fatal uncongested crashes involving trucks (Figure 19c). For nearly half of fatal congested crashes, a truck is at-fault. Therefore, a sizable portion of fatal congested crashes could possibly be prevented if truck drivers received advanced warning of congestion.

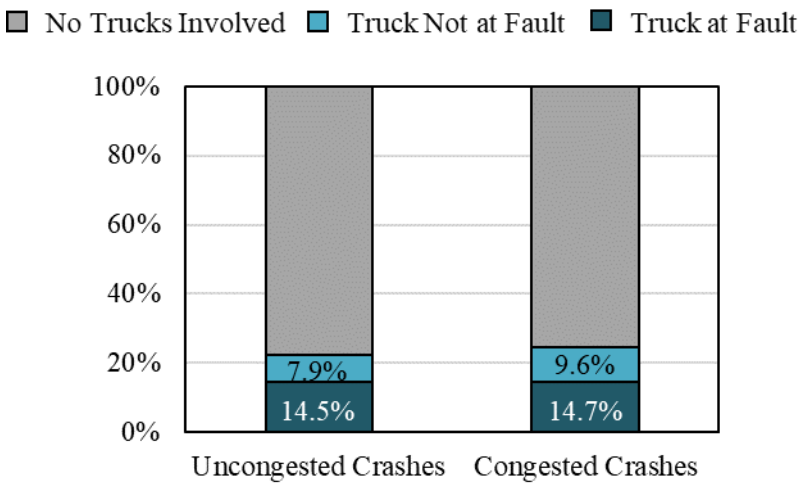

(a) Property damage only crashes

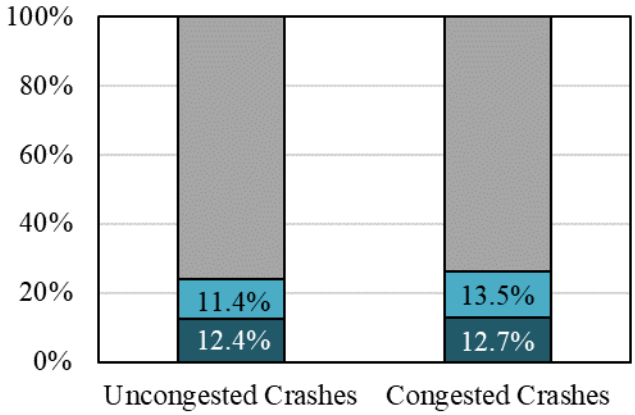

(b) Personal injury crashes

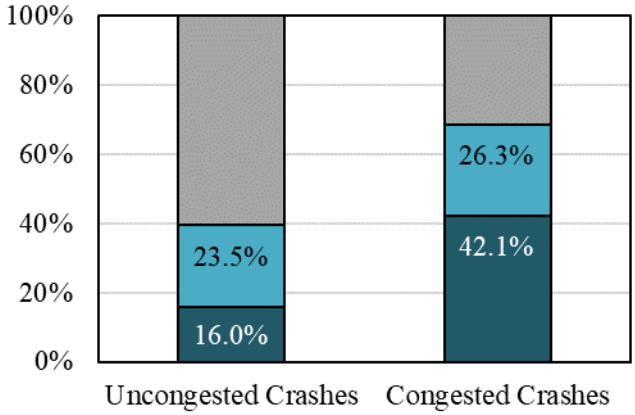

(c) Fatal crashes

Figure 19 Percent of crashes that involved commercial vehicles, 2014-2015

The duration of the congestion prior to each crash was considered. Figure 20 is a cumulative frequency diagram of queue duration for all crashes, congested crashes not involving trucks, and congested crashes involving trucks. Of 30,159 crashes in 2014-2015, 18.5% had congestion visible in the connected vehicle data at least 1 minute prior to the occurrence of the crash. Ten percent of all crashes had congestion visible at least 33 minutes prior to the crash. Of the congested crashes not involving trucks, 36.3% had congestion visible at least 1 hour prior to the crash. For congested crashes involving trucks, 44.3% had congestion at least 1 hour prior to the crash. This suggests some crashes could feasibly be prevented with advanced warning to truck drivers.

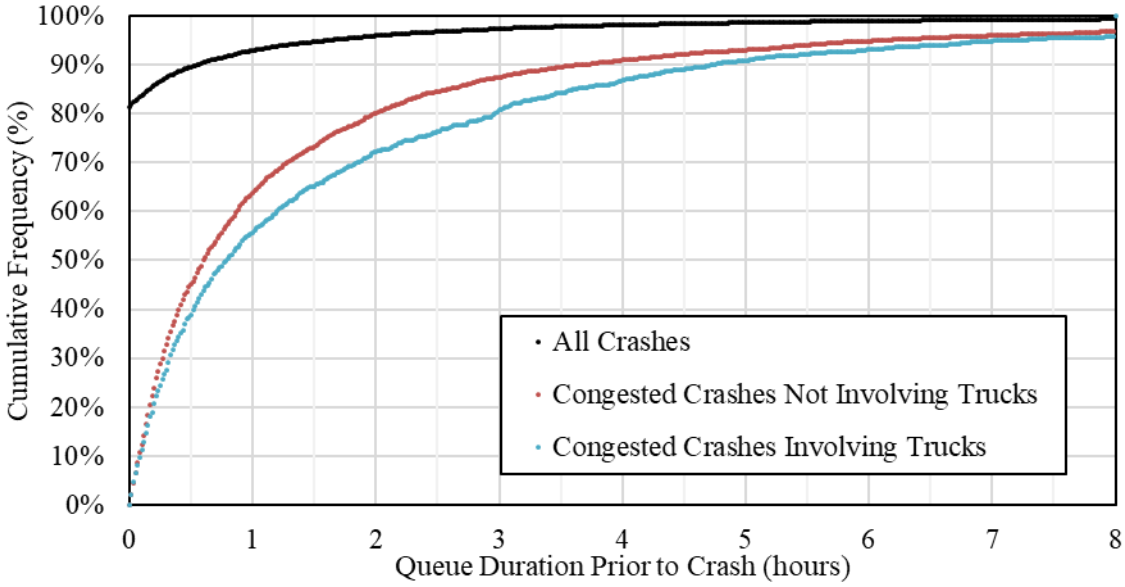

Figure 20 Duration of queue in connected vehicle data prior to all crashes, 2014-2015

4.4 Contribution

This study demonstrates the importance of opportunities for the reduction of queueing. Crash data were associated to determine that the crash rate increased by 24.0 and 20.6 times in 2014 and 2015, respectively, when interstates in Indiana were congested. Of all interstate crashes in two years, 18.5% had congestion visible in the connected vehicle at least one minute prior to the occurrence of the crash. There is a clear opportunity to reduce interstate crashes and improve safety by mitigating congestion and alerting drivers.

5. QUEUE ALERTS

It is not uncommon for queueing to occur in advance of a work zone, which presents the risk of back-of-queue crashes. This chapter discusses a system developed for INDOT to provide alerts to stakeholders, such as public safety and traffic management personnel, in a manner that does not require constant monitoring of data, extensive physical infrastructure, or the deployment of personnel to the field. Figure 21 shows an example of a queue alert sent as an email and viewed on a smartphone.

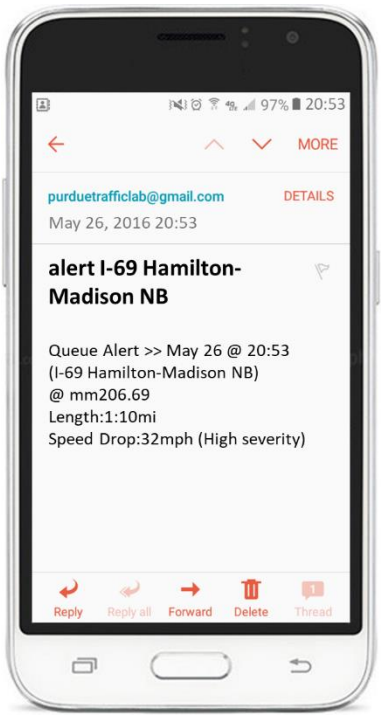

Figure 21 Sample queue alert email viewed on a smartphone

5.1 Overview

Figure 22 provides a basic overview of the inputs, outputs, and potential users of the queue alert system in Indiana. The system utilizes the real-time connected vehicle data for locating queues within pre-defined work zones. Notification thresholds define what conditions warrant an alert. The queue alert algorithm takes these inputs and

generates two products: an alert sent to stakeholders via email or text and an online dashboard where stakeholders can view the progression of queues over time.

Archived connected vehicle speed data crossed-referenced with construction contracts were utilized to develop a heuristic for the alert distribution process. Behaviors of past queues were used to fine tune the parameters in the heuristic for real-time implementation. Initially, the alert system was deployed to a small subset of in-house users for tuning.

Six classifications of alert types were developed to correspond to different queueing behaviors, as detailed in Table 3. The initial “Queue Alert” is sent when a queue initially forms. “Queue Expanding,” “Queue Shifting,” and “Queue Intensifying” are sent whenever the severity of the queue increases. The “Check-in” alert is sent in the case of a stable queue so that users are reminded that the queue is still there. Lastly, the “Queue Cleared” alert is sent after the queue has disappeared from the data.

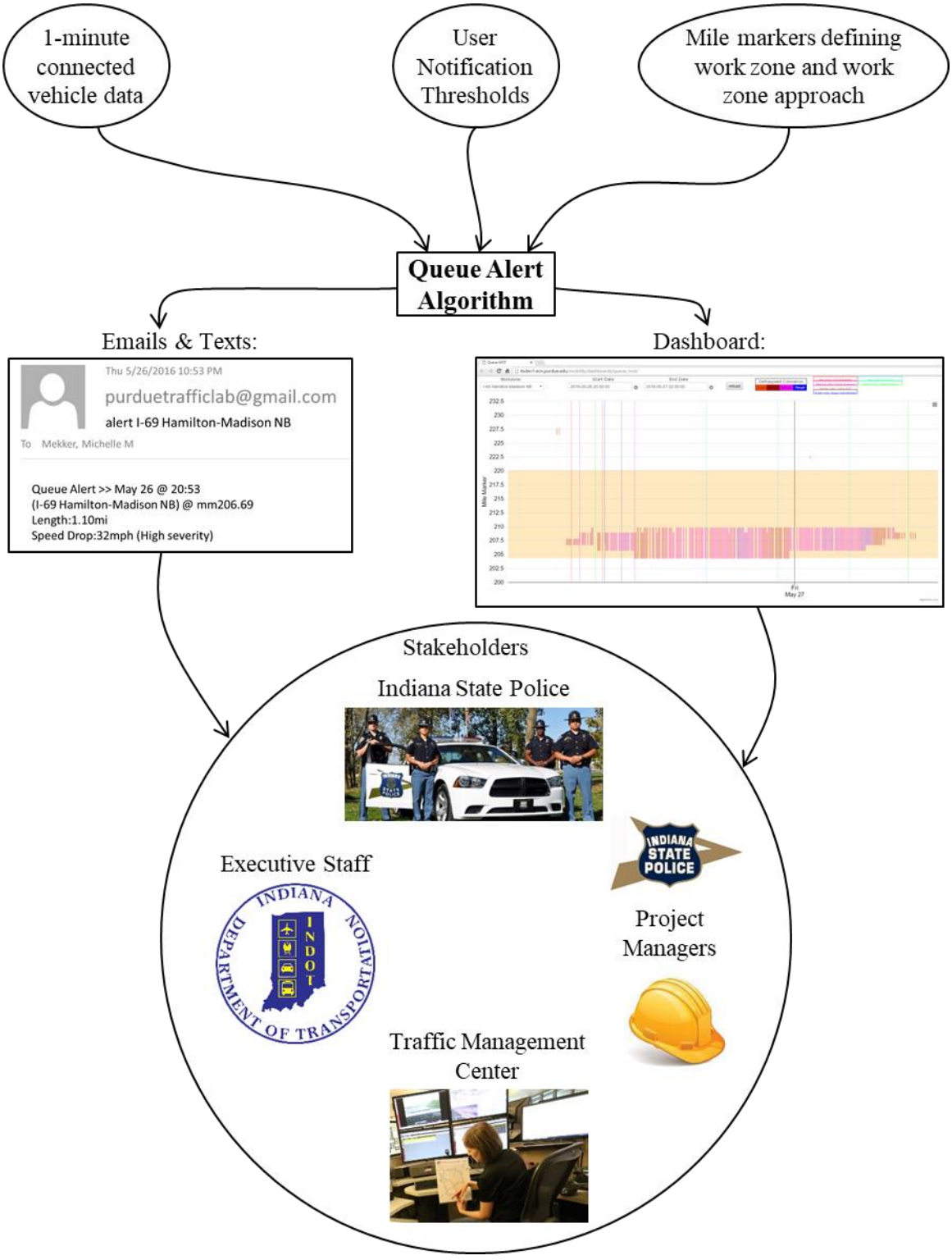

Figure 22 Queue alert information flow diagram

Table 3 Types of Alerts and Corresponding Queue Behavior

Alert Type	**Description of Queue Behavior**
Queue Alert	Queue has formed
Queue Expanding	Length of queue has increased
Queue Shifting	Back of the queue has shifted further upstream
Queue Intensifying	Speed drop at the back of the queue has increased
Check-in	Queue still exists but has not expanded, shifted, or intensified
Queue Cleared	Queue has dissipated

5.2 Selected Work Zones

After the initial development and tuning of the queue alert system, it was deployed for small scale beta-testing within INDOT. To filter the queue alerts geographically, groups of segments that are of interest, such as work zone areas, can be defined to only report queues occurring on those segments. Four stationary work zones were chosen as test beds for the service (Figure 23). Alerts were only generated for queues that occurred in the coverage area (Table 4) of one of the work zones.

Figure 23 Map of selected work zones for testing of queue alert system

Table 4 Overview of Selected Work Zones

Label	Route	Work Zone Location (Mile Posts)	Queue Alert System Coverage (Mile Posts)
C2	I-65	167-176	157-186
C4	I-70	6.8-8.7	0-18.7
G5	I-69	205-220	200-230
S2	I-65	8-16.5	2.5-26.5

5.3 Algorithm

Figure 24 shows the structure of the database used for the queue alert system. Each table includes the variables (units, if applicable), variable types, and example values. In “Workzones”, each work zone is defined by a series of connected vehicle data segments with unique IDs (*segid*) that are in the work zone (*is_workzone* = 1) or in the coverage area around the work zone (*is_workzone* = 0). Each work zone is given a name (*workzone_name*), start date (*startdate*), and end date (*enddate*). “Workzones” is connected to “Paths” via matching *segid*s. “Path” relates each segment on a road (*roadname*) to its relative position on the road. For example, segment 4320677 is the 208th segment on I-65 N when traveling north from mile post 0. This allows the queue alert system to identify adjacent segments. By matching *segid*s, the starting mile posts (*startmp*) and ending mile posts (*endmp*) of the segments and work zones are known.

In real time, “Speeds” is populated with an average speed (*speed*) for the current minute (*tstamp*) for every *segid*. Contiguous congested segments are grouped together as a single queue in “Queues” by associating “Speeds,” “MilePosts,” and “Paths”. Each queue in this table has an associated timestamp (*tstamp*), *roadname*, INDOT District (*district*), starting mile post (*qstartmp*), ending mile post (*qendmp*), *length*, *speeddelta*, and *threshold*. The *speeddelta* is the magnitude of the decrease in speed at the back of the queue. The *threshold* is the congestion threshold used to define the contiguous congested segments: 45 MPH, 35 MPH, 25 MPH, 15 MPH, or 5 MPH. To filter the queue alerts geographically, the “Workzones” and “Queues” tables are used in conjunction so that only queues occurring in the work zones of interest are reported.

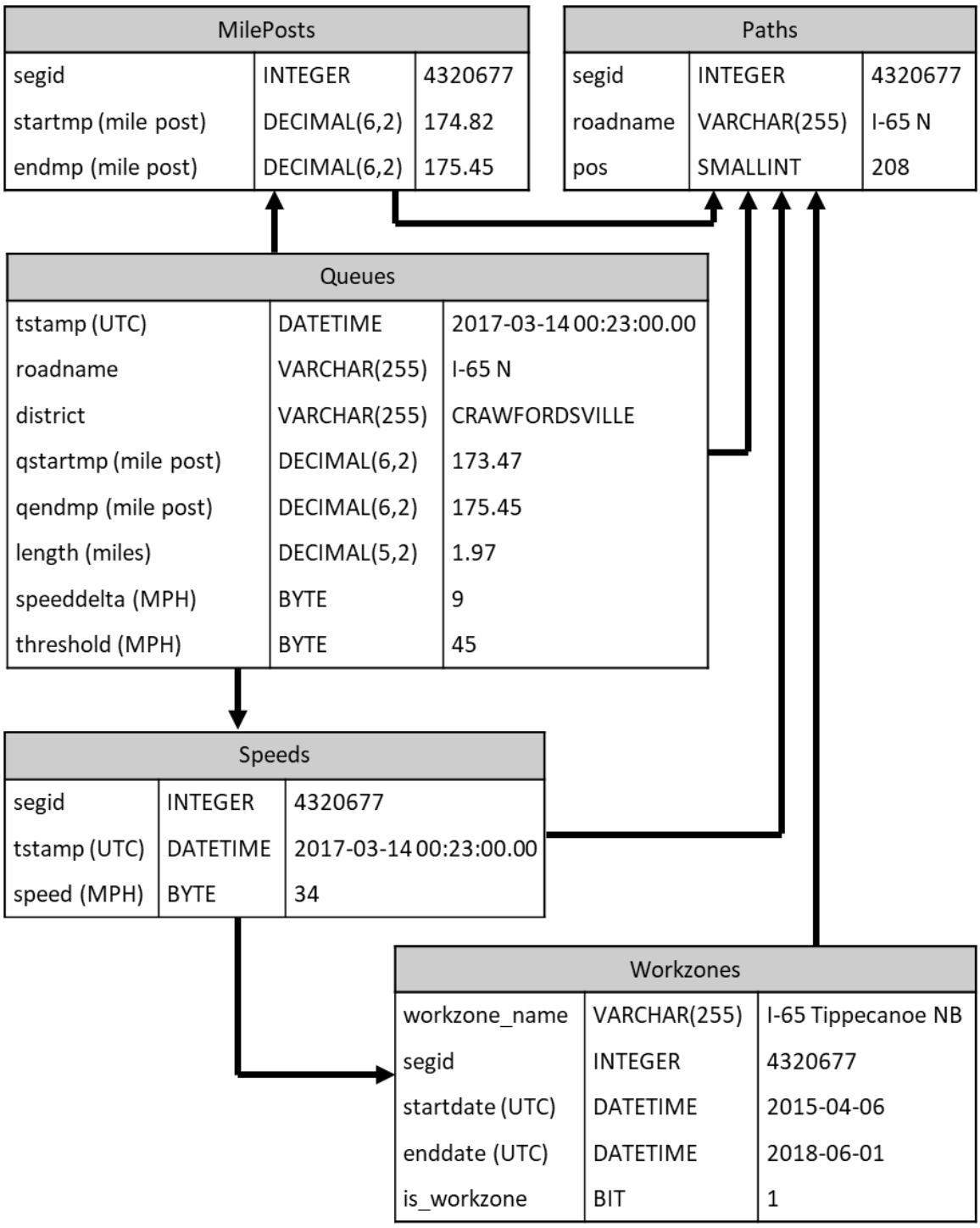

Figure 24 Database model for queue alert system

Using this database structure, additional logic is employed to track changes in queues spatially and temporally (Figure 25). Only queues with a *threshold* matching the selected congestion threshold (45 MPH) and that overlap a selected work zone are considered. Queue persistence over time is addressed by mapping new queues to existing queues that have occurred over an overlapping spatial boundary and within a pre-defined time window. This logic allows queue properties, such as duration, *length*, back-of-queue shockwave location, and *speeddelta* to be tracked over time. A non-alerting period is maintained to filter data anomalies. This feature requires any new queue to persist for a certain amount of time before an initial alert is sent to limit the amount data noise and increase confidence in the alert. Data noise can be due to occasional stopped vehicles reporting low speeds that do not interfere with the flow of traffic or sporadic blips within segments that are adjacent to queue boundaries. The goal of the non-alerting period is to prevent user-desensitization and to build user confidence in the reporting system. Queues that persist over long periods of time and the eventual moment of queue clearance triggers additional alerts to update and close out the status of the queues.

The conditions for the six different classifications of alerts are detailed in Figure 25. The initial "Queue Alert" is sent after three conditions are met: the non-alerting period is overcome (default = 4 out of 5 minutes), the *length* exceeds a specified magnitude (default = 1 mile), and the *speeddelta* exceeds a specified magnitude (default = 15 MPH). No other alerts can be sent for a queue before the initial "Queue Alert" is sent. "Queue Shifting" is sent when the back-of-queue shockwave (*qstartmp*) shifts further upstream by a specified distance (default = 1 mile). "Queue Expanding" is sent when the queue *length* increases by more than a specified magnitude (default = 1 mile). "Queue Intensifying" is sent when the *speeddelta*, or the change in speed at the back-of-queue shockwave, increases by a specified amount (default = 10 MPH). The "Check-in" alert is sent in the case of a stable queue that has not had any update alerts ("Queue Shifting", "Queue Expanding", or "Queue Intensifying") within a specified amount of time (default = 60 minutes). Lastly, the "Queue Cleared" alert is sent after the queue has disappeared from the data for a specified amount of time (default = 10 minutes). Each queue in the current minute is run through this algorithm, which runs every minute.

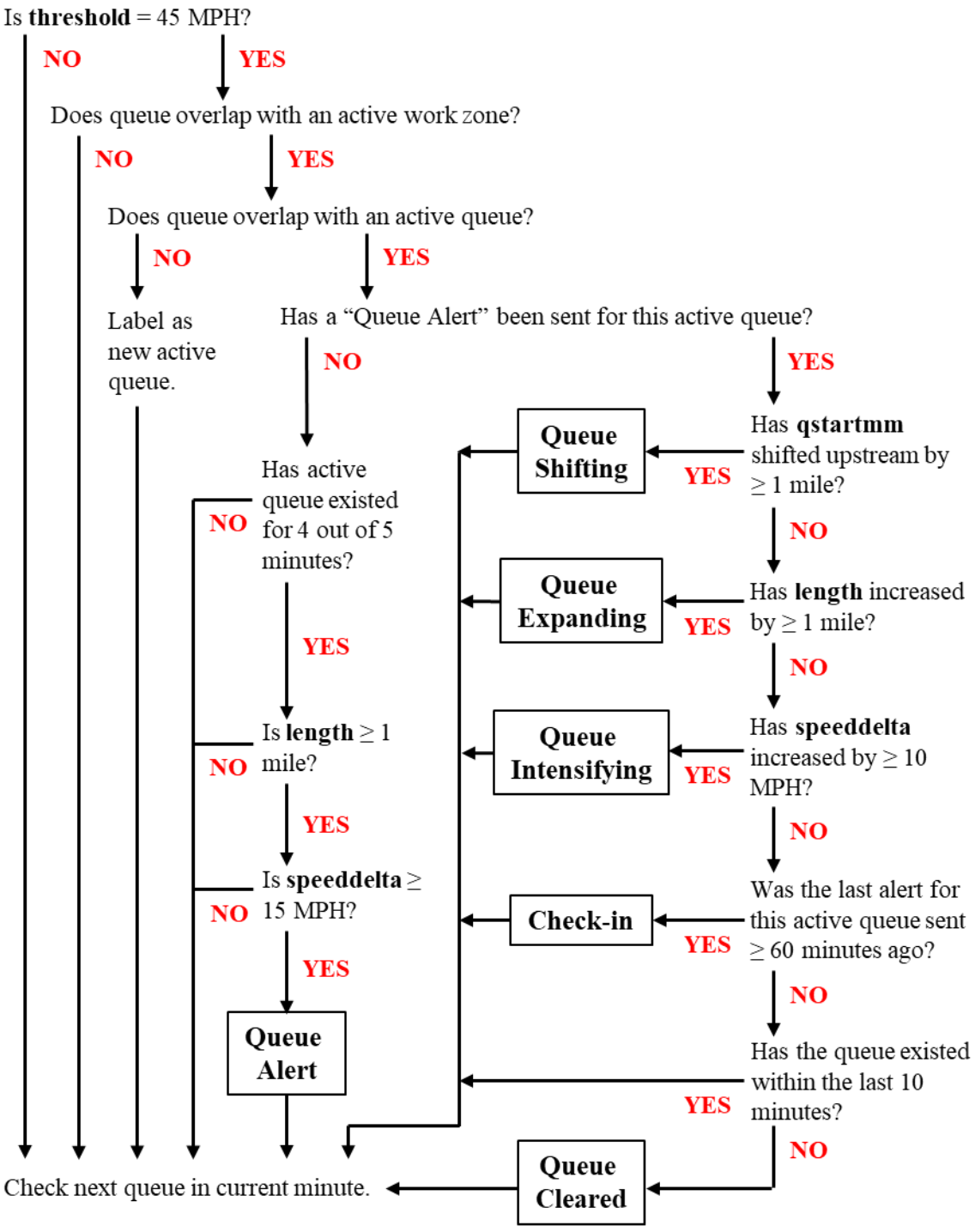

Figure 25 Queue alert logic tree

5.4 Validation

Alerts were distributed via either SMS messages or emails, as chosen by each individual user, for May through June of 2016. Users could choose any combination of the work zones for which they wished to receive alerts. Figure 26a shows a plot of the number of unique alerts that a single user would have been sent during the months of May and June if they were subscribed to all four work zones.

Figure 26b and Figure 26c show the number of alerts for each direction of the G5 work zone, I-69 N and I-69 S, respectively. This work zone has the most congestion of the four work zones due to its proximity to Indianapolis. On some days during this time period, a single direction could generate more than fifty alerts (see 5/4/16 and 5/6/16 for I-69 NB (Figure 26b) and 5/20/16 for I-69 SB (Figure 26c)). The work zone had recurring congestion from both commuter traffic and construction activities. The corridor typically experiences a high frequency of crashes and has extensive coverage by INDOT cameras. The existing infrastructure of deployed cameras made this corridor ideal for validating the queue alert system. The next two subsections will detail two queue case studies (callout ‘i’ and callout ‘ii’ in Figure 26b) from the G5 work zone on I-69 N. The alerts for these case studies were generated in real-time as the events occurred.

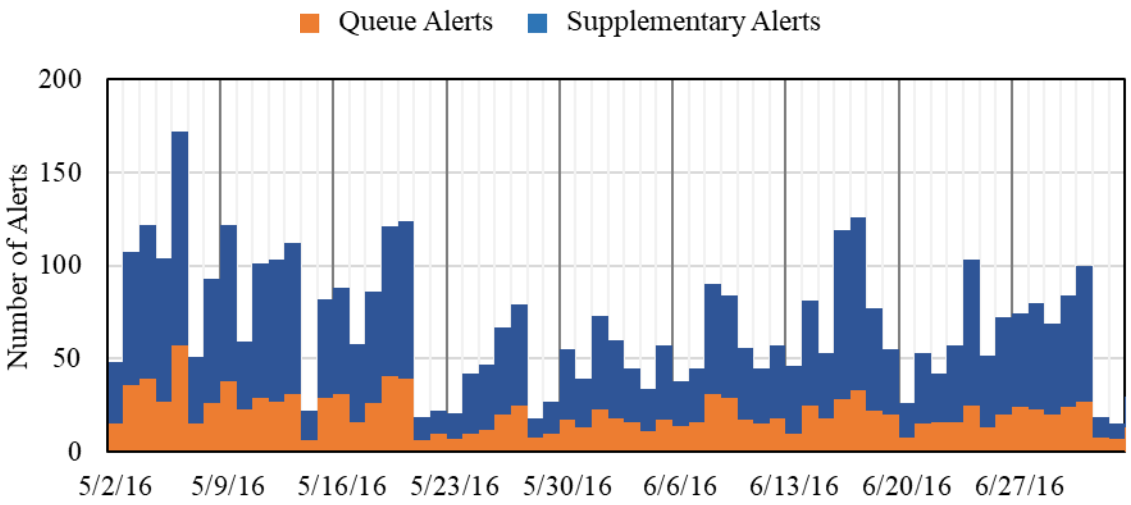

(a) Alerts for four work zones

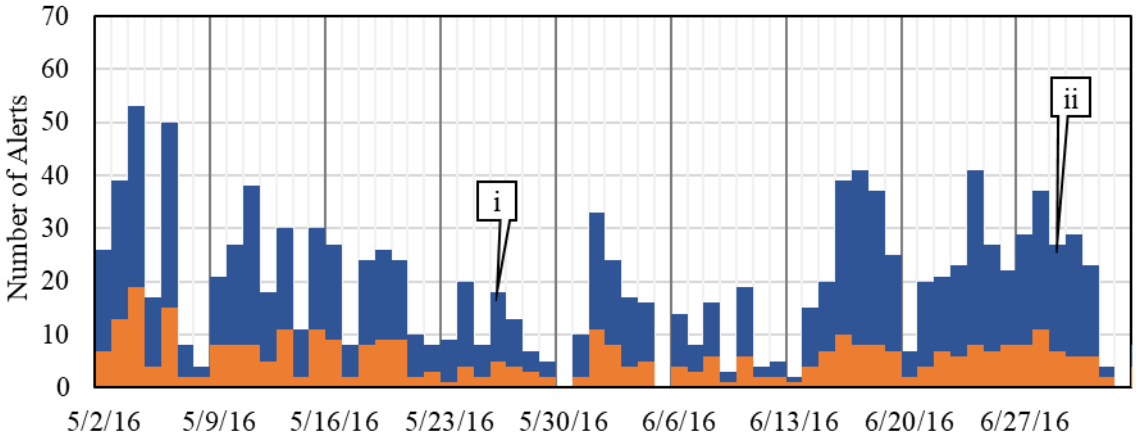

(b) Alerts for G5N work zone (I-69 N)

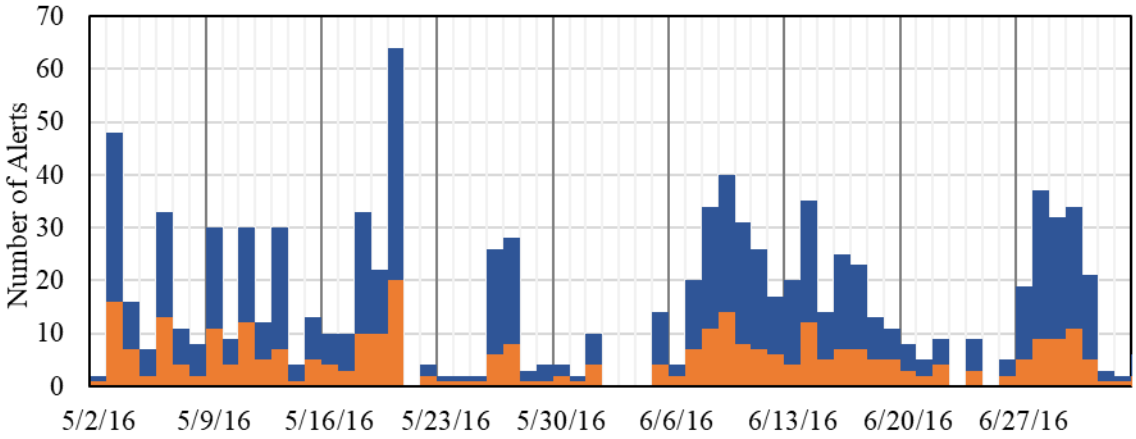

(c) Alerts for G5N work zone (I-69 S)

Figure 26 Number of unique alerts sent for May-June 2016

5.4.1 Case Study ‘i’

The first case study was a queue that formed at mile post 208 on I-69 N as a result of a scheduled lane closure on the evening of May 26, 2016. Figure 27a is a heat map of the queue throughout the evening. The heat map gives a qualitative view of the system over both space and time. Direction of travel is from the bottom of the graph to the top. The shorter vertical lines represent the location and severity of the queue. The darker color gradations represent higher magnitude *speeddeltas* at the back of the queue, as noted in the legend of Figure 27a. The long vertical lines that span the entire height of the graph (callout ‘d’ in Figure 27a) represent individual alerts and correlate to the alert times and types described in the previous section. The horizontal bar of orange shading (callout ‘e’ in Figure 27a) represents the location of the work zone. These graphs were integral for the validation process and were used to retroactively assess a queueing incident. Callouts ‘a’, ‘b’, and ‘c’ in Figure 27b correspond to nearby camera locations and match up with callouts ‘a’, ‘b’, and ‘c’ in Figure 27a.

The queue first appeared in the data at 20:50. However, following the rules of the algorithm, the initial “Queue Alert” was not sent until the queue had existed for at least 4 out of 5 minutes. The “Queue Alert” was sent at 20:53 (callout ‘a’ in Figure 27a) and the email is shown in Figure 21. The message was short and simple, giving only the critical information regarding the queue.

Using INDOT traffic cameras, the cause and progression of the queue over time was observed and compared to the data. Figure 28a, Figure 28b, and Figure 28c correspond to the callouts of the same letter in Figure 27. Figure 28a shows an image of the front of the queue when the initial alert (callout ‘a’ in Figure 27) was first sent out. The queue can be seen in the northbound travel lanes on the right (callout ‘I’ in Figure 28a). Also visible in the photo is an arrow board and workers on the shoulder preparing to close the right lane (callout ‘ii’ in Figure 28a). Vehicles had already begun to shift into the left lane and slow down. Brake lights can be observed on many of the vehicles in the queue in the image.

At the same location four minutes later (callout ‘b’ in Figure 27), drums had been staged along the right shoulder (callout ‘iii’ in Figure 28b). The speed drop at the back of

the queue is approximately 45 MPH at this point in time. Figure 28c is a photo from a camera located in the middle of the queue at 21:19 (callout ‘c’ in Figure 27). Vehicles can be seen occupying both lanes with very small headways. The queue extends out of view of the camera and further upstream. In total, 11 alerts were sent for this single queue, which endured for over four and a half hours.

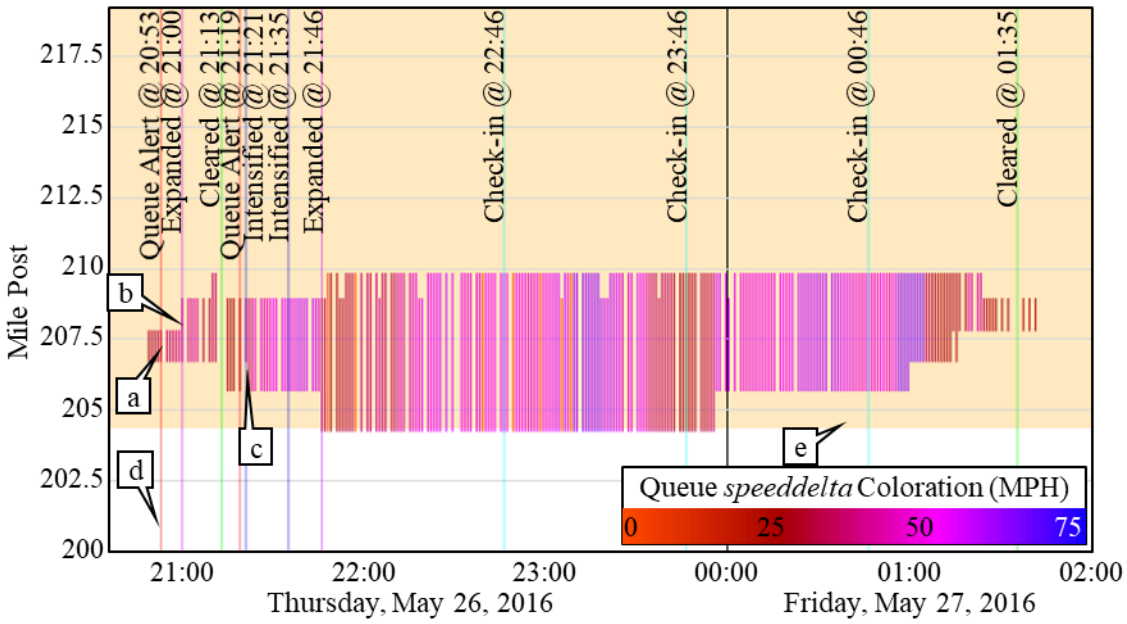

(a) Queue heat map

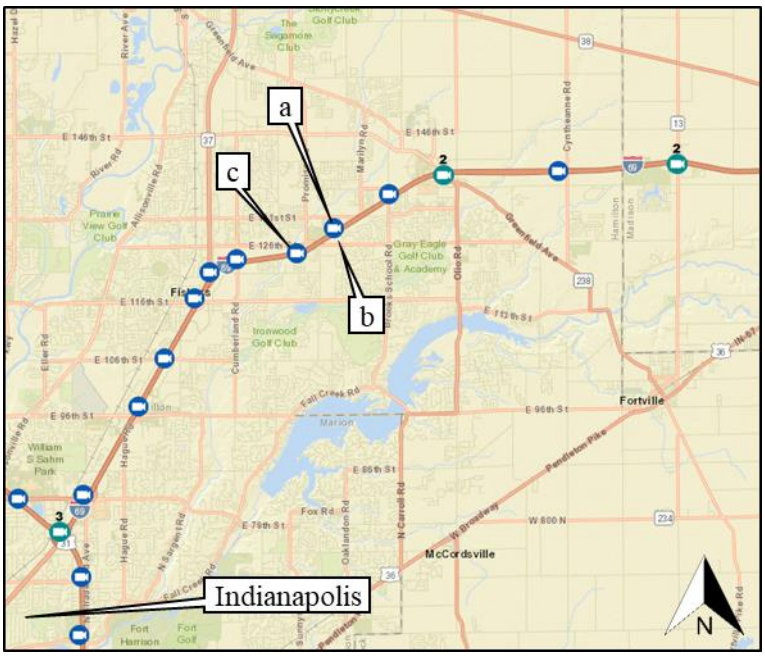

(b) Map of camera locations on I-69

Figure 27 Case study of a WZ queue on I-69 N at mile post 208 on May 26, 2016

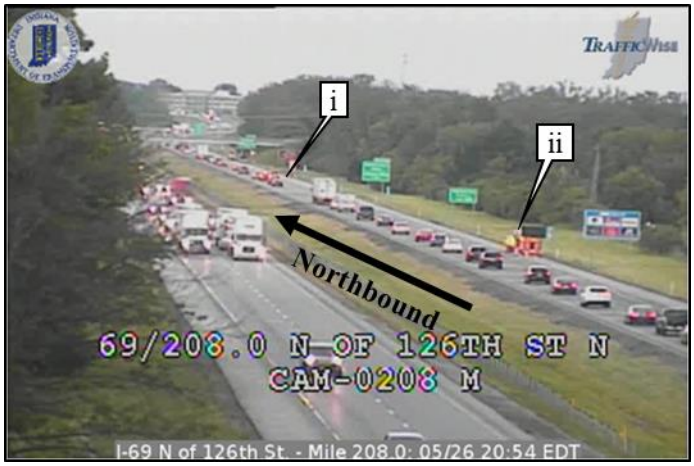

(a) Mile post 208.0 at 20:54

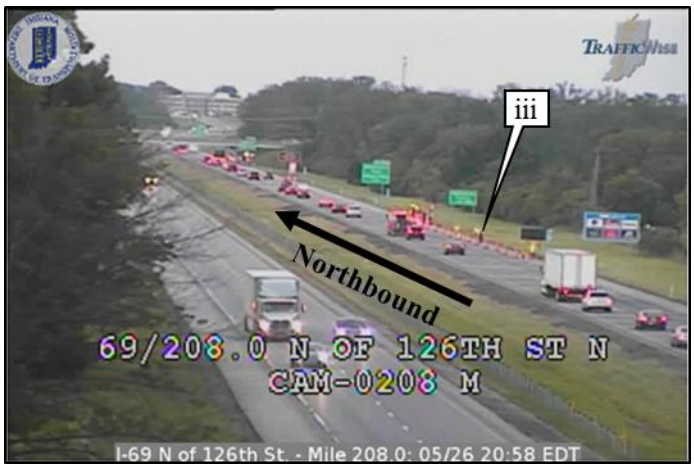

(b) Mile post 208.0 at 20:58

(c) Mile post 207.2 at 21:19

Figure 28 Camera views corresponding to callouts ‘a’, ‘b’, and ‘c’ in Figure 27

5.4.2 Case Study ‘ii’

The queue in this case study (Figure 29) occurred on June 29, 2016 at mile post 212.3 of I-69 NB. This example is based upon queueing associated with a crash. In Figure 29a, direction of travel is from the bottom of the graph to the top. Figure 29b shows the location of cameras and callouts from Figure 29a.

Figure 30 shows camera views of the crash location and corresponding queue. Figure 30a, Figure 30b, and Figure 30c correspond to the callouts in Figure 29. Two vehicles can be seen on the shoulders of the I-69 N lanes shortly after the crash occurs (callout ‘i’ in Figure 30a). After only a few minutes, the queue was already about 2 miles long and an initial queue alert was sent (callout ‘ii’ in Figure 30b). Over time, the queue oscillated and there were various backward-forming and backward-recovery shockwaves. Nearly an hour and a half after the crash occurred, tow trucks arrived on scene to extract the damaged vehicles (callout ‘iii’ in Figure 30c). Approximately a half hour later, the crash scene was cleared but it took another half hour for the queue to fully dissipate.

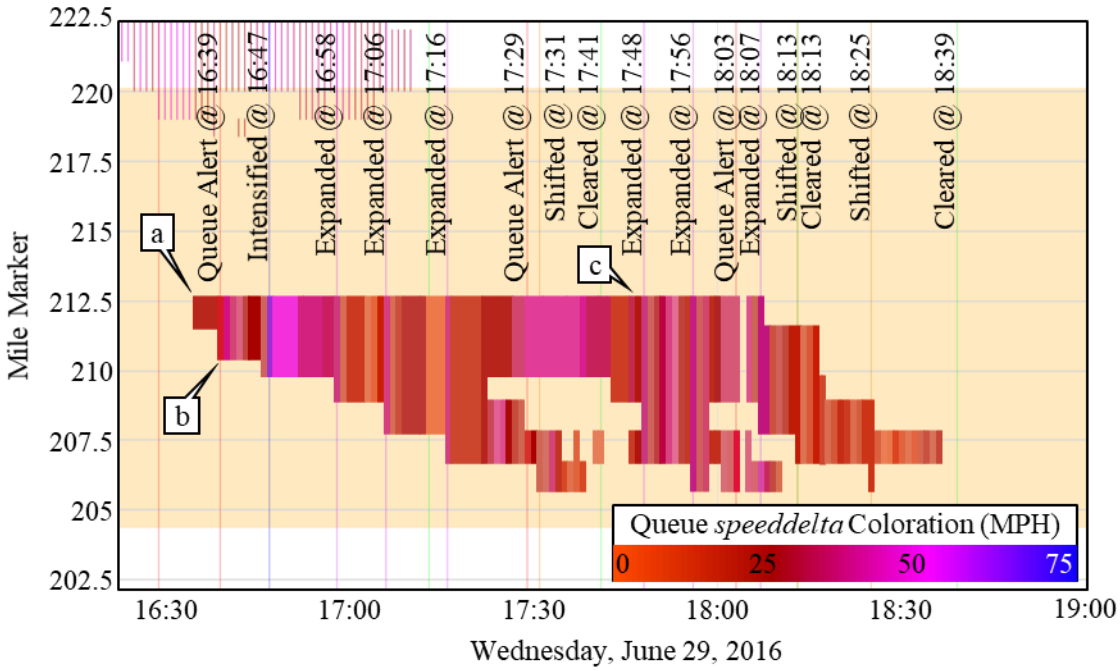

(a) Queue heat map

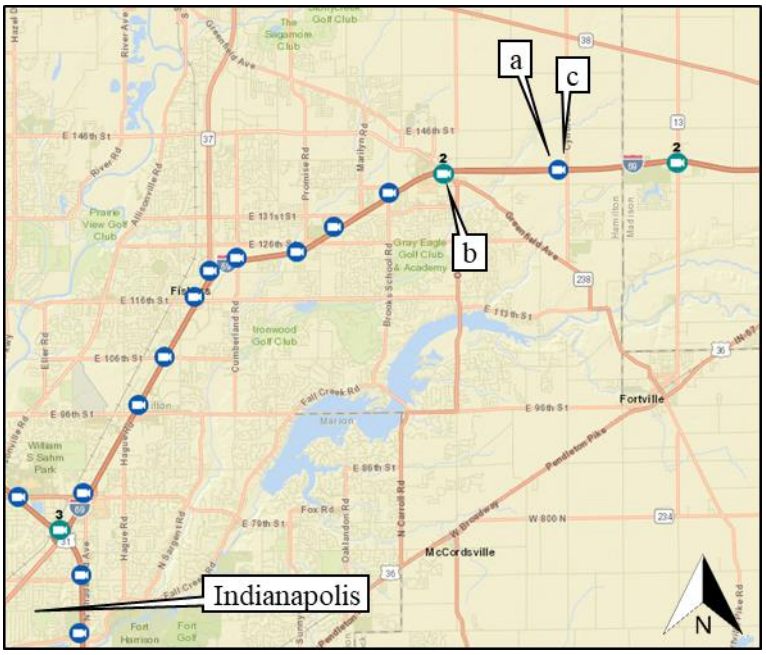

(b) Map of camera locations on I-69

Figure 29 Case study of a crash queue on I-69 N at mile post 212.3 on June 29, 2016

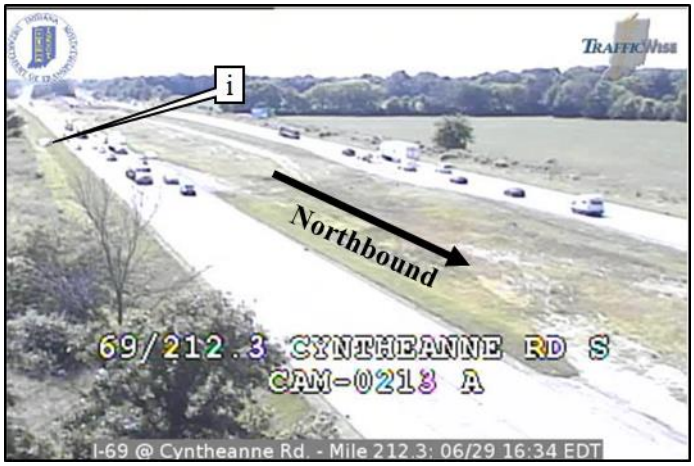

(a) Mile post 212.3 at 16:24

(b) Mile post 210.2 at 16:38

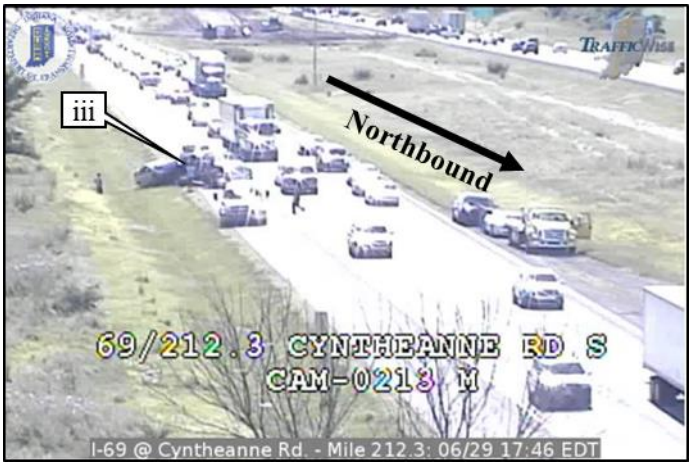

(c) Mile post 212.3 at 17:46

Figure 30 Camera views from callouts ‘a’, ‘b’, and ‘c’ in Figure 29

5.5 Contribution

This queue alert system could potentially be used to dynamically monitor and review work zone activities. For example, if a queue grows to unacceptable lengths or persists for a significant amount of time, officials and contractors could potentially change or halt activities within the work zone to mitigate the queue. It could also be especially useful in work zones where there is little to no coverage by existing infrastructure, such as cameras, or is too far away for officials to make frequent inspection trips.

As the system is now, the system can help officials locate and identify queues within work zones regardless of the cause of the queue. In the future, this service could potentially assist safety officials in locating crashes that have occurred outside of standard video coverage areas and prior to being called in by participants or passersby. Officials in the field would be able to monitor how clean-up activities are impacting traffic mobility and safety upstream of the crash.

This study has shown that it is feasible to deploy a system that sends targeted alerts that can potentially help public safety and traffic management personnel make more informed decisions during incidents. Extending this system to be integrated with vehicle telematics to provide direct in-vehicle notification is a feasible next step that could significantly reduce back of queue crashes.

6. WORK ZONE REPORT

Maintenance of traffic (MOT) plans implemented during construction may involve multiple stages depending on the schedule and scope of work activities. Ideally, traffic management personnel would monitor traffic and use the observed impacts to calibrate the queue models and/or make dynamic changes to the MOT plan as needed. However, with dozens of construction projects underway at any given time, monitoring work zones via regular in-person visits can consume significant manpower. Furthermore, work zones may have subtle changes on a near daily basis that can significantly impact work zone queueing. Active monitoring of all active work zones within an agency's jurisdiction may not be feasible. To assist INDOT in dynamic monitoring and assessment of interstate work zones, a weekly work zone report and web-based tools were developed, referred to as dashboards. A dashboard is a visual tool that allows the user to see the status of a system (or a part of a system) in a simple format, similar to how the dashboard of a car allows the driver to easily determine their speed and fuel level.

6.1 Overview

The work zone reports and associated dashboards have been in use by INDOT since May 2016. The reports and dashboards have undergone numerous iterations and improvements. This dissertation discusses the most current formats. Figure 31 shows the components of the report, which were compiled into a slide deck. The components are constructed using a mix of database queries, spreadsheet graphing, and automated online dashboards. There is potential to automate more of the components in the future. Each of the report components will be covered in detail in the following subsections.

In its current state, the work zone report is split into separate slide decks by INDOT district. Each slide deck begins with an overview slide (discussed in more detail below). Each work zone within the district has a set of 4 dedicated slides comprised of the different report components. Each report focuses on data from a single week, Monday to Monday.

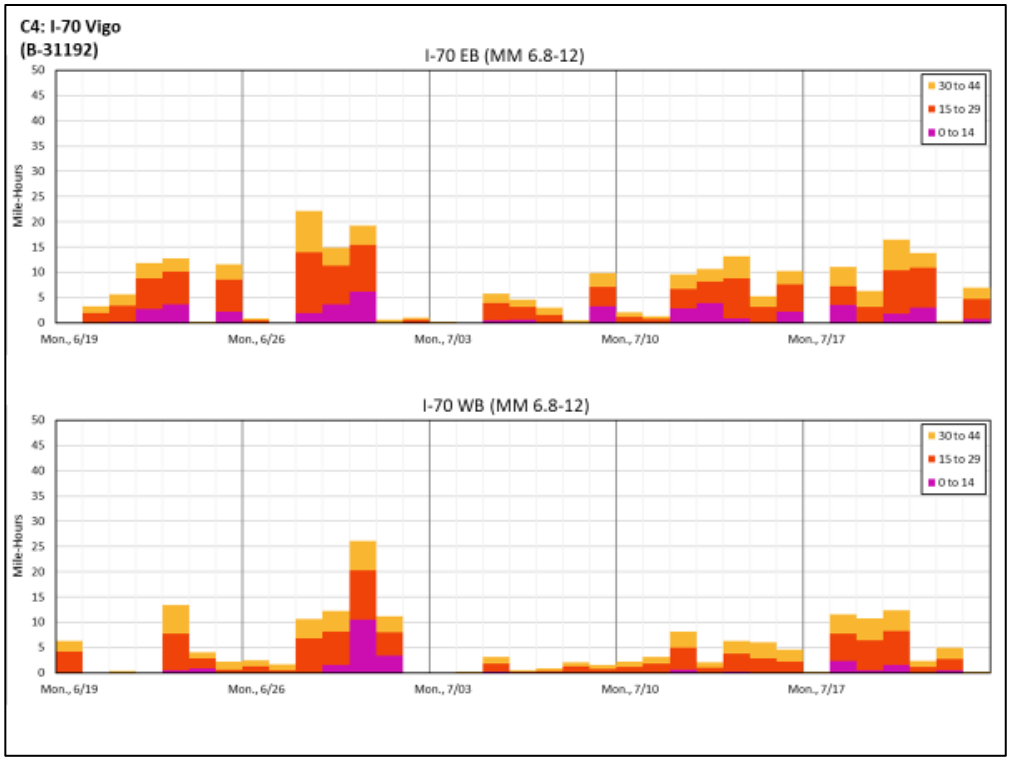

(a) Page 1

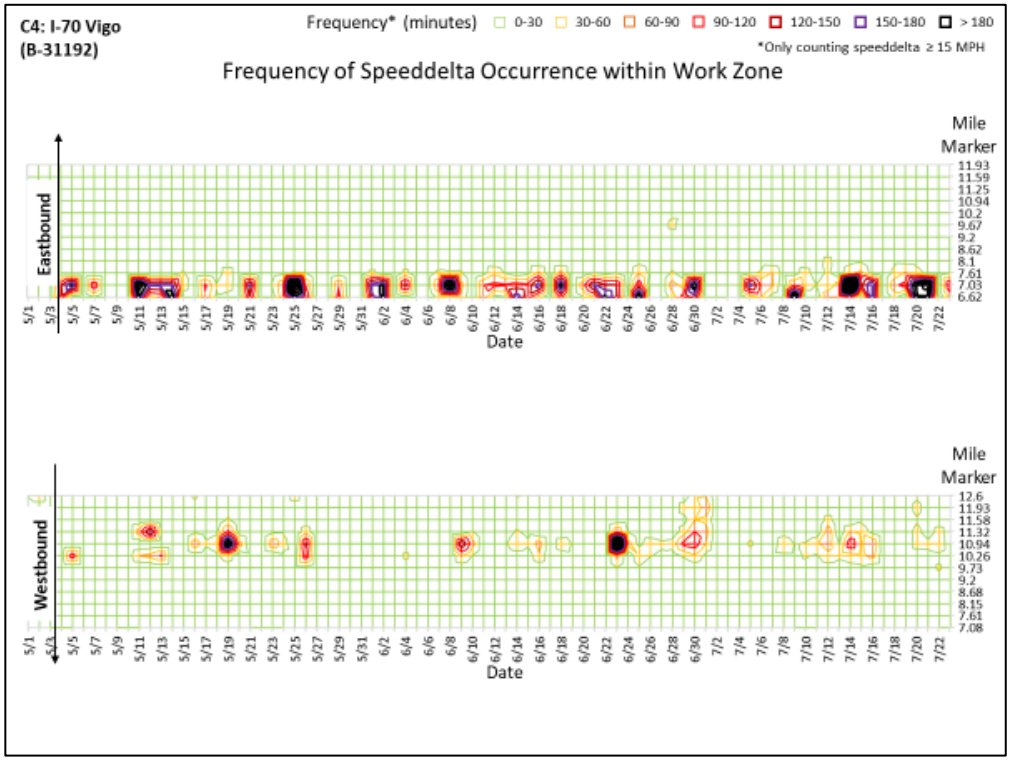

(b) Page 2

Figure 31 Work zone report sample

Figure 31 continued

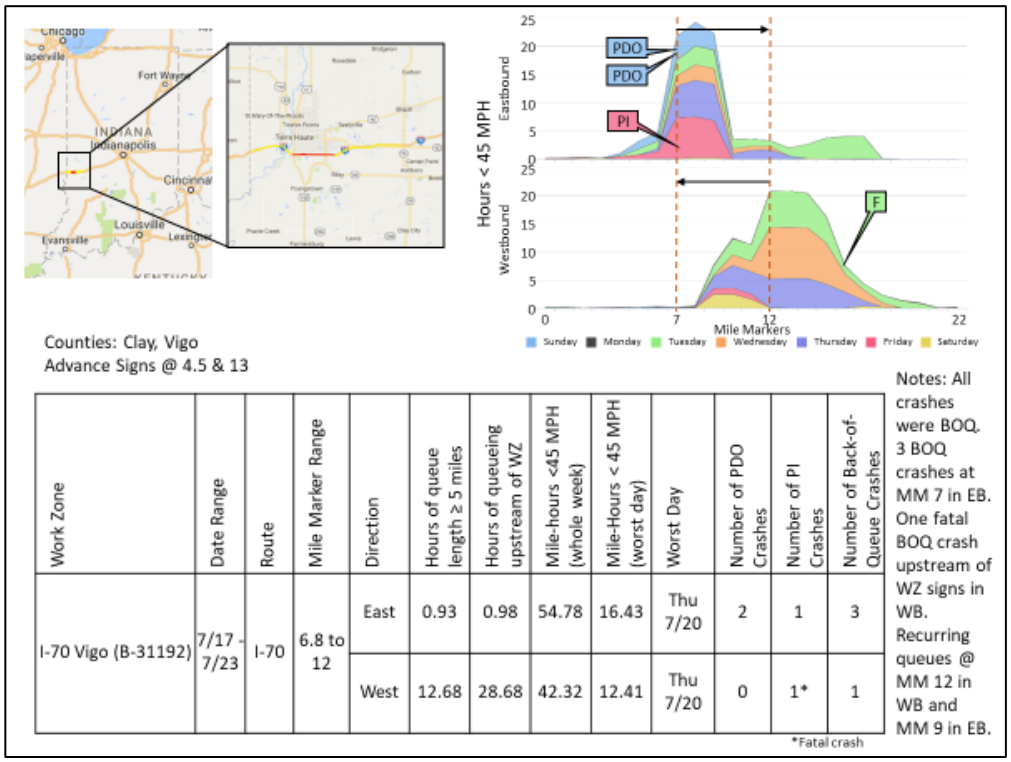

Counties: Clay, Vigo
Advance Signs @ 4.5 & 13

Work Zone	Date Range	Route	Mile Marker Range	Direction	Hours of queue length ≥ 5 miles	Hours of queueing upstream of WZ	Mile-hours <45 MPH (whole week)	Mile-Hours < 45 MPH (worst day)	Worst Day	Number of PDO Crashes	Number of PI Crashes	Number of Back-of-Queue Crashes
I-70 Vigo (B-31192)	7/17 - 7/23	I-70	6.8 to 12	East	0.93	0.98	54.78	16.43	Thu 7/20	2	1	3
				West	12.68	28.68	42.32	12.41	Thu 7/20	0	1*	1

*Fatal crash

Notes: All crashes were BOQ. 3 BOQ crashes at MM 7 in EB. One fatal BOQ crash upstream of WZ signs in WB. Recurring queues @ MM 12 in WB and MM 9 in EB.

(c) Page 3

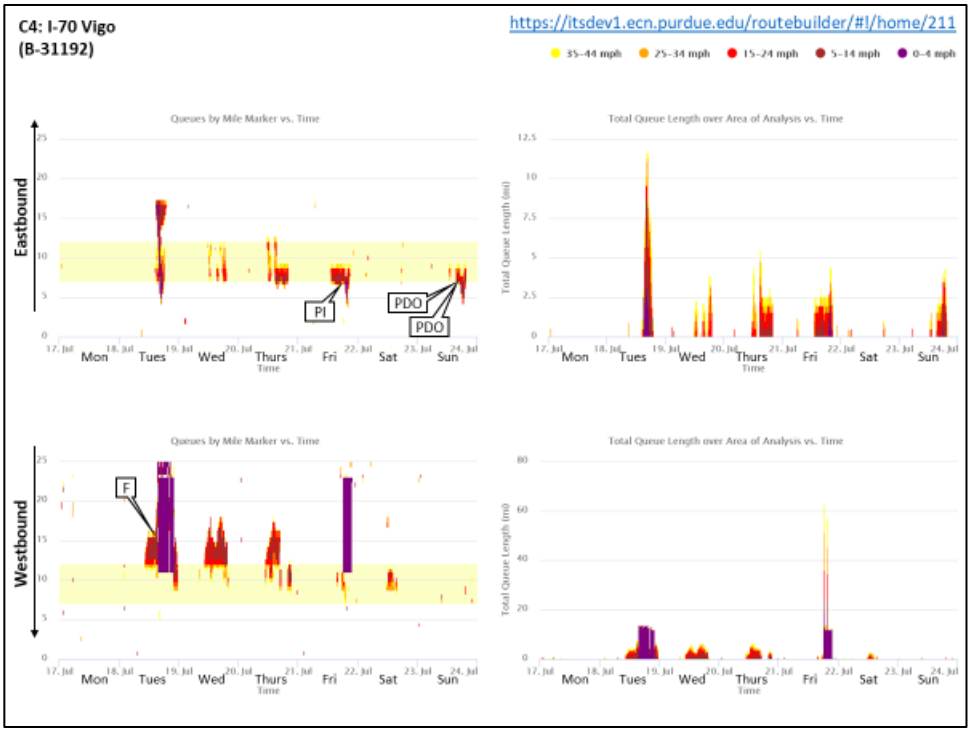

(d) Page 4

6.1.1 Mile-Hours of Congestions Plots

Figure 31a, the first page of the report for a work zone, includes two plots of mile-hours by day, one for each direction. Each column in the graph represents the total number of mile-hours of operation within each speed bin in one day within the work zone. It does not include the congestion that extends or occurs outside of the work zone. These plots allow personnel to view overall performance and quickly identify days or weeks that had more severe congestion. The 4 weeks prior to the current week are included in the plot to provide context and to show any emerging trends. The database query for this performance measure is provided in detail in Appendix A. This performance measure is typically displayed with a stacked column graph.

Also included in the work zone report is a summary of the total congestion observed the INDOT district (Figure 32). The top graph is the sum of all congestion in the work zones within that district. The middle plot has the same total values of congestion sorted by work zone instead of by speed bin. The final, bottom plot shows the total congestion on all interstate segments, work zone and non-work zone, within the district. This view is particularly useful for district managers. The impact of district- or region-wide events, such as weather or holidays, within work zones and the entire district can be observed. Patterns of congestion within the work zone that are also observed within the district can be more easily attributed to non-work zone factors.

Figure 32 District-wide view of mile-hours of congestion

6.1.2 Frequency of Speeddelta

Figure 31b, the second page of the report for a work zone, includes two heat maps of speeddelta frequency by day and longitudinal location. As described briefly in the previous chapter, the speeddelta is the magnitude of the change in speed at the back of the queue, or the difference between the average speeds of two adjacent segments. If vehicles are decelerating, the speeddelta will be positive (upstream speed minus downstream speed). In this plot, a threshold of speeddelta greater than or equal to 15 MPH is used so as to eliminate noise from minor changes in speed. The color scale corresponds to the duration of speeddelta ≥ 15 MPH each day. Due to the nature of the connected vehicle data segmentation, each horizontal line in the grid represents the point between two adjacent segments. The distance between these points are not to scale in these plots. In these heat maps, the darker colored spots represent locations where vehicles slowed down more frequently during that day. Horizontal dark bands typically represent recurring congestion at a particular point. Vertical dark bands typically

represent a single incident, such as a crash or weather event. The database query for this performance measure are provided in Appendix B. This performance measure is typically displayed with a wireframe contour plot.

6.1.3 Congestion Profile and Summary Table

At the top of Figure 31c, the third page of the report for a work zone, there is a map of the work zone location within Indiana. Next to this map are two congestion profiles for the work zone in the current week. The congestion profile was originally developed as part of the *Indiana Mobility Report* [71], [72], [73], [74] and can be generated via the "Congestion Profile" online dashboard [81] (Figure 33). These plots include both the work zone and up to 10 miles upstream and downstream of the work zone. The congestion profile shows the hours of congestion by mile post and by day. It is a useful longitudinal representation of congestion within and around the work zone. Significant traffic incidents with large queues are typically represented by a wide band of color corresponding to the day of the incident. Stacked bands of similar width typically represent recurring congestion at a particular location.

For use in the work zone report, the user must define the following inputs. First, the route and mile post range (called "Mile Marker" in the dashboard) must be selected. It is recommended that the user select a mile post range that includes 10 miles on either end of the work zone. For example, the C4 work zone on I-70 in Vigo County starts at mile post 6.8 and ends at mile post 12. In the "Congestion Profile" dashboard, the user would select the route as I-70 and a mile post range of 0 (because -3.2 is not a valid mile post) to 22. The user must then select the date range of interest. For the full report, one week, Monday to Monday, is selected, such as "2017-07-17 to 2017-07-23". The user must ensure that all days of the week and times of day are selected to ensure completeness. The user may select a congestion threshold if desired. The default threshold is 45 MPH. The user should leave the grouping as "Day of Week" for the report. The "Generate Graph" button must be clicked to update the graphs. The user may download the graph images using the hamburger menu icons to the top right of each graph.

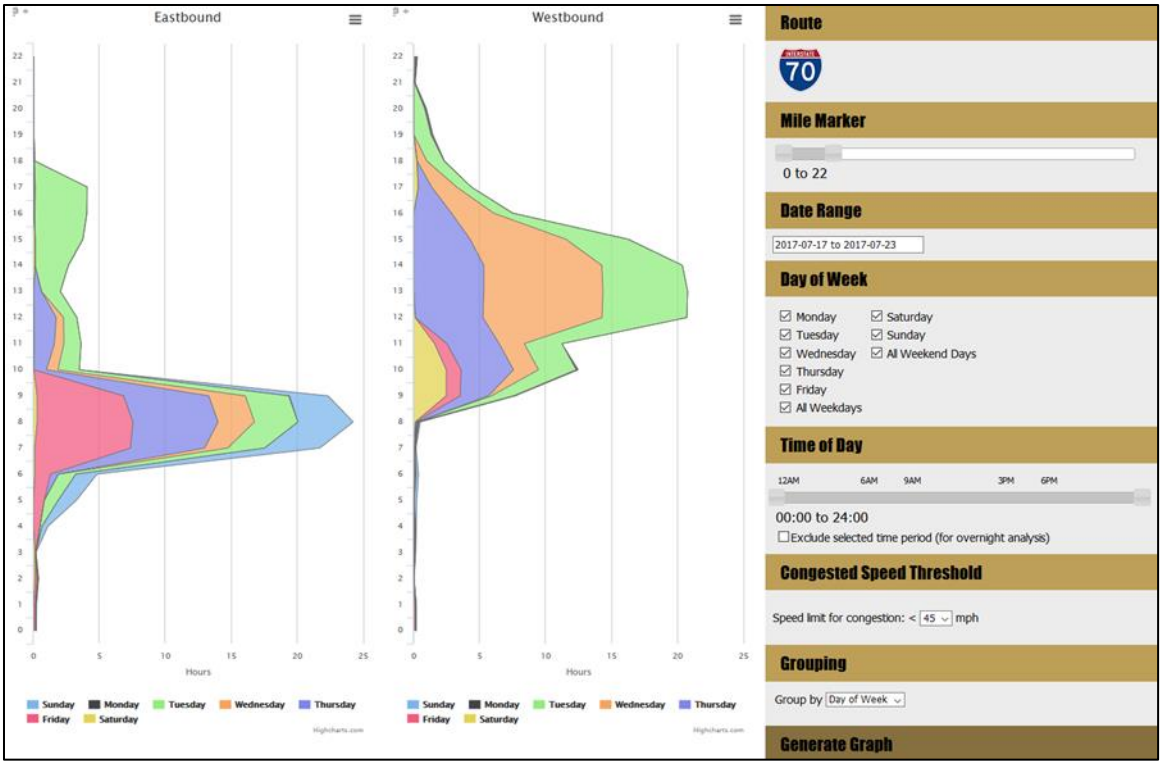

Figure 33 "Congestion Profile" online dashboard [81]

At the bottom of Figure 31c is a summary table for the current week. The work zone label, name, and contract number are followed by the date range of the current week, route, and mile post range. The performance measures are split by direction and are for the current week only. In the 6th column is the number of hours when there was a queue of length greater than or equal to 5 miles within or overlapping the work zone. This is a good measure of the duration of severe traffic incidents. In the 7th column is the number of hours when there was a queue extending upstream of the work zone boundary. This measure is important to traffic and project managers in regard to the placement of advance warning signs and queue length modeling. The database query for the hours of queueing $\geq$ 5 miles and hours of queueing upstream of the work zone are provided in Appendix C. Columns 8-10 deal with the mile-hours of congestion in the work zone for the whole week and the "worst" day. These measures are useful when compared to performance in previous weeks and for determining the impact of recurring congestion relative to single incidents.

Columns 11-13 show the number of crashes related to the work zone. All crashes that occurred within the work zone, regardless of the cause, were included. In addition, any crashes that occurred in relation to congestion from within the work zone were also included. Back-of-queue crashes were of particular concern and were categorized as "within" or "upstream of" a work zone. A back-of-queue crash within a work zone occurs downstream of the advance work zone warning signs ("Road Work Ahead") and upstream of the "End Road Work" signs (Figure 34a). A back-of-queue crash upstream of a work zone occurs upstream of the advance work zone warning signs and at the back of a queue extending from within the work zone (Figure 34b). The number of property damage only (PDO) and personal injury (PI) crashes are also shown. Fatal crashes, due to their rarity, are included in the number of personal injury crashes but are called out in the table with a '*' and in the notes.

Each crash counted in the summary table is also plotted on the congestion profiles and on the plots on page 4 of the report. Crashes called out on the congestion profiles are colored according to the day of occurrence and point to the corresponding longitudinal location. A crash pointing to the x-axis (0 hours of congestion) was not associated with congestion. A crash pointing to a corresponding band of color (i.e. a blue-Sunday crash pointing to a blue-Sunday band) was associated with congestion. A crash called out on page four points to the exact time and location of the crash. Plotting the crashes in this manner can reveal patterns. Multiple crashes that occurred in a single day and at different but nearby locations may be indicative of congestion crashes. Multiple crashes that occurred over multiple days and at the same location may be indicative of a recurring physical hazard.

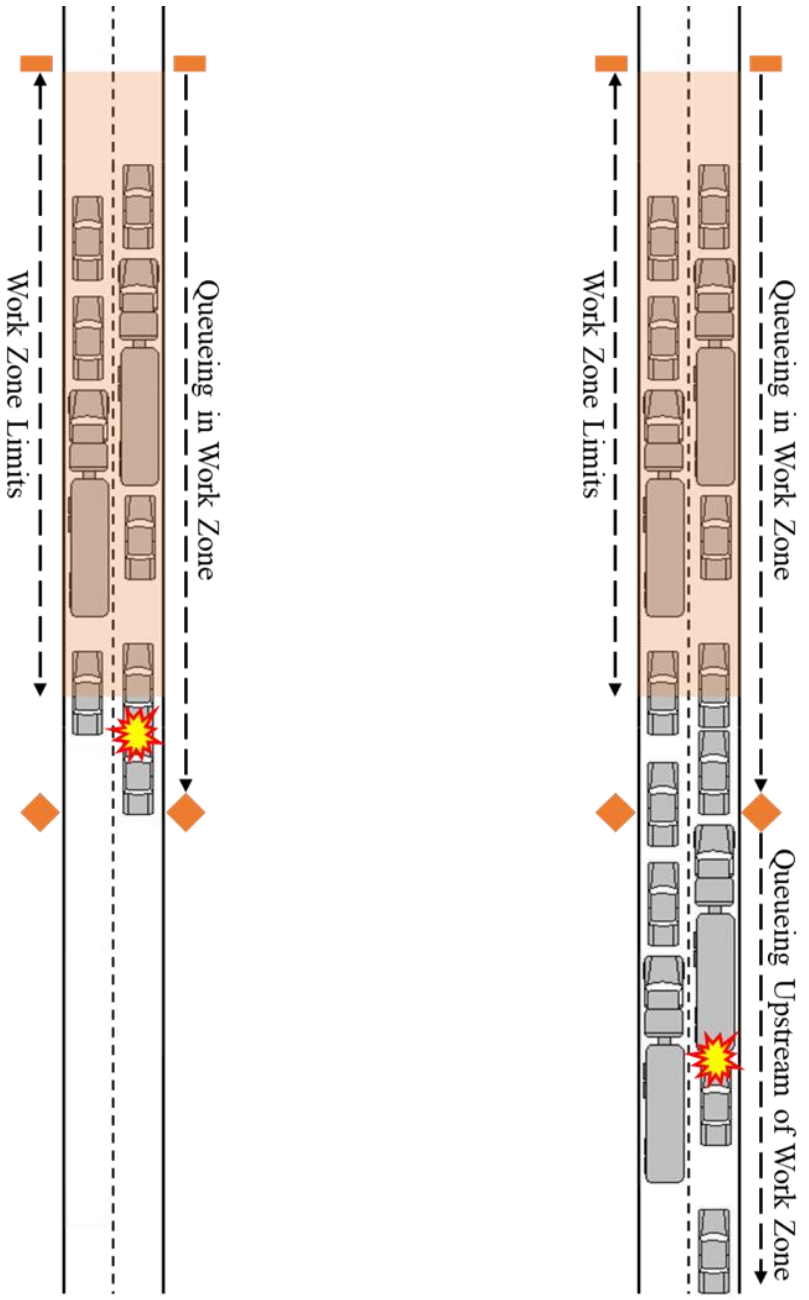

(a) Within work zone (b) Upstream of work zone

Figure 34 Conceptualization of work zone back-of-queue crashes

6.1.4 Route Builder

The previous sections discuss aggregate measures and visualizations of the congestion within the work zone. However, it is often useful to view the data in an unaggregated manner. Figure 27a and Figure 29a are queue heat maps that were

generated using an online dashboard called “Queue MOT” [82] (Figure 35). This dashboard displayed queues and the corresponding queue alert notifications for pre-defined work zones and a selected date range. This tool did not require any management of spreadsheets or static files. In work zones with INDOT cameras present, the user could mouse over the queue and view static, minute-by-minute images. This dashboard was utilized for the work zone report for the Summer 2016 construction season. The tool was useful for investigating specific ongoing incidents or identifying patterns over a historic range of dates. However, users could only select from the pre-defined work zones and could only view one heat map at a time.

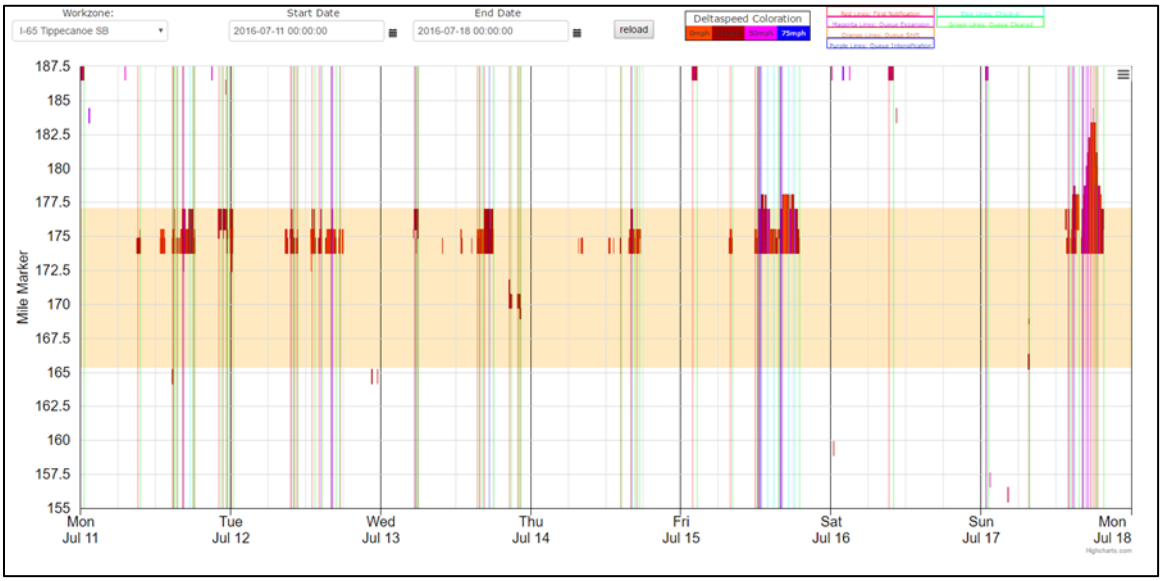

Figure 35 “Queue MOT” online dashboard [82]

The “Route Builder” dashboard [83] evolved from the “Queue MOT” dashboard. The new dashboard, show in Figure 36, allows users to easily define work zone boundaries and displays four graphs instead of one. Each direction has two graphs: total queue length (“Total Queue Length over Area of Analysis vs. Time”) and the queue heat map (“Queues by Mile Markers vs. Time”). The total queue length graphs are useful to traffic managers for comparing predicted to actual queue lengths. The two directions, placed side by side, can also be easily compared.

For use in the work zone report, the user must define the following inputs. First, the route, area of analysis, and work zone area must be selected. The unit for both the

"Area of Analysis" and the "Workzone Area" is mile post. The "Area of Analysis" includes the work zone and the recommended 10 miles on either end of the work zone. The "Workzone Area" is defined by the work zone limits. For example, the C4 work zone on I-70 in Vigo County starts at mile post 6.8 and ends at mile post 12. In the "Route Builder" dashboard, the user would select the route as I-70, an "Area of Analysis" of 0 to 22, and a "Workzone Area" of 7 to 12. The map on the dashboard will change to reflect the selected "Area of Analysis" (yellow) and "Workzone Area" (red). The user must then select the date range of interest. For the full report, one week, Monday to Monday, is selected, such as "2017-07-17 to 2017-07-23". Users may also input the times of scheduled lane restrictions or work activities, which will shade the selected times in yellow on the total queue length graphs. This allows users to easily identify congestion that happened during those times. Otherwise, the user may uncheck all days. The shaded yellow area in the queue heat maps represents the work zone area. Using this tool, traffic management and safety officials can monitor queues in real-time or as part of an after-action review of traffic management activities.

In the "Total Queue Length over Area of Analysis vs. Time" graphs, the x-axis is the time axis and the y-axis is the total queue length in miles. In the "Queues by Mile Marker vs. Time" graphs, the x-axis is the time axis and mile posts are on the y-axis. For the northbound, eastbound, and inner loop directions, the direction of travel is up (increasing mile posts) on the graph. For the southbound, westbound, and outer loop directions, the direction of travel is down (decreasing mile posts) on the graph. As stated above, the shaded yellow area represents the work zone area. The solid yellow, orange, red, dark red, and purple shapes represent queues over time and space. The user can choose their desired congestion threshold by clicking on the speed bins in the legend.

An added feature of the "Route Builder" dashboard is the "Generate Link" button. This allows users to generate a unique URL that corresponds to their selected locations and dates. This link can be shared with colleagues to generate discussion or to easily share findings.

Figure 36 "Route Builder" online dashboard [83]

6.2 Data Interpretation Examples

While the work zone reports alone cannot always diagnose the exact cause of work zone congestion, the data within the report can provide valuable information to traffic management personnel. Appropriate interpretation of the information is important so that informed decisions can be made about further action. The following case studies provide examples of work zone report data interpretations.

6.2.1 Non-recurring Incident

On October 12, 2017, there was a crash resulting in an overturned semi-truck at mile post 161 on I-65 S (Figure 37), which is located in work zone C1. The resulting queue presents an example of a non-recurring incident (and non-recurring congestion) within a work zone. Some easy-to-identify markers of non-recurring incidents are listed below. Note that these are general observations, not an all-inclusive list of rules. Some of these observations apply to the example in Figure 37.

- In the mile-hour plots on page 1 of the work zone report, there are higher frequencies of slower speeds (purple) on the day of the incident (Figure 37a).
- In the mile-hour plots on page 1 of the work zone report, there is a significant difference in the mile-hours of congestion on the day of the incident compared to other days in that week (Figure 37a).
- There is a dark, vertical band on the day of the incident in the “Frequency of Speeddelta” plot on page 2 of the work zone report.
- In the congestion profile on page 3 of the report, the colored band for that day (in this case, the purple-Thursday band) is visibly larger than the other days (Figure 37c).
- There are no queues of similar shape or duration at similar times and/or locations during the rest of the week in the queue heat map on page 4 of the report (Figure 37d).
- A crash occurred at the location of the front of the queue and up to 0.5 hours prior to the initial formation of the queue (Figure 37d).
- A significant weather event occurred on that day.

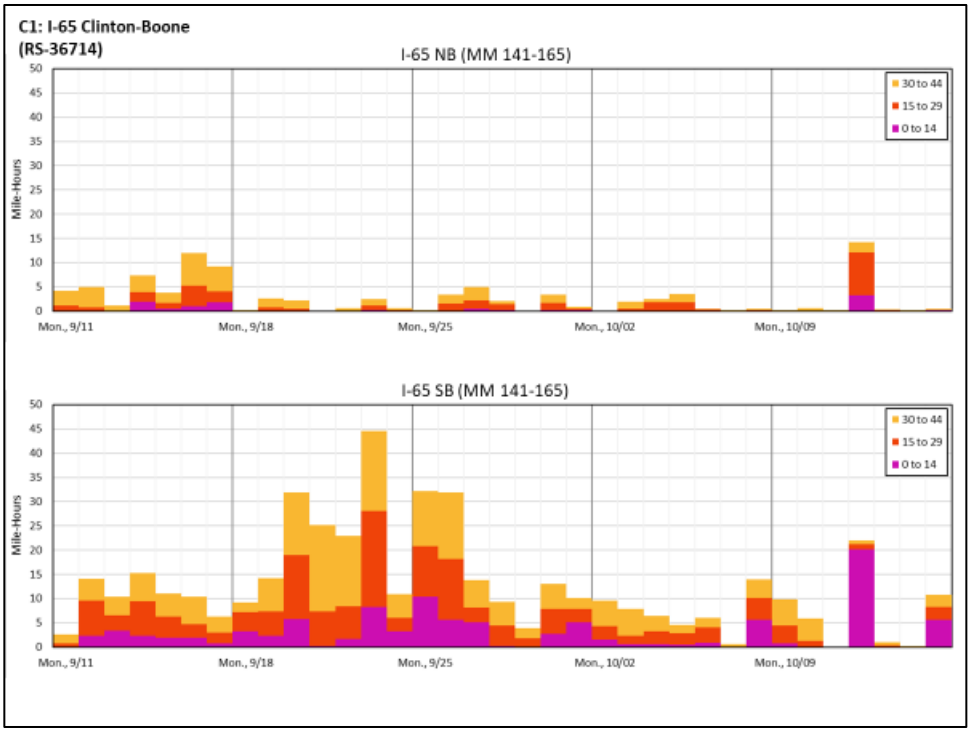

(a) Page 1

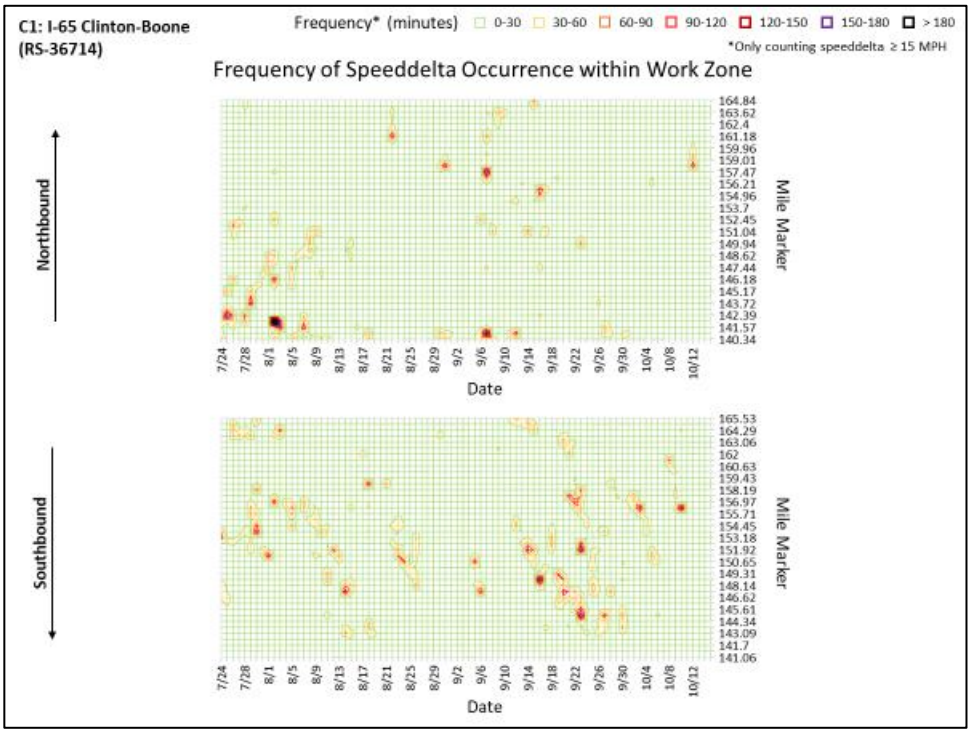

(b) Page 2

Figure 37 Example of non-recurring incident

Figure 37 continued

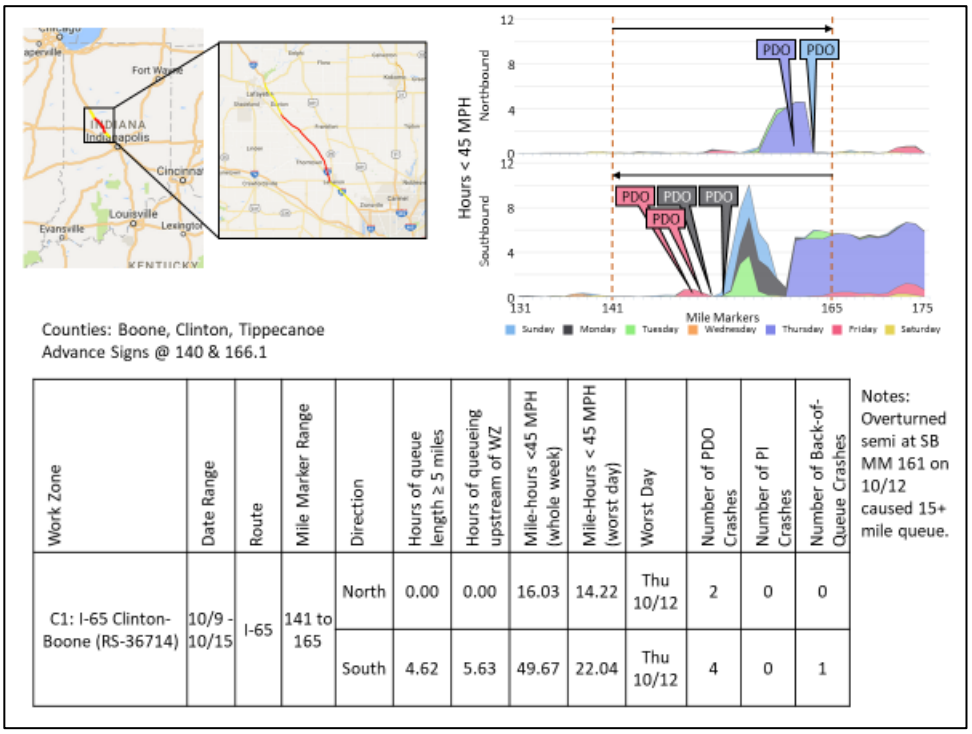

Work Zone	Date Range	Route	Mile Marker Range	Direction	Hours of queue length ≥ 5 miles	Hours of queueing upstream of WZ	Mile-hours <45 MPH (whole week)	Mile-Hours < 45 MPH (worst day)	Worst Day	Number of PDO Crashes	Number of PI Crashes	Number of Back-of-Queue Crashes
C1: I-65 Clinton-Boone (RS-36714)	10/9 - 10/15	I-65	141 to 165	North	0.00	0.00	16.03	14.22	Thu 10/12	2	0	0
				South	4.62	5.63	49.67	22.04	Thu 10/12	4	0	1

Notes: Overturned semi at SB MM 161 on 10/12 caused 15+ mile queue.

(c) Page 3

(d) Page 4

6.2.2 Recurring Congestion

During the week of October 16-22, 2017, there was recurring congestion in both directions of the C4 work zone on I-70 in Vigo County (Figure 38). The queues typically formed in the afternoon at approximately mile post 8. During these times, there were lane closures in both directions at this location in the work zone. The resulting queues present an example of recurring congestion within a work zone. Some easy-to-identify markers of recurring congestion are listed below. Note that these are general observations, not an all-inclusive list of rules. Some of these observations apply to the example in Figure 38.

- In the mile-hour plots on page 1 of the work zone report, there are lower frequencies of slower speeds (purple) throughout the week (Figure 38a).
- In the mile-hour plots on page 1 of the work zone report, the mile-hours of congestion each day remains relatively constant (Figure 38a).
- There is a dark, horizontal band in the “Frequency of Speeddelta” plot on page 2 of the work zone report (Figure 38b).
- In the congestion profile on page 3 of the report, the colored bands for each day have consistent widths (Figure 38c).
- There are queues of similar shape or duration at similar times and/or locations during the week in the queue heat map on page 4 of the report (Figure 38d).

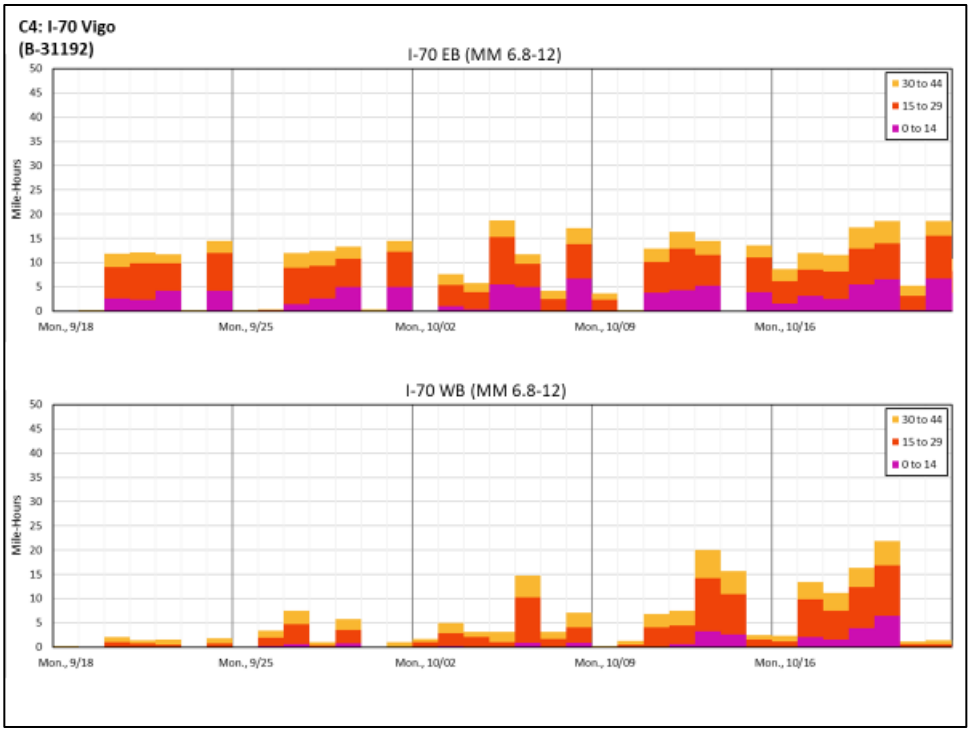

(a) Page 1

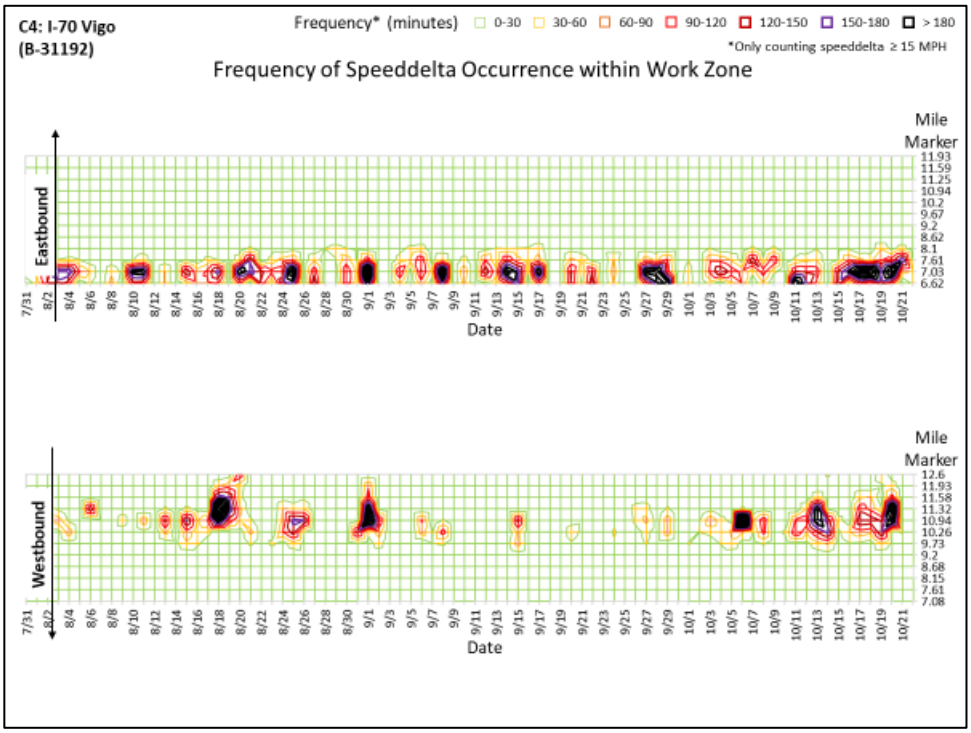

(b) Page 2

Figure 38 Example of recurring congestion

Figure 38 continued

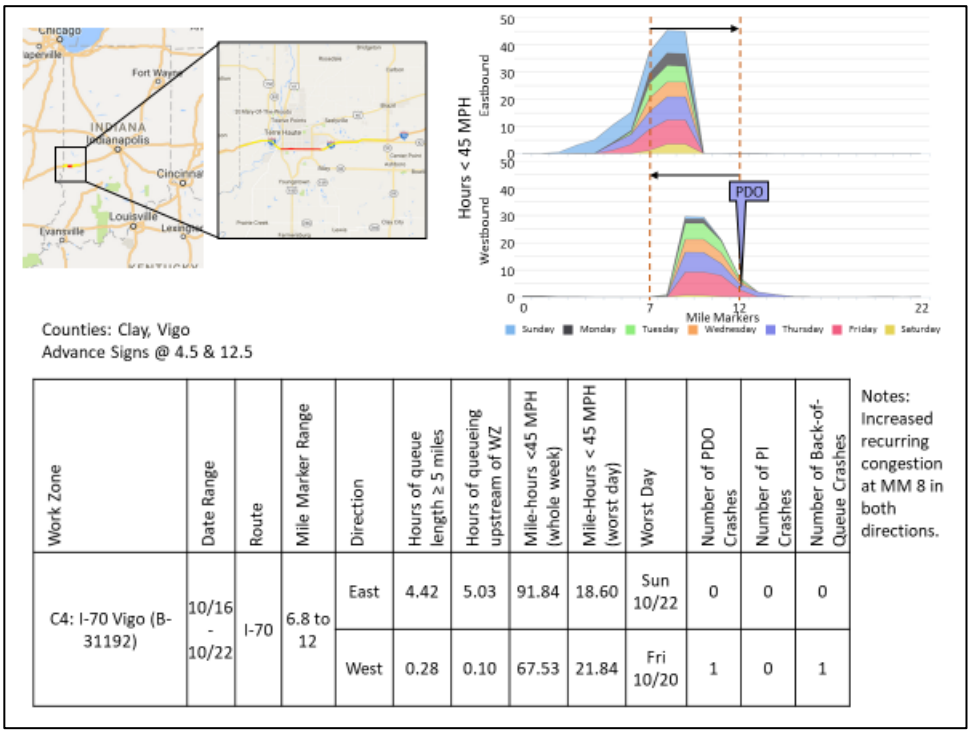

Work Zone	Date Range	Route	Mile Marker Range	Direction	Hours of queue length ≥ 5 miles	Hours of queueing upstream of WZ	Mile-hours <45 MPH (whole week)	Mile-Hours < 45 MPH (worst day)	Worst Day	Number of PDO Crashes	Number of PI Crashes	Number of Back-of-Queue Crashes
C4: I-70 Vigo (B-31192)	10/16 - 10/22	I-70	6.8 to 12	East	4.42	5.03	91.84	18.60	Sun 10/22	0	0	0
				West	0.28	0.10	67.53	21.84	Fri 10/20	1	0	1

Notes: Increased recurring congestion at MM 8 in both directions.

(c) Page 3

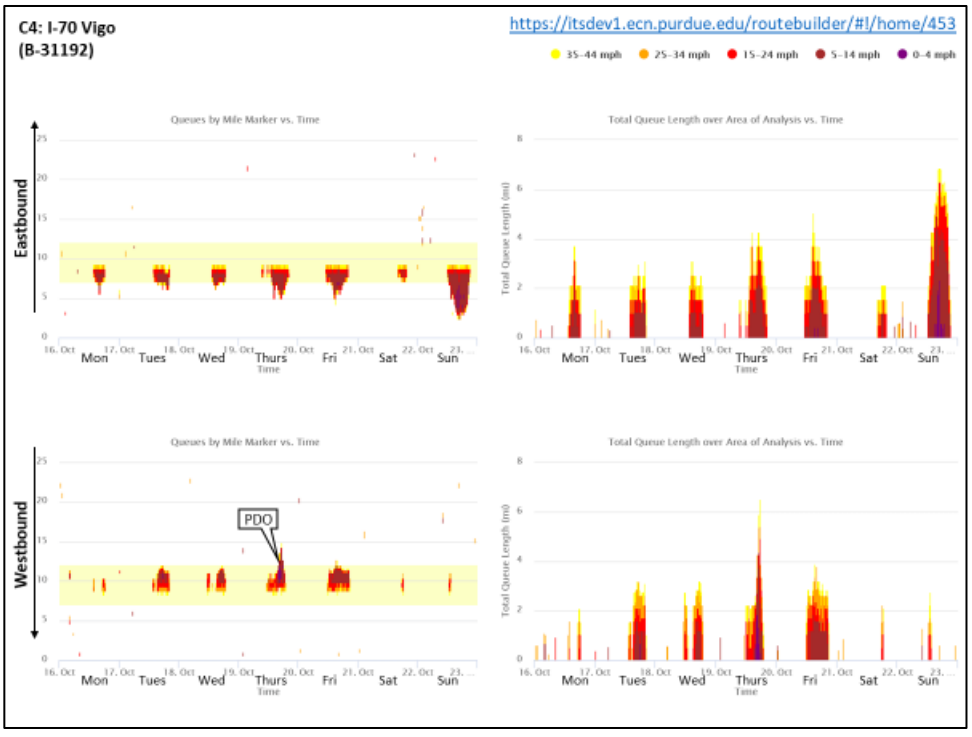

(d) Page 4

6.2.3 Moving Operations

During the week of September 18-24, 2017, there was work zone-related congestion in both directions of the C1 work zone on I-65 in Clinton County and Boone County (Figure 39). In the northbound direction, there were brief, moving queues overnight (September 19-20). These queues were caused by slow-moving maintenance vehicles. Over time, the short queue shifts north with the maintenance vehicles. In the southbound direction, there was recurring overnight congestion. In this case, the queue did not shift throughout the night. Instead, the queue formed in a different location each night due to construction crews working on different, static sections each night. The resulting queues present examples of moving operations (both recurring and non-recurring) within a work zone. Some easy-to-identify markers of moving operations are listed below. Note that these are general observations, not an all-inclusive list of rules. Some of these observations apply to the example in Figure 39.

- In the mile-hour plots on page 1 of the work zone report, there are lower frequencies of slower speeds (purple) throughout the week (Figure 39a).
- There are no consistent horizontal or vertical bands in the "Frequency of Speeddelta" plot on page 2 of the work zone report (Figure 39b).
- In the congestion profile on page 3 of the report, recurring congestion at different locations each day may be characterized by colored bands for each day of consistent widths at different locations (Figure 39c, southbound). For the brief, moving queues, there may be no visible impact in the congestion profile.
- For the recurring congestion at different locations, there are queues of similar shape or duration at similar times but different locations during the week in the queue heat map on page 4 of the report (Figure 38d, southbound). Queues caused by slow-moving maintenance vehicles typically look like thin slanted lines in the queue heat map (Figure 38d, northbound).

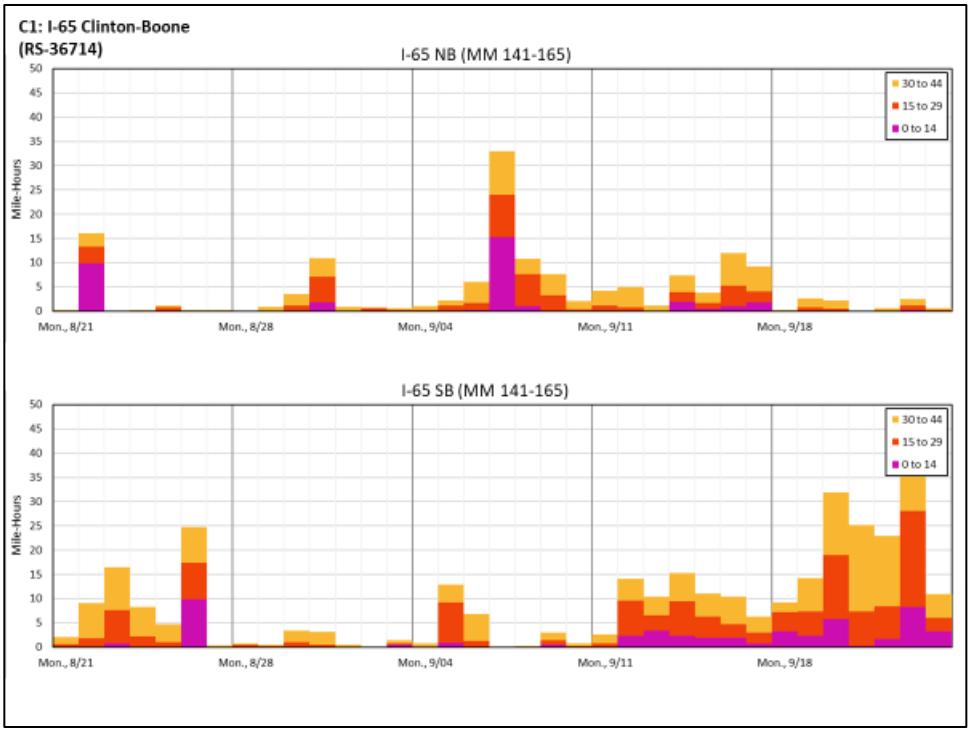

(a) Page 1

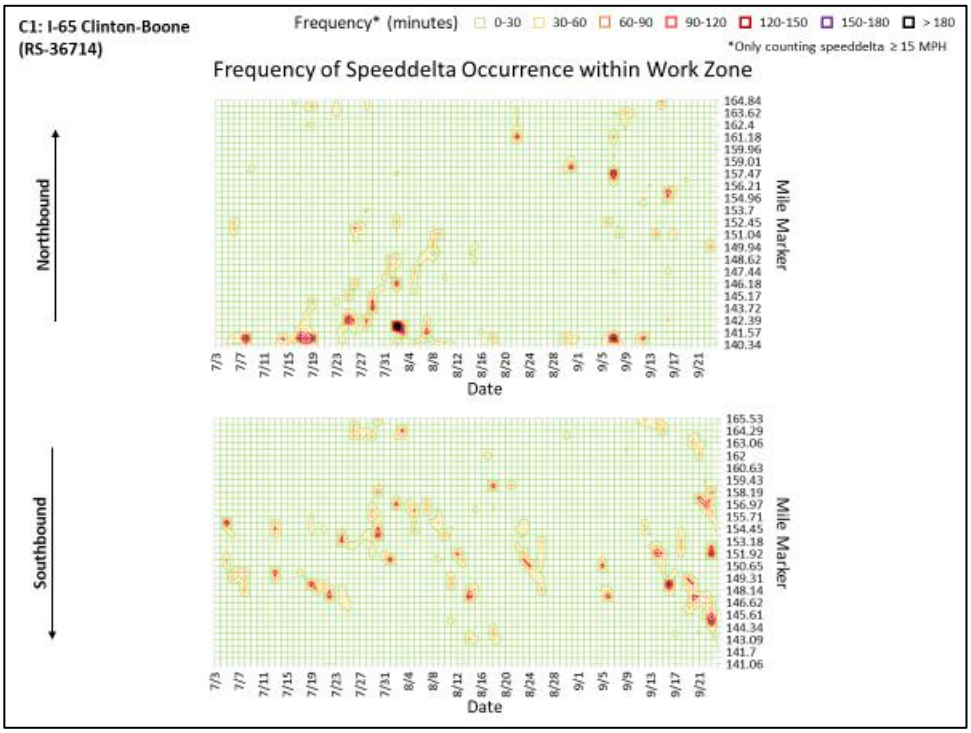

(b) Page 2

Figure 39 Example of moving operations

Figure 39 continued

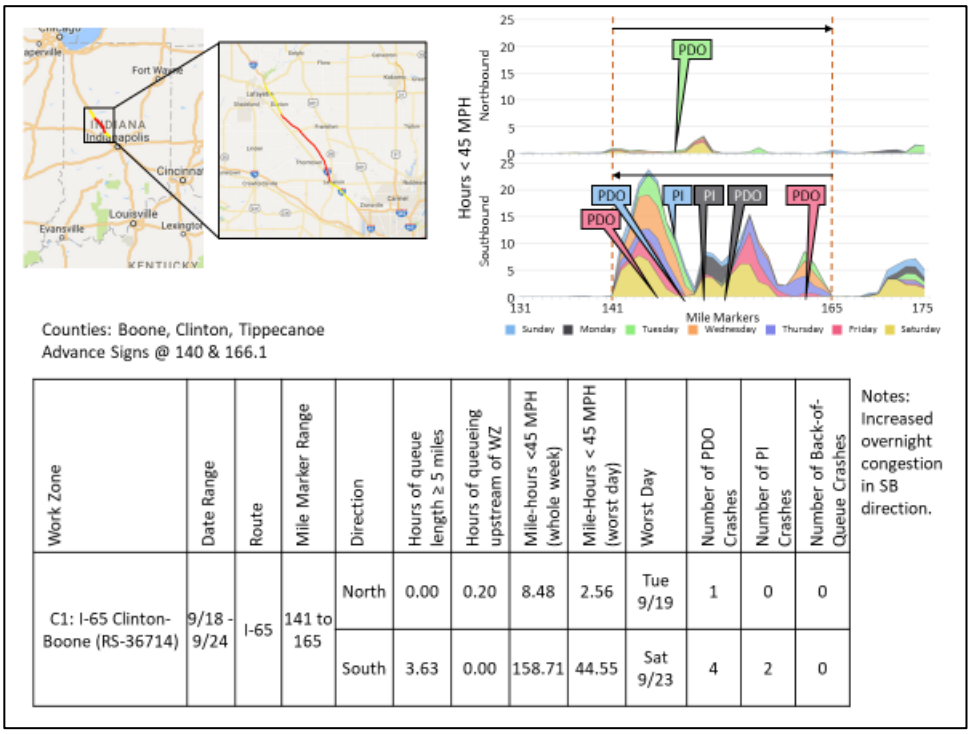

Work Zone	Date Range	Route	Mile Marker Range	Direction	Hours of queue length ≥ 5 miles	Hours of queueing upstream of WZ	Mile-hours <45 MPH (whole week)	Mile-Hours < 45 MPH (worst day)	Worst Day	Number of PDO Crashes	Number of PI Crashes	Number of Back-of-Queue Crashes
C1: I-65 Clinton-Boone (RS-36714)	9/18 - 9/24	I-65	141 to 165	North	0.00	0.20	8.48	2.56	Tue 9/19	1	0	0
				South	3.63	0.00	158.71	44.55	Sat 9/23	4	2	0

Notes: Increased overnight congestion in SB direction.

(c) Page 3

(d) Page 4

6.2.4 Road Closure

On I-70 W on July 18, 2017, there was a fatal back-of-queue crash at mile post 16 that caused the closure of I-70 W for approximately 6 hours (Figure 40). In the queue heat map following that fatal crash, there is a purple rectangle. This rectangular queue presents an example of a road closure. The "Route Builder" dashboard treats missing data (instances when there are no vehicles on the roadway) as roadway segments with speed of 0-4 MPH (purple). Missing data is not shown in any of the other work zone report figures or performance measures. Some easy-to-identify markers of road incidents are listed below. Note that these are general observations, not an all-inclusive list of rules. Some of these observations apply to the example in Figure 40.

- There is a purple rectangle in the middle of a "normal" queue (Figure 40d).
- There is no evidence of this rectangular queue in any of the other work zone report figures (Figure 40a, Figure 40b, and Figure 40c). In other words, there is less congestion in the other figures than is shown in the queue heat map.
- There was a severe crash up to 1 hour prior to the appearance of the purple rectangle (Figure 40d).
- There was queueing further upstream and around the same time as the purple rectangle (indicative of vehicles being detoured) (Figure 40d).

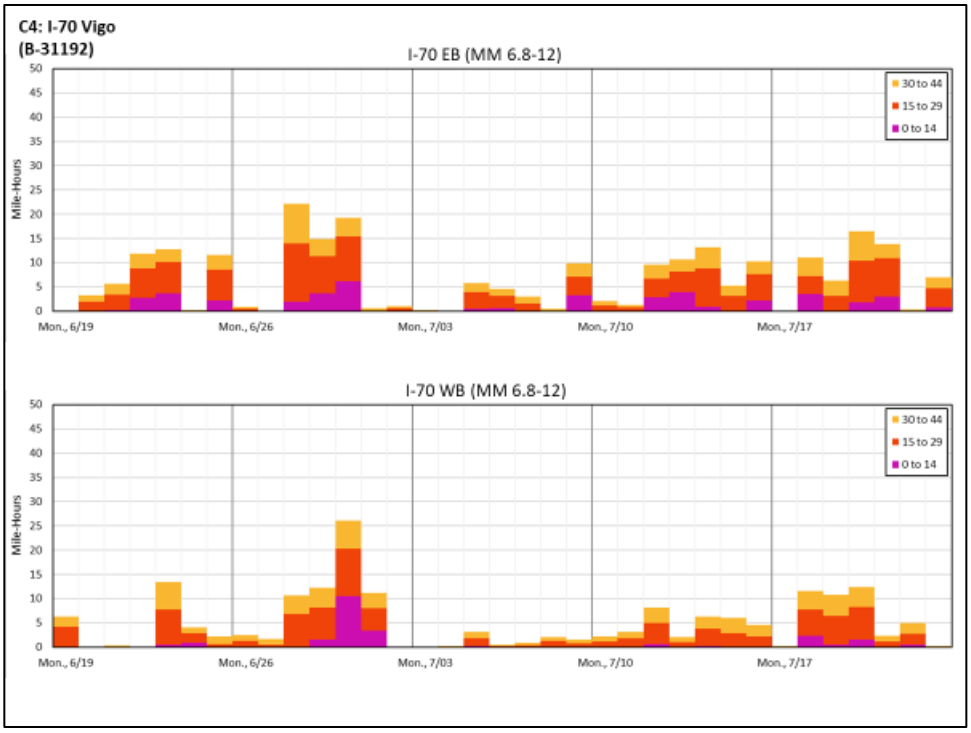

(a) Page 1

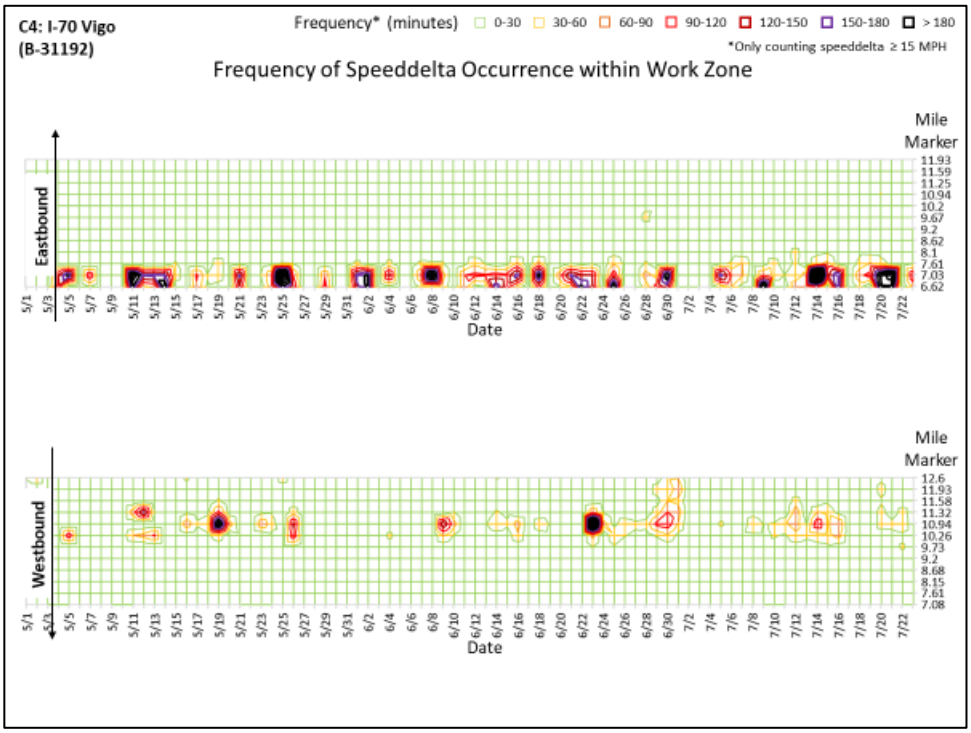

(b) Page 2

Figure 40 Example of a road closure

Figure 40 continued

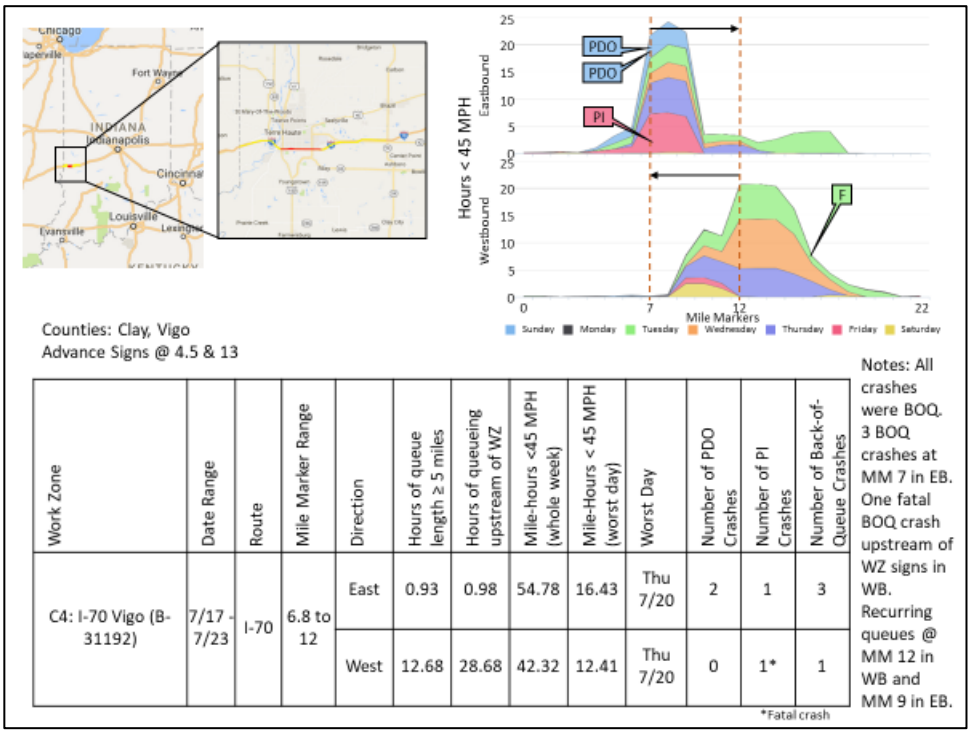

Work Zone	Date Range	Route	Mile Marker Range	Direction	Hours of queue length ≥ 5 miles	Hours of queueing upstream of WZ	Mile-hours <45 MPH (whole week)	Mile-Hours < 45 MPH (worst day)	Worst Day	Number of PDO Crashes	Number of PI Crashes	Number of Back-of-Queue Crashes
C4: I-70 Vigo (B-31192)	7/17 - 7/23	I-70	6.8 to 12	East	0.93	0.98	54.78	16.43	Thu 7/20	2	1	3
				West	12.68	28.68	42.32	12.41	Thu 7/20	0	1*	1

*Fatal crash

Notes: All crashes were BOQ. 3 BOQ crashes at MM 7 in EB. One fatal BOQ crash upstream of WZ signs in WB. Recurring queues @ MM 12 in WB and MM 9 in EB.

(c) Page 3

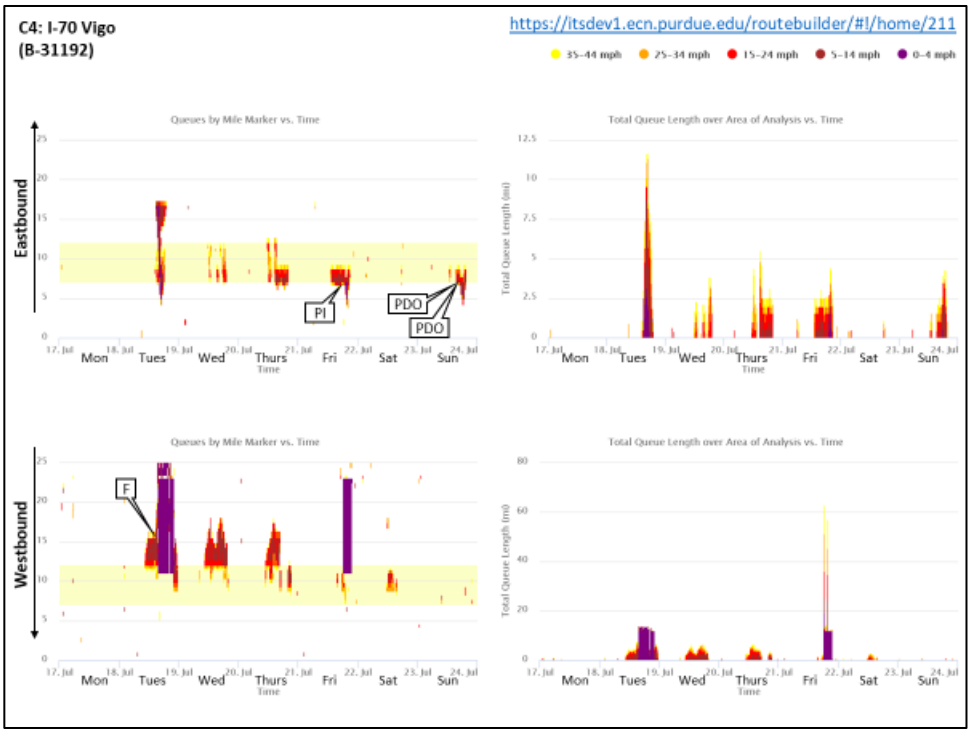

(d) Page 4

6.2.5 Data Error

The most common data error that users will encounter is missing data. This error may look very similar to a road closure. On I-65 N between mile posts 220 and 230, there were approximately 4.5 hours on May 19, 2017, with no data (Figure 41). At first glance, this would appear to be a road closure. However, there was no queueing immediately before, after, or near this block of missing data. Upon closure inspection of the raw data, it was determined that there was an error in the data during this time period. Some easy-to-identify markers of data errors are listed below. Note that these are general observations, not an all-inclusive list of rules. Some of these observations apply to the example in Figure 41.

- There are no visible signs of congestion near the incident on any of the other report figures.
- In the queue heat map, there was no queueing immediately before, after, or near this block of missing data (Figure 41d).
- There were no crashes nearby in time or space.
- There is no discernable reason for the road to have been closed.

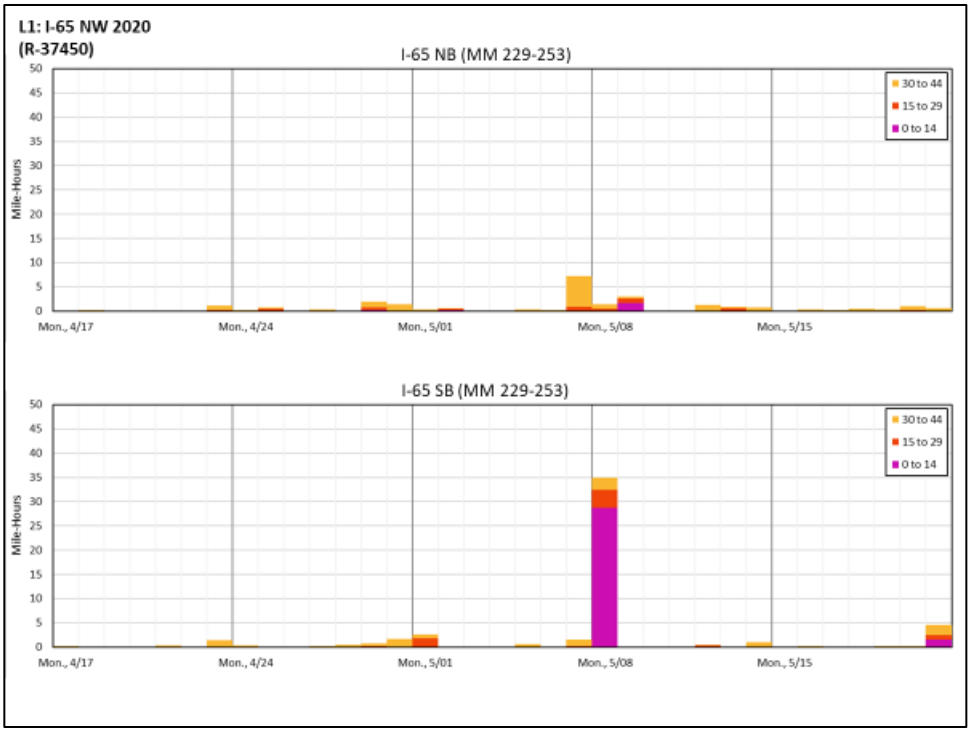

(a) Page 1

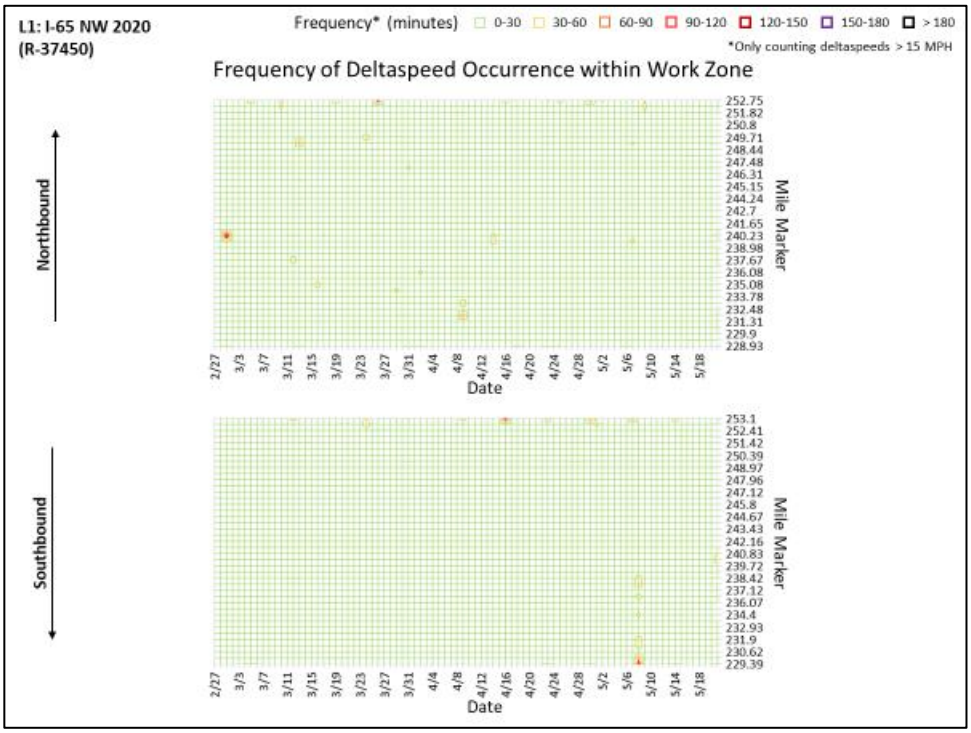

(b) Page 2

Figure 41 Example of a data error

Figure 41 continued

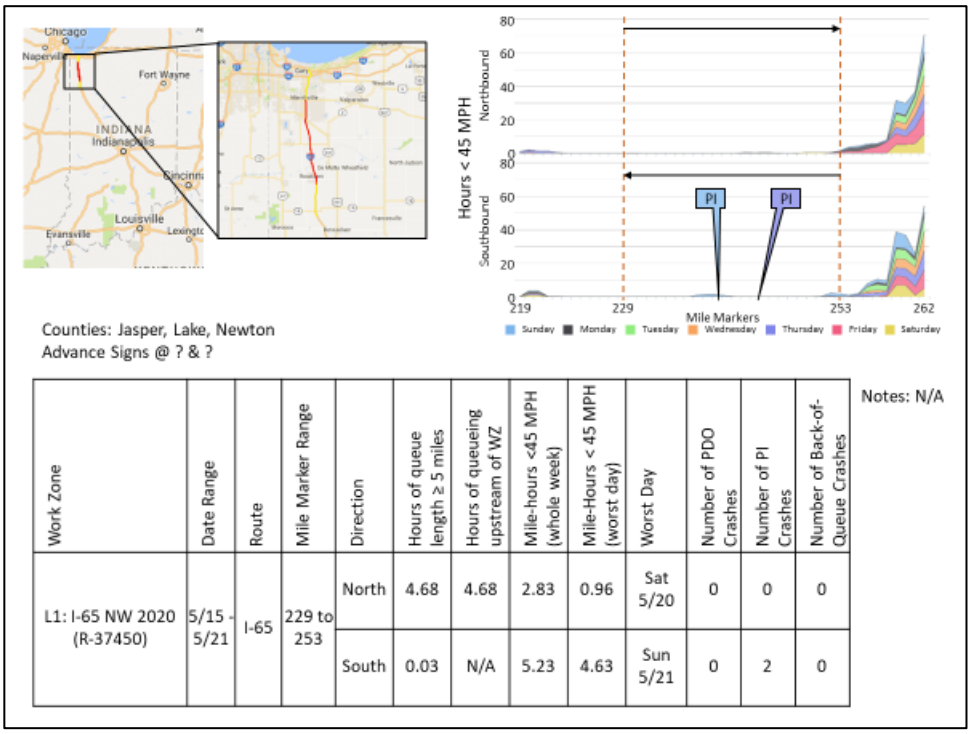

Work Zone	Date Range	Route	Mile Marker Range	Direction	Hours of queue length ≥ 5 miles	Hours of queueing upstream of WZ	Mile-hours <45 MPH (whole week)	Mile-Hours < 45 MPH (worst day)	Worst Day	Number of PDO Crashes	Number of PI Crashes	Number of Back-of-Queue Crashes
L1: I-65 NW 2020 (R-37450)	5/15 - 5/21	I-65	229 to 253	North	4.68	4.68	2.83	0.96	Sat 5/20	0	0	0
				South	0.03	N/A	5.23	4.63	Sun 5/21	0	2	0

Notes: N/A

(c) Page 3

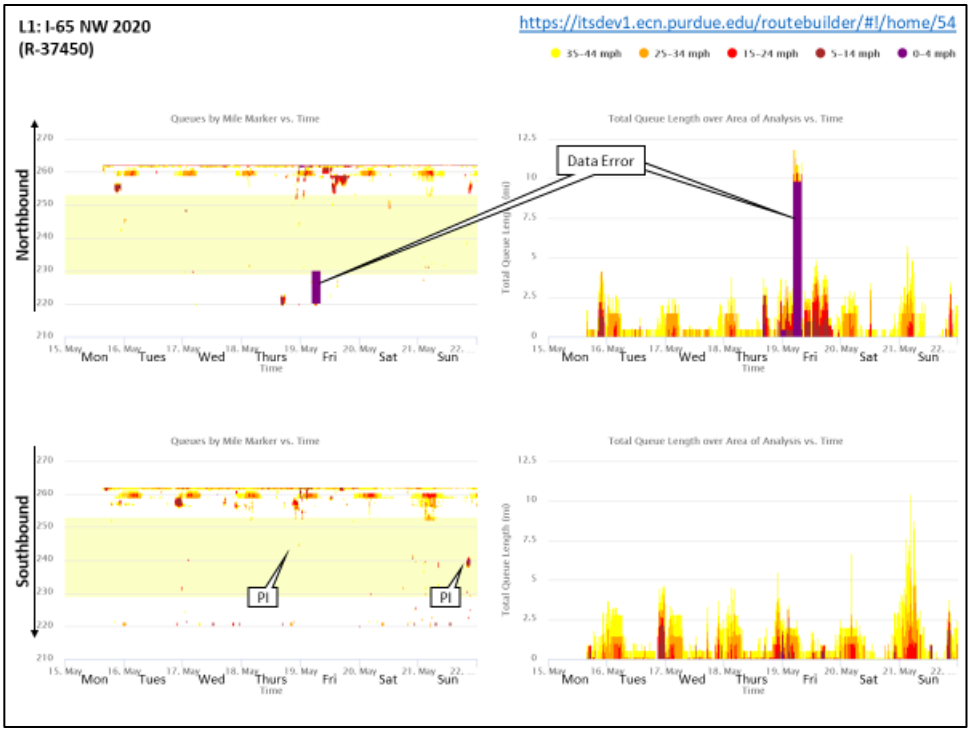

(d) Page 4

6.3 Long-Term Analyses

In addition to the weekly work zone reports, some long-term analyses of the work zones were conducted to emphasize the impact of work zones on mobility and safety and to demonstrate the potential impact on policy. Congestion crashes over a 5-month period were analyzed. Observed queueing in the work zones was compared to congestion policy limits. Finally, cursory economic analyses were conducted for two of the long-term work zones.

6.3.1 Work Zone Congestion Crashes

Among the 30,159 crashes on Indiana interstates in 2014 through 2015 (discussed in Chapter 4), 3,079 were labelled by the investigating officer as being related to construction (Figure 42a) and 5,594 were found to be related to congestion (Figure 42b). Of these two sets, 763 crashes occurred during congestion and were related to construction (Figure 42c). Of interest is the effect of congestion within the work zone versus upstream of the work zone on crashes.

In Chapter 4, a statewide data set of crashes was used for analysis. In this subsection, a smaller data set (1,098 crashes that occurred within the selected works zones (Table 2) between May and August of 2017) was analyzed. Each of these crashes was defined as occurring within or upstream of a work zone (Figure 34) and were compared to the connected vehicle data to determine to duration of queueing prior to the crash. Of these 1,098 crashes, 768 (25.7%) were congestion crashes and had queueing visible in the connected vehicle data at least 1 minute prior to the crash. It was also found that 60.7% of congested crashes upstream of the work zone had congestion visible in the data at least 1 hour prior to the crash, compared to 46.2% of congested crashes within the work zone.

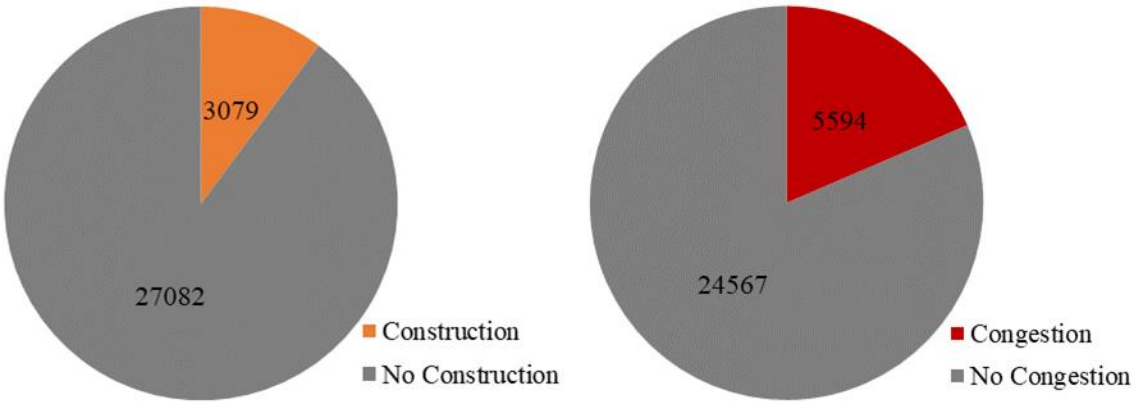

(a) Crashes related to construction (b) Crashes related to congestion

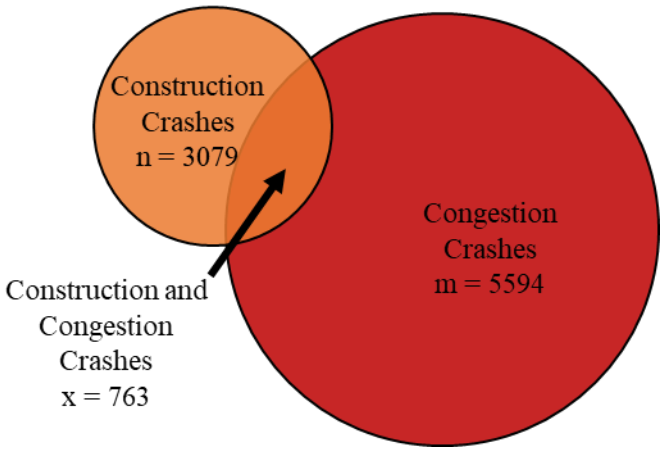

(c) Construction and congestion crashes

Figure 42 Comparing crashes associated with work zones and congestion (2014-2015)

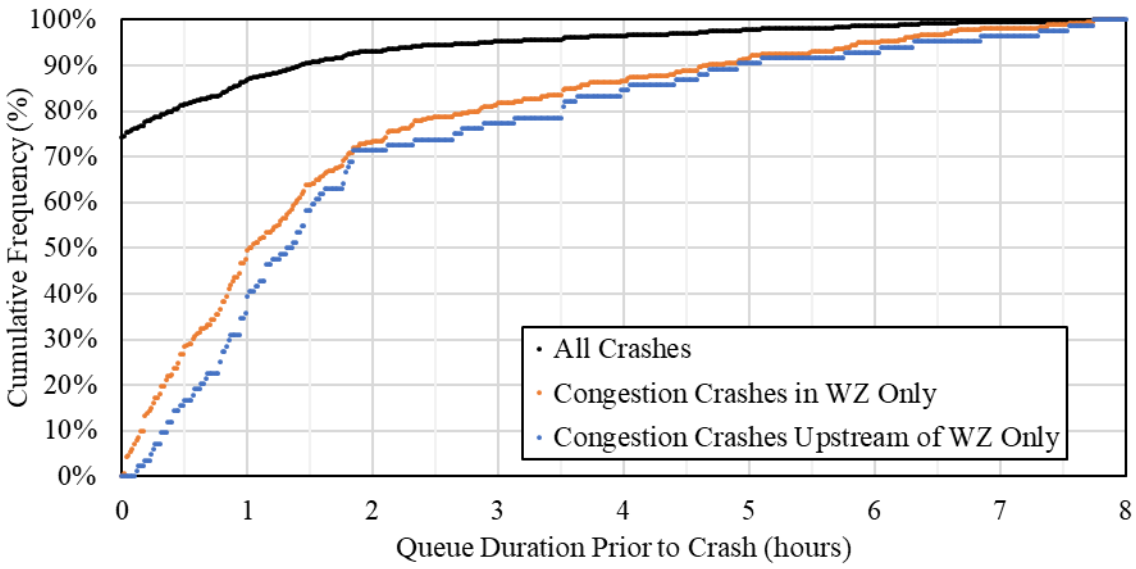

Figure 43 Duration of queue in connected vehicle data prior to work zone crashes

The congestion crash rates within and upstream of the work zones (Table 5) were calculated as in Section 4.3. Within the work zone, the congestion crash rate only included congestion crashes and mile-hours of congestion that occurred within the boundaries of the work zone (Figure 34a). The congestion upstream of the work zone included congestion crashes and mile-hours of congestion that extended upstream of the work zone (Figure 34b). Depending on the congestion threshold used for the connected vehicle data, the congestion crash rate upstream of the work zone was 1.271 to 3.576 times greater than the congestion crash rate within the work zone.

Table 5 Congestion Crash Rates Within and Upstream of Work Zones

Speed Threshold (MPH)	**Congested Crash Rate Within Work Zones (crashes per mile-hour)**	**Congested Crash Rate Upstream of Work Zones (crashes per mile-hour)**	**Crash Rate Ratio**
45	0.016	0.020	1.271
35	0.022	0.030	1.343
25	0.040	0.058	1.441
15	0.096	0.176	1.830
5	0.735	2.629	3.576

6.3.2 Congestion Policy Limits

The *Interstate Highways Congestion Policy* [6] defines an interstate queue as "the length of pavement occupied by a line or lines of closely spaced vehicles travelling below 30 MPH." The policy also states the following limitations for queueing on interstates:

- No queues of any length should be permitted to exceed 6 continuous hours or 12 total hours in any calendar day.
- Queues greater than 0.5 miles in length should not be permitted to exceed 4 continuous hours.
- Queues greater than 1.0 mile in length should not be permitted to exceed two continuous hours.
- Queues greater than 1.5 miles in length should not be permitted.

In Indiana, interstates work zones must be designed so that none of these limits are passed. The policy lists when and where certain roadway restrictions, such as lane or shoulder closures, may be implemented. However, exceptions may be made if modeling results show that expected queueing will not exceed the limitations. Due to the nature of the connected vehicle data, only the last condition can be checked for the selected work zones. It would be difficult to check for queueing less than 1.5 miles due to the length of the connected vehicle data segments.

Table 6 details the observed queueing in each of the selected work zones between April 1, 2017, and September 1, 2017. For two different speed thresholds (35 MPH and 25 MPH), the hours of queueing greater than 1.5 miles in length, the maximum observed queue length, and the median observed queue length were calculated. In Table 6, the median observed queue lengths in bold are greater than the 1.5-mile limit.

Table 6 Observed Queueing Past Congestion Policy Limits in Selected Work Zones

	35 MPH Threshold			25 MPH Threshold		
Work Zone	**Hours of queueing > 1.5 miles**	**Maximum Observed Queue Length (miles)**	**Median Observed Queue Length (miles)**	**Hours of queueing > 1.5 miles**	**Maximum Observed Queue Length (miles)**	**Median Observed Queue Length (miles)**
C1N	154.12	4.49	**1.75**	104.58	8.77	**1.59**
C1S	186.85	8.87	**1.90**	135.85	8.28	**1.83**
C2N	85.50	11.70	**1.75**	48.42	11.7	**1.64**
C2S	62.29	7.30	**2.44**	44.14	6.86	**1.95**
C3N	47.41	5.48	0.82	32.54	4.90	0.64
C3S	42.76	4.74	1.08	28.71	4.32	0.70
C4E	294.39	7.69	**1.57**	154.85	6.48	1.10
C4W	196.48	22.47	**2.08**	102.70	22.47	**1.58**
F1N	62.69	8.51	**1.63**	28.59	7.45	1.20
F1S	31.06	11.76	1.24	20.76	11.13	1.19
F2N	32.41	5.25	0.90	13.24	4.16	0.72
F2S	14.77	5.68	0.60	9.60	5.49	0.60
G1N	6.34	4.02	0.87	3.97	3.80	0.64
G1S	80.13	9.68	1.18	24.89	5.76	1.18
G2N	49.38	7.73	0.98	14.62	6.99	0.60
G2S	18.85	5.86	1.21	7.78	4.99	0.63
G3IL	123.19	11.53	**1.55**	47.50	11.04	1.20
G3OL	29.77	14.40	1.15	14.79	7.03	1.38
G4N	0	0.84	0.39	0	0.84	0.39
G4S	55.27	10.68	1.31	18.67	8.90	0.86
G5N	166.53	10.68	**1.86**	118.78	10.68	**1.78**
G5S	110.93	7.91	1.28	82.83	6.84	1.24
G6IL	75.01	5.43	**2.63**	21.39	4.49	**1.75**
G6OL	16.37	7.05	0.60	5.49	6.15	0.60
L1N	38.68	6.58	**1.81**	28.30	6.58	**1.81**
L1S	31.35	9.97	1.10	20.36	9.97	1.03
L2N	55.77	5.32	0.77	22.92	4.23	0.70
L2S	77.80	4.60	1.47	20.67	3.33	0.82
L3E	309.67	10.80	**2.48**	141.93	10.24	**2.49**
L3W	715.03	21.90	**1.93**	366.12	18.76	1.33
L4E	150.44	14.09	**1.77**	63.71	12.21	1.26
L4W	150.37	6.28	0.02	110.22	9.25	0.02
S1N	0.66	2.49	0.68	0.53	3.12	0.94
S1S	16.54	7.62	1.14	10.16	6.32	0.86
S2N	15.38	8.99	1.15	11.23	6.25	1.15
S2S	49.69	10.50	2.08	41.67	10.50	**2.12**

Values in **bold** are median observed queues lengths greater than the policy limit of 1.5 miles.

In the C1 work zone (I-65 in Clinton and Boone counties), single lane closures were pre-approved in the *Interstate Highways Congestion Policy* [6] for the hours of 21:00 to 06:00. Construction activities in this work zone involved nighttime resurfacing at changing locations throughout the 5-month time period. The median observed queue length in this work zone was 1.59 miles in the northbound direction and 1.83 miles in the southbound direction. Queue modeling showed that the congestion policy limits would not be exceeded. Figure 44 is a plot of the number of days where queueing exceeded 1.5 miles by hour of day. The shaded area represents times during which lane closures were not approved. The color grade represents the number of minutes of observed queueing in that hour of day. For example, in the southbound direction (Figure 44b), there were 40 days where queueing greater than 1.5 miles was observed for at least 1 minute in hour 22. There were 2 days where queueing greater than 1.5 miles was observed for the entirety of hour 22. There was also recurring queueing greater than 1.5 miles earlier than the approved closure time. In cases such as this, traffic managers may want to consider changing the pre-approved closure times, recalibrating the queueing models, or ensuring that the closures are occurring at the appropriate times with the appropriate traffic control.

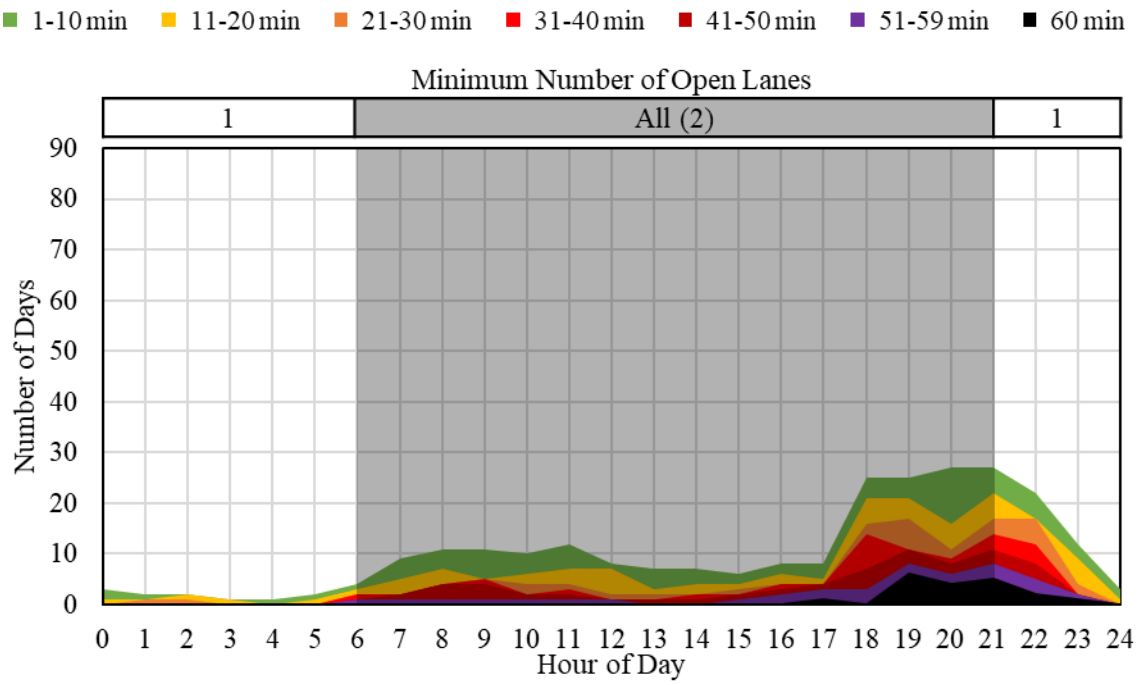

(a) C1N

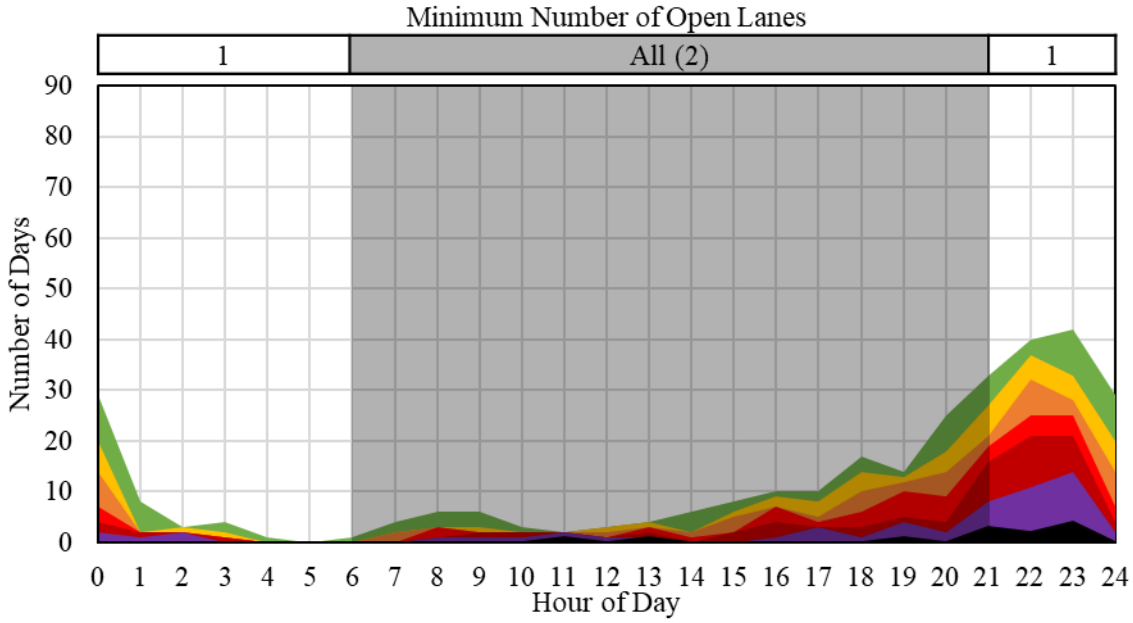

(b) C1S

Figure 44 Days with queueing greater than 1.5 miles by hour of day (C1)

In the C4 work zone (I-70 in Vigo County), the pre-approved times for a lane closure are 21:00 to 06:00. Modeling results showed that a lane closure would not cause queueing in excess of congestion policy limits at any time of day. An exception was approved for lane closures in this work zone at any time, except for 16:00-19:00 on Fridays and Sundays. However, queueing greater than 1.5 miles was observed in both directions during the daytime lane closures (Figure 45). In the eastbound direction, there were 70 days where queueing exceeded 1.5 miles in the 16th hour. Additionally, the maximum observed queue length far exceeded the predicted maximum queue length (22.47 miles vs. 1.2 miles in the westbound direction). In future work zones in this area, traffic managers may want to reconsider allowing daytime lane closures.

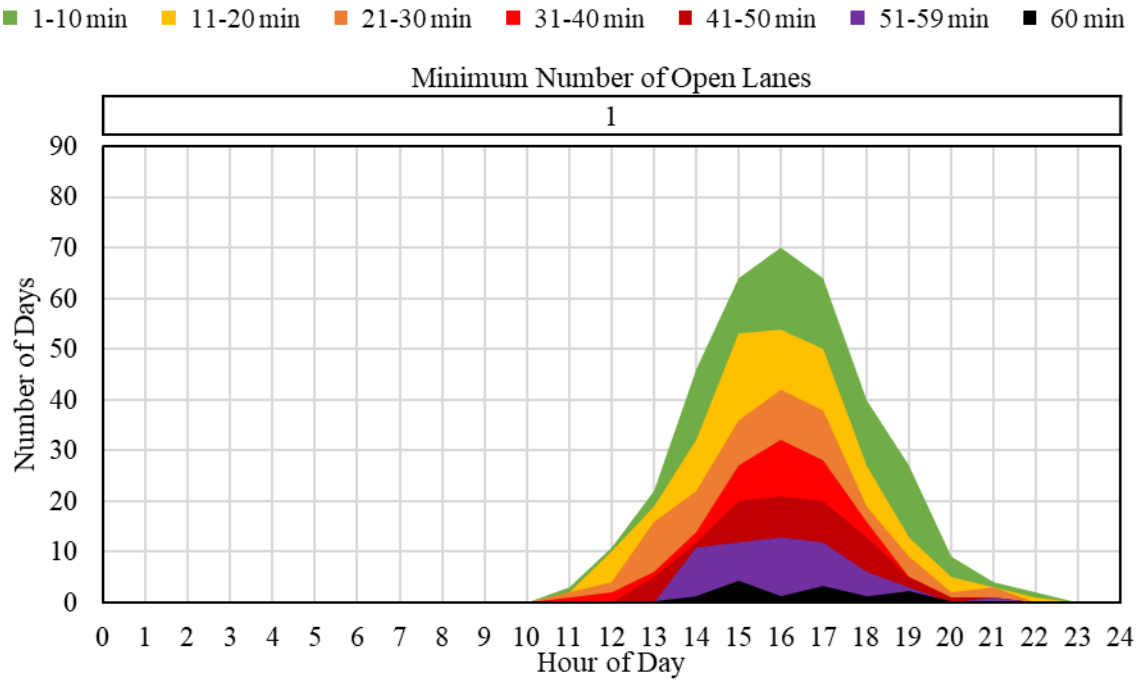

(a) C4E

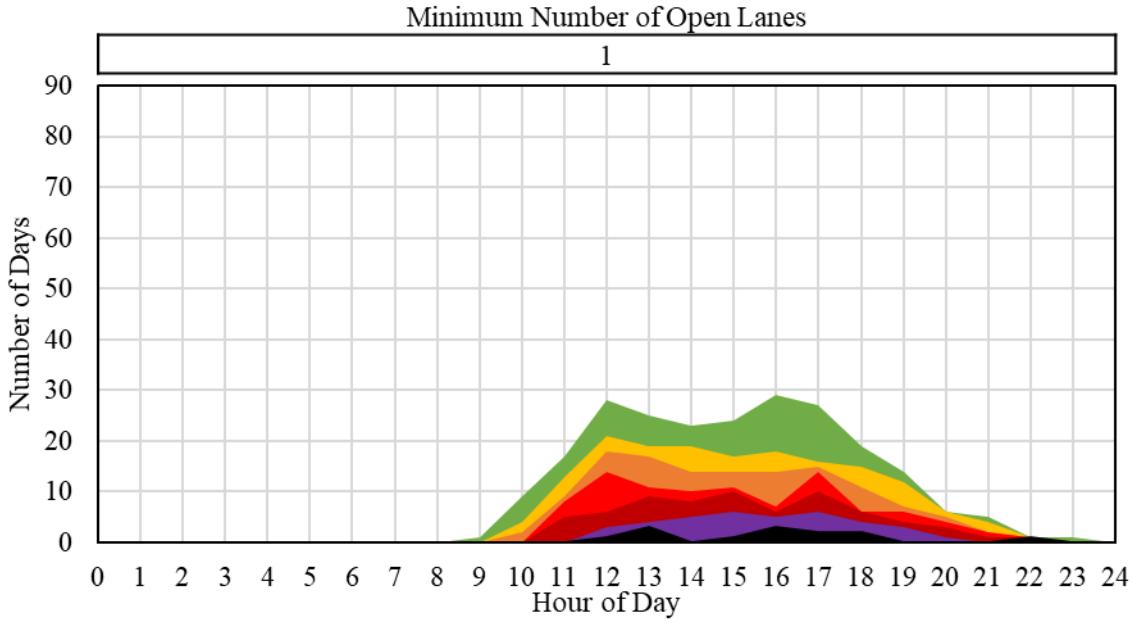

(b) C4W

Figure 45 Days with queueing greater than 1.5 miles by hour of day (C4)

Figure 46 shows a case with significant queueing greater than 1.5 miles. This workzone, L3 (I-80/I-94 in Lake County), is an urban area with some of the highest traffic volumes in the state of Indiana. There is recurring congestion in this area during normal roadway conditions. This work zone was approved for 1-, 2-, and 3-lane closures during different time periods overnight (shown by the shaded areas in Figure 46). However, most of the queueing greater than 1.5 miles occurred during the day, when there were no lane closures. Contextual understanding of the work zone location is important when considering queueing in work zones.

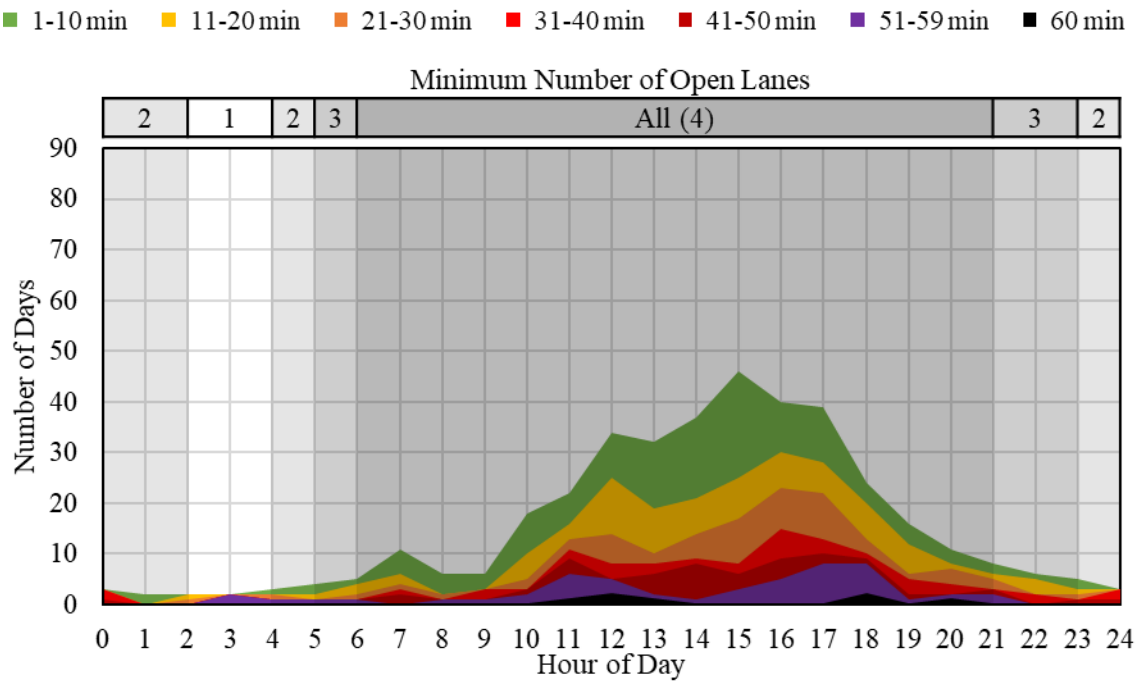

(a) L3E

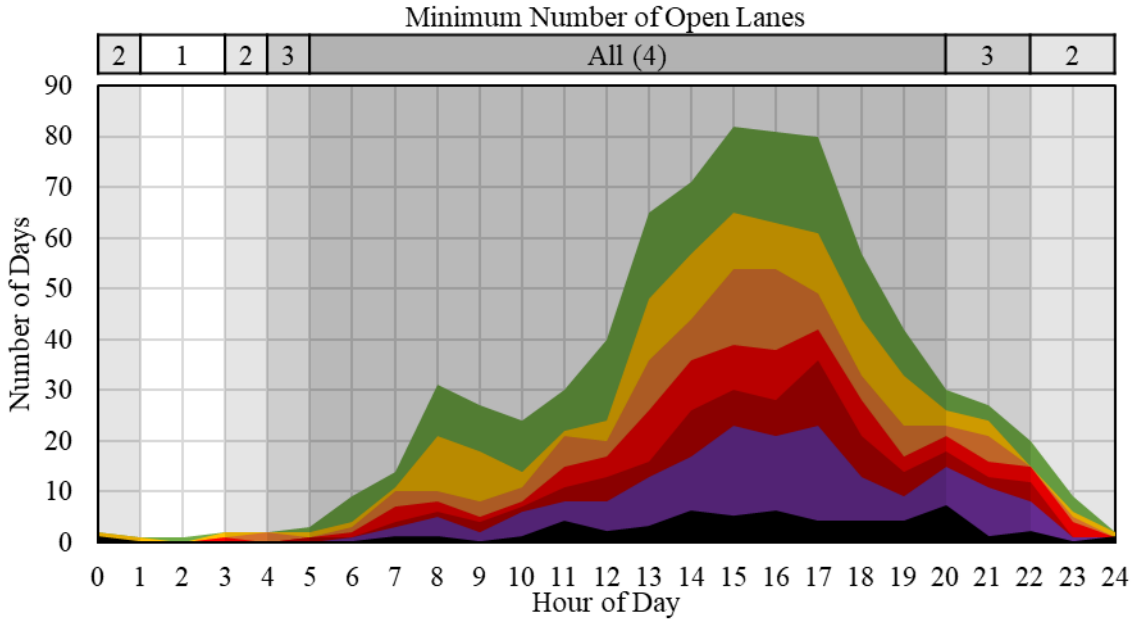

(b) L3W

Figure 46 Days with queueing greater than 1.5 miles by hour of day (L3)

6.3.3 Economic Analysis

For the C2 and C4 work zones, an economic analysis was conducted for a 3-year period in which the work zones were active (2015-2017). For comparison, nearby interstate segments of equal length that had construction activities, aside from minor maintenance activities, were selected. To compare to C2 (I-65, mile posts 167-176), I-65 between mile posts 181 and 190 was selected. Over this three-year period, there were several work zones that overlapped with C4 as defined in Table 2. Therefore, the work zone area in this analysis was defined as I-70 between mile posts 0 and 20. The corresponding non-work zone area was selected as I-70 between mile posts 20 and 40.

First, the economic impact of congestion was calculated. The chosen methodology is similar to that of the *Urban Mobility Scorecard* [75]. The total delay was calculated and multiplied by the value of time. To calculate the total delay in this study, the first step was to calculate the mile-hours of congestion by speed bin (30-45 MPH, 15-30 MPH, and 0-15 MPH) for each hour in the 3-year period for each study segment. For example, between 10:00 and 11:00 on January 2, 2015, on I-65 between mile posts 167 and 176: 4.02 miles were 30-45 MPH, 0.63 miles were 15-30 MPH, and 0.16 miles were 0-15 MPH. Using the midpoint of these speed bins, the travel times on these distances were calculated. Also, the travel time at free-flow speed (70 MPH for passenger cars and 65 MPH for commercial vehicles) was calculated for these same distances. Then, the difference between the free-flow and congested travel times multiplied by the number of vehicles traveling through the study segment during that hour was taken as the total delay, in vehicle-hours, during that hour. The hourly volumes were retrieved from INDOT's Traffic Count Database System [84].

Figure 47 compares the cumulative delay over time in vehicle-hours by vehicle type for the work zone segment and the non-work zone segment on I-65. The total vehicle-hours of delay over 3 years in the I-65 work zone was 4.39 times greater than in the non-work zone segment. Figure 48 compares the cumulative delay over time in vehicle-hours by vehicle type for the work zone segment and the non-work zone segment on I-70. The total vehicle-hours of delay over 3 years in the I-70 work zone was 4.57 times greater than in the non-work zone segment.

To convert the total delay to the cost of congestion the value of time needed to be defined. For commercial vehicles, the annual values of average marginal costs per hour of operation, calculated by the American Transportation Research Institute [85, p. 23], were used. The cost per hour was multiplied by the commercial vehicle-hours of delay. For passenger vehicles, the vehicle-hours of delay was first converted to person-hours of delay using a vehicle occupancy value of 1.25 [75, p. A14]. Then, the value of time for persons in passenger vehicles was taken as the median hourly wage for all occupations in Indiana from the Bureau of Labor Statistics [86].

Figure 49 compares the cumulative cost of congestion over time by vehicle type for the work zone segment and the non-work zone segment on I-65. The total cost of congestion over 3 years in the I-65 work zone was 4.09 times greater than in the non-work zone segment. Figure 50 compares the cumulative cost of congestion over time by vehicle type for the work zone segment and the non-work zone segment on I-70. The total cost of congestion over 3 years in the I-70 work zone was 4.37 times greater than in the non-work zone segment.

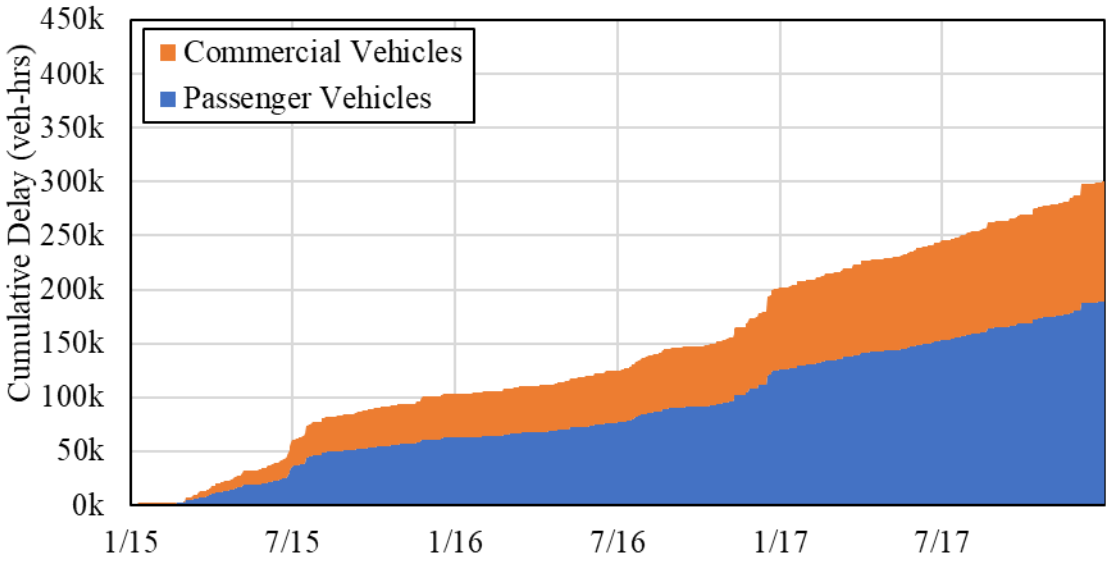

(a) I-65, mile post 167-176 (work zone)

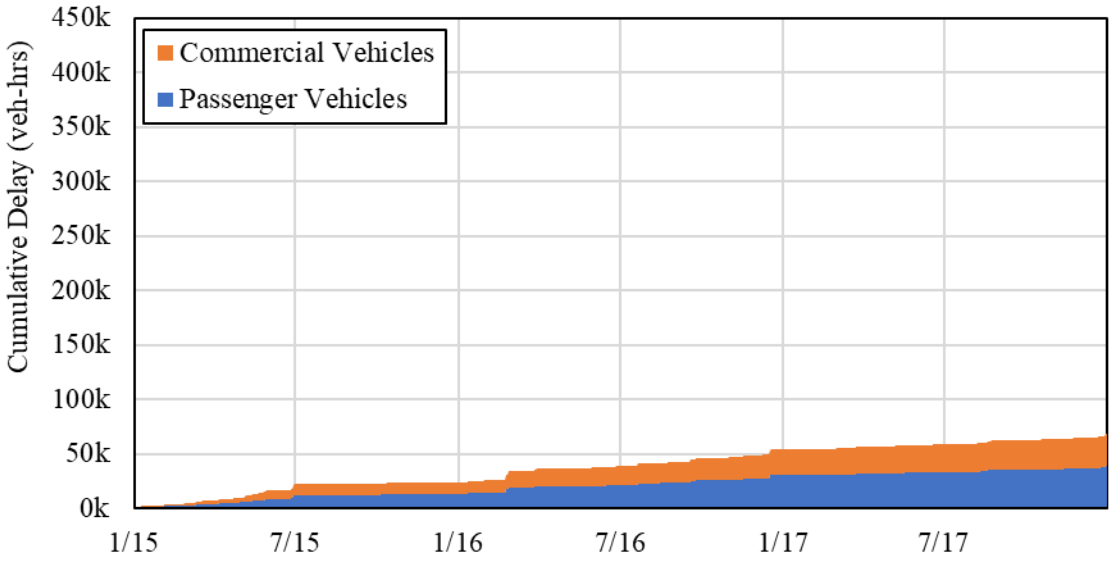

(b) I-65, mile post 181-190 (non-work zone)

Figure 47 Cumulative vehicle-hours of delay by vehicle type over time on I-65

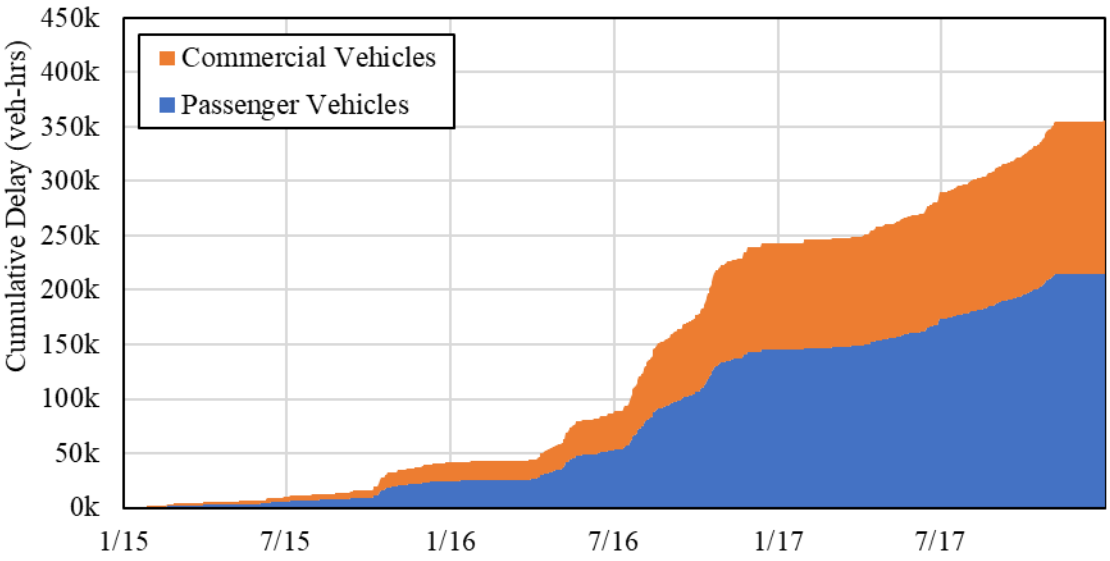

(a) I-70, mile post 0-20 (work zone)

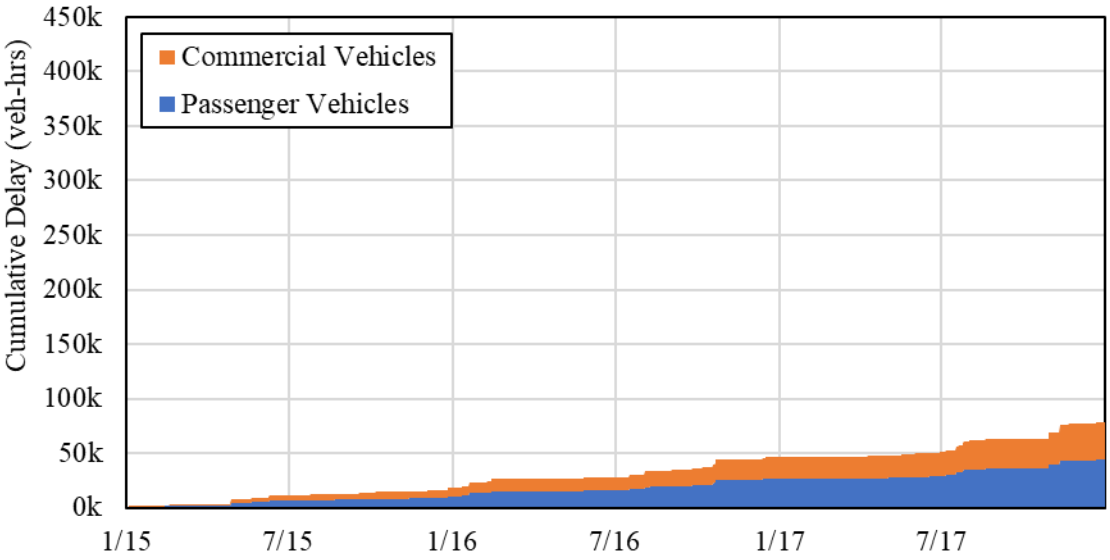

(b) I-70, mile post 20-40 (non-work zone)

Figure 48 Cumulative vehicle-hours of delay by vehicle type over time on I-70

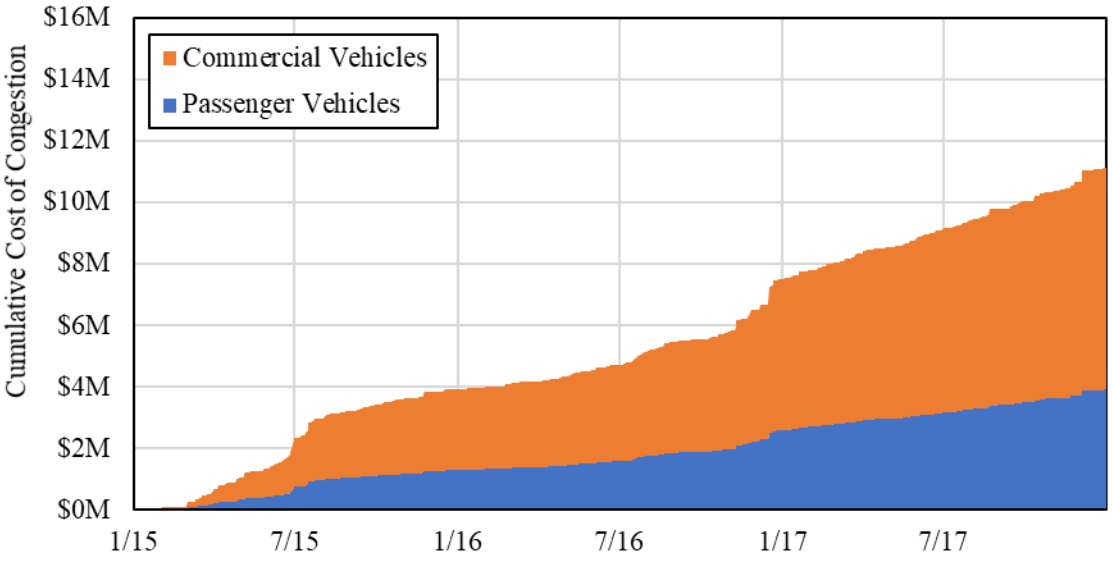

(a) I-65, mile post 167-176 (work zone)

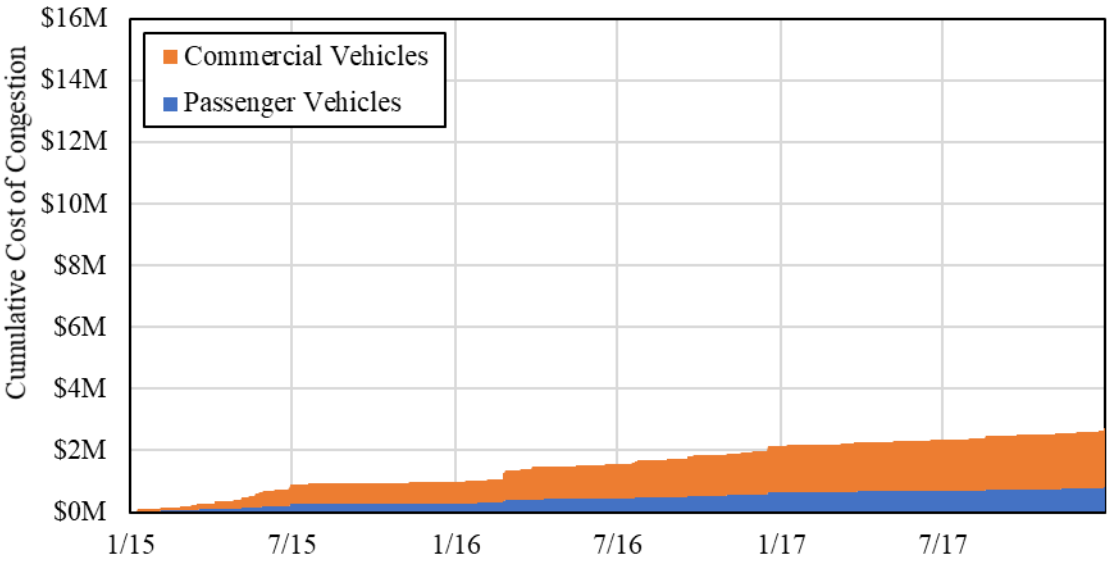

(b) I-65, mile post 181-190 (non-work zone)

Figure 49 Cumulative cost of congestion by vehicle type on I-65

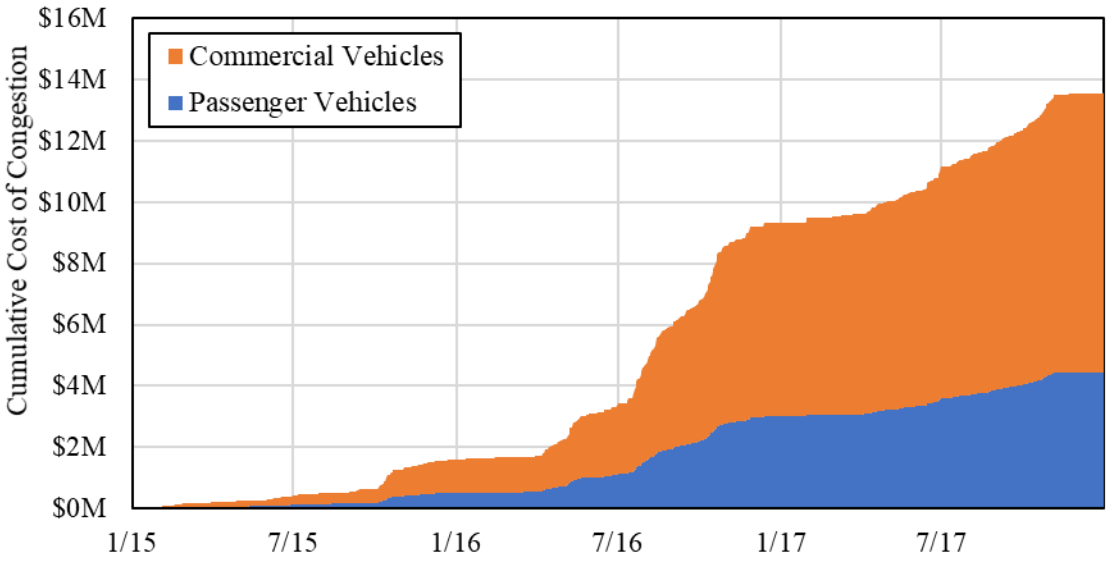

(a) I-70, mile post 0-20 (work zone)

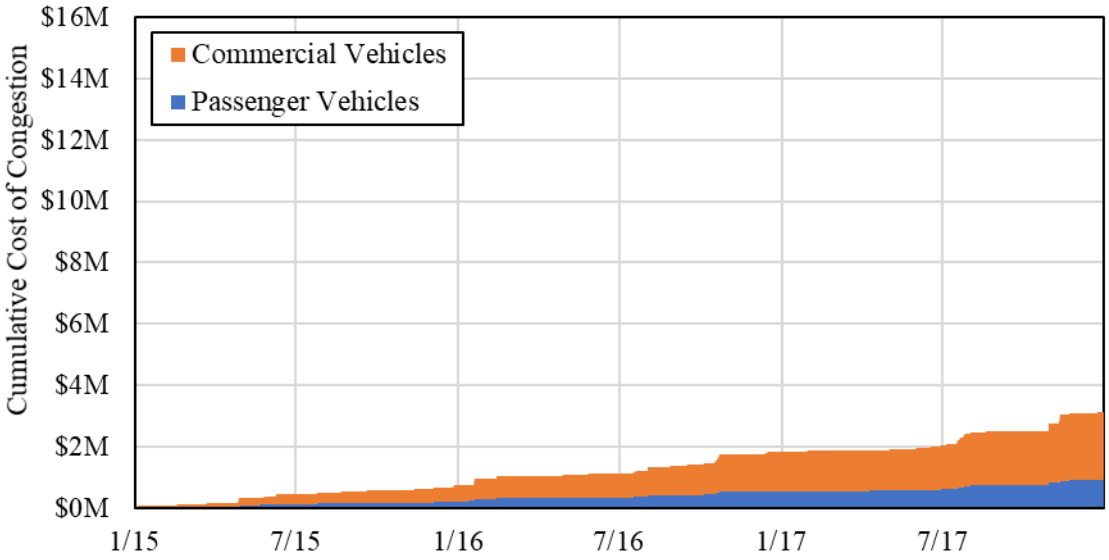

(b) I-70, mile post 20-40 (non-work zone)

Figure 50 Cumulative cost of congestion by vehicle type on I-70

Second, the economic impact of crashes was calculated. Figure 51a shows the number of crashes by severity for each study segment in the 3-year period. There were 16 fatal crashes, which are listed in Table 7. Figure 51b shows the number of damaged vehicles, injuries, and fatalities in the study segments.

The cost of these crashes was calculated using two methods. One method multiplied the number of crashes of a specified severity by the average cost of a crash of that type. The average costs of crashes by severity was taken from a 2005 FHWA report [87] and converted to 2017 dollars. The second method uses the economic unit cost per damaged vehicle, person injured, and person killed [88], also converted to 2017 dollars.

Figure 52a compares the cost of congestion and the cost of crashes (calculated suing the average cost per crash by severity) of the different study segments. The total costs of the I-65 and I-70 work zone segments are 2.58 and 3.31 times greater, respectively, than the non-work zone segments, in this case. Overall, the economic impact of the work zones was 2.96 times greater than the non-work zones.

Figure 52b compares the cost of congestion and the cost of crashes (calculated using the average cost per crash outcome) of the different study segments. The total costs of the I-65 and I-70 work zone segments are 3.57 and 3.00 times greater, respectively than the non-work zone segments, in this case. Overall, the economic impact of the work zones was 3.23 times greater than the non-work zones.

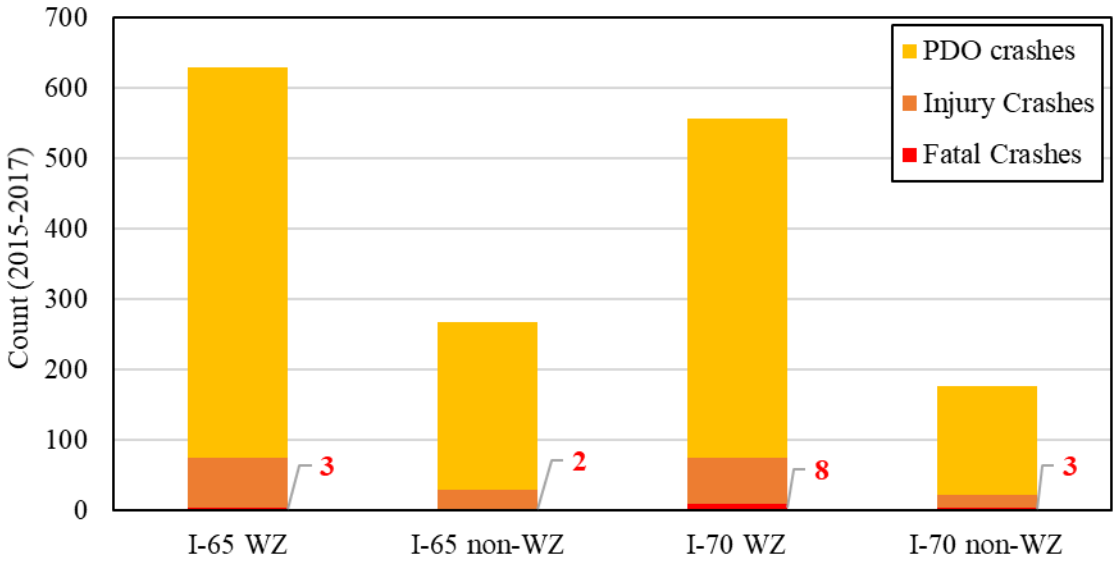

(a) By crash severity

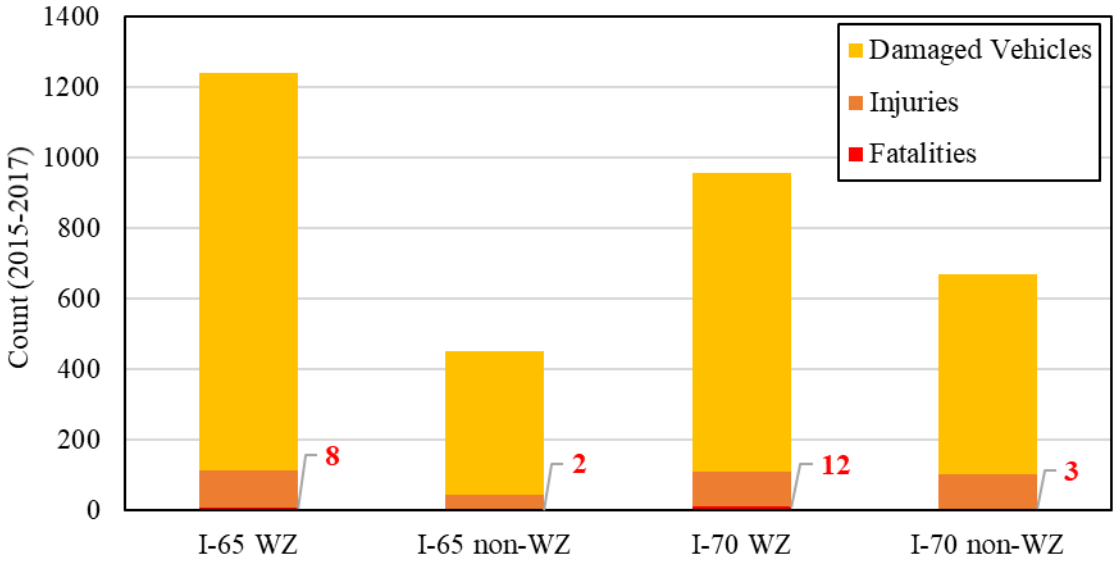

(b) By crash outcome

Figure 51 Comparison of crashes by study segment, 2015-2017

Table 7 Summary of Fatal Crashes in Study Segments, 2015-2017

	Date	Location	Description	Num. of Injuries	Num. of Fatalities
I-65 WZ	7/23/2015 23:54	I-65 S MP 177	Work zone back-of-queue crash	1	5
	5/20/2017 02:05	I-65 S MP 168	Ran off road, possible lane incursion	8	1
	12/5/2017 15:15	I-65 S MP 172	Work zone back-of-queue crash	2	2
I-65 non-WZ	3/10/2015 21:52	I-65 N MP 188	Dense fog	4	1
	3/10/2015 22:30	I-65 N MP 188	Dense fog	3	1
I-70 WZ	5/5/2015 01:33	I-70 E MP 11	Ran off road, OWI	0	1
	6/2/2015 13:00	I-70 W MP 7	Pedestrian action	1	1
	10/6/2015 13:40	I-70 E MP 10	Illegal U-turn	0	1
	4/23/2016 06:05	I-70 W MP 13	Hit and run, pedestrian	0	1
	5/13/2017 16:55	I-70 E MP 4	Back-of-queue crash	0	4
	7/18/2017 02:46	I-70 W MP 17	Work zone back-of-queue crash	4	2
	8/6/2017 17:00	I-70 W MP 10	Work zone back-of-queue crash	1	1
	11/20/2017 10:36	I-70 E MP 1	Ran off road, tire failure	0	1
I-70 non-WZ	4/27/2015 17:50	I-70 W MP 22	Ran off road, OWI	0	1
	6/9/2015 03:48	I-70 E MP 28	Deer in road, pedestrian	1	1
	7/21/2017 17:29	I-70 W MP 27	Back-of-queue crash	2	1

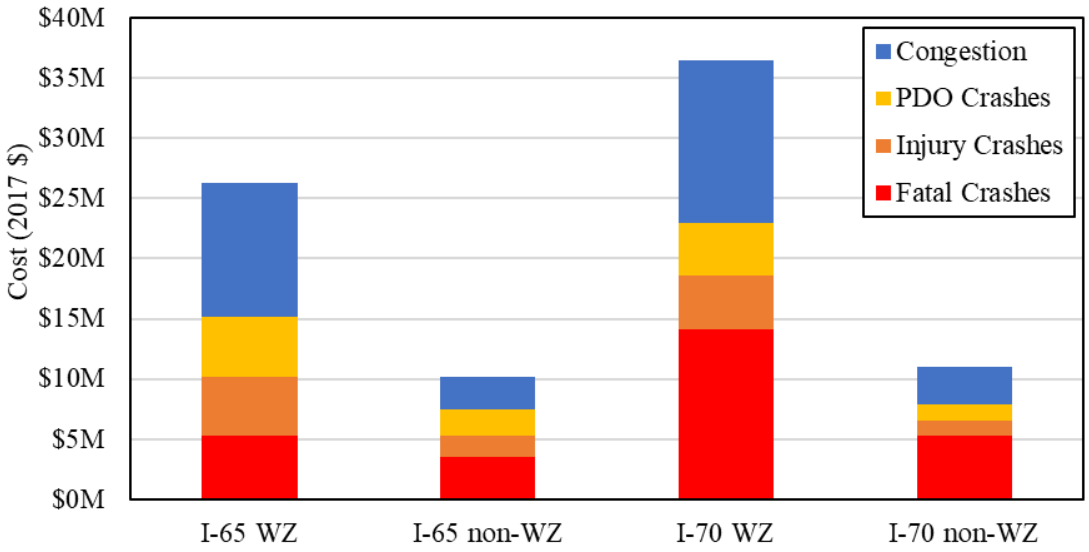

(a) Cost of congestion and crashes by severity

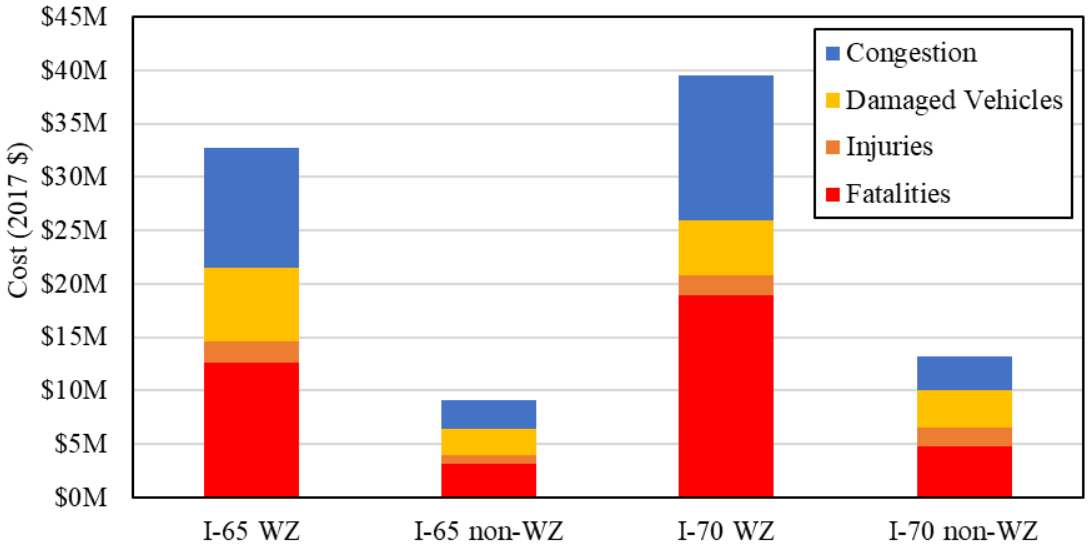

(b) Cost of congestion and crash outcomes

Figure 52 Comparison of cost of congestion and crashes, 2015-2017

6.4 Contribution

The weekly work zone reports and dashboards have already provided and will continue to provide INDOT traffic management personnel with valuable information. Active monitoring of work zones using these tools allow for more efficient use of time and resources. Managers can make informed decisions regarding the deployment of assets, enforcement, or the disbursement of information to the public.

7. MOBILE LIDAR FOR WORK ZONE INSPECTION

Between August 2016 and November 2017, work zone geometric data was collected via mobile LiDAR on 15 separate occasions and covering approximately 930 directional lane-miles (Table 8). In this chapter, the deployment process for the mobile LiDAR system will discussed. Advantages and disadvantages of this data source are summarized. Finally, a number of case studies were selected for detailed discussion on how connected vehicle data can be used to identify work zones with significant congestion, and how LiDAR can be used to identify geometric conditions that deviate from designs and are likely to contribute to the work zone queueing.

Table 8 Summary of Lane-Miles of Mobile LiDAR Data Collection

Date	Work Zone	Lane-Miles
8/12/2016	C2	60
10/12/2016	C2	60
11/5/2016	C4	36
12/1/2016	C3	68
4/7/2017	C2	30
5/1/2017	C3	73
5/2/2017	C4	40
5/11/2017	L1	61
5/18/2017	C2	64
6/1/2017	C1	73
9/18/2017	C4	80
9/19/2017	L1	84
10/2/2017	C2	76
10/3/2017	G5	76
10/31/2017	L1	46

7.1 Deployment Process

The locations for LiDAR data collection were selected from the set of work zones listed in Table 2. The selections were based on the work zone traffic performance observed in the weekly work zone reports. Most potential sites were selected when there

was recurring congestion or crashes at a consistent location or time. However, some sites were recommended for data collection based upon visual observations.

Upon selecting a data collection site, a team consisting of at least 3 persons and 2 vehicles was deployed (Figure 53). One vehicle was equipped with the mobile LiDAR unit. The second vehicle was equipped with flashing emergency lights. The second vehicle was intended as a shadow vehicle, which would alert other drivers to the slow-moving research vehicles. A driving speed of 40 MPH was selected for the research vehicles. This speed balances the impact on traffic and the density of the resulting data point cloud. The 3-person team consisted of two drivers and one technician to manage the equipment. As the technology matures, an equivalently dense point cloud may be achievable at higher speeds, necessitating only one vehicle.

Figure 53 Two-vehicle deployment for LiDAR data collection

Depending on the distance of the data collection site from the home base of the equipment (West Lafayette, IN, in this case), a preparation site would need to be chosen for set-up before and take-down after the data collection run. Set-up typically included mounting the LiDAR unit on the vehicle, staging calibration materials, calibrating the LiDAR unit, and taking down the calibration materials (Figure 54). System calibration was necessary to sync the two individual LiDAR scanners, the GPS unit, the accelerometer, and the camera that make up the mobile LiDAR unit. The set-up and calibration process typically took between 0.5 and 1 hour.

The area selected for data collection typically consisted of the entire length of the work zone plus the distance to the nearest interstate exits in both directions. For example, work zone C2 was on I-65 between mile posts 167 and 176. The nearest exits outside of the work zone boundaries were Exit 178 (IN-43) and Exit 158 (IN-28). The data

collection route for this work zone began on I-65 S at Exit 178, changed direction at Exit 158, and ended on I-65 N at Exit 178 for a total of 40 miles. At a speed of 40 MPH, this data collection run would take approximately 1 hour. The research vehicles would remain in the right lane except in cases of emergency vehicles on the shoulder or lane closures. If the work zone had split lanes (i.e. the right and left lanes separated by a median or barrier), two passes would be made through the work zone, one for each lane. In the future, agencies could use their authority to change direction via median crossovers and limit the time spent for data collection. This would be most useful in situations where there is a very specific area of interest within a long work zone.

After the data collection is completed, the equipment is packed up, which typically took 0.5 hour. The entire process included: travel to the site, set-up, calibration, data collection, take-down, and travel from the site. For the 15 data collection occasions in Table 8, with varied distances to and the desired lengths of the data collection sites, the entire data collection process ranged from 2 to 8 hours.

(a) Mounting of LiDAR unit

(b) Calibration set-up

Figure 54 Set-up and calibration prior to data collection

7.2 Advantages and Disadvantages

It is important to note that the system used in this study was incapable of real-time data processing. After the data collection process was completed and the data transferred to the appropriate party, it typically took 1-2 days of data processing to produce a point cloud depending on the size of the data set (and length of the data collection site). For additional data processing, such as automatic lane width extraction, another 1-2 days would be needed after data collection. If a narrower area or specific feature of interest is specified, the time needed for data processing can be reduced. Because the mobile LiDAR unit used in this study included a camera, features observed in the point cloud could be compared with camera imagery. This made it easier to identify and measure specific work zone features.

All agencies apply highly reflective glass beads or elements to pavement markings to improve night visibility. Well-maintained retro-reflective markings provide very high contrast in LiDAR point clouds (Figure 9c) and can be easily extracted via automated processes. However, extraction requires manual processing if markings are old and have poor retro-reflectivity characteristics.

Environmental conditions need to be considered when using LiDAR. Unlike video data collection, LiDAR can be used at night. In one nighttime lane closure, workers in reflective gear standing in front of a flood light were more visible in the LiDAR point cloud than could be visually observed by the driver. However, in nighttime scenarios, it may be difficult to compare the LiDAR point cloud with corresponding camera images. Additionally, LiDAR performance significantly degrades when there is precipitation. Precipitation can also be damaging to the equipment. When planning a data collection run, it is necessary to check and plan around the weather in the area.

As mentioned briefly above, the speed at which the mobile LiDAR travels affects the density of the data point cloud. Slower speeds will produce denser point clouds but may be less safe on high speed facilities, such as freeways. In this study, 40 MPH was chosen because it was the minimum allowable speed on Indiana interstates. All data collection runs were conducted with two vehicles: the vehicle mounted with the mobile LiDAR and a shadow vehicle equipped with strobe lights to alert other drivers to the

slow-moving vehicles. As LiDAR technology matures and sampling frequency increases, these speed constraints will not be a concern. In fact, there are currently LiDAR systems that can be deployed at 70 MPH that will provide sufficient resolution, but their cost exceeded the budget of this study.

Lastly, the LiDAR data is reproducible. LiDAR data was collected along US-231 S near West Lafayette and I-70 W near Terre Haute on multiple occasions (Figure 55). On US-231 S, three different runs were made. Between the 11/30/2016 and 2/11/2017 runs, the root mean square error was 0.049 ft. Between the 11/30/2016 and 8/17/2017 runs, the root mean square error was 0.099 ft. On I-70 W, aside from the movement of drums for a lane closure, the lane markings and concrete barriers in this work zone remained the same between the 11/5/2016 and 5/22/2017 runs. For the 20-mile data set on I-70, the root mean square error of the lane width measurements was 0.054 ft.

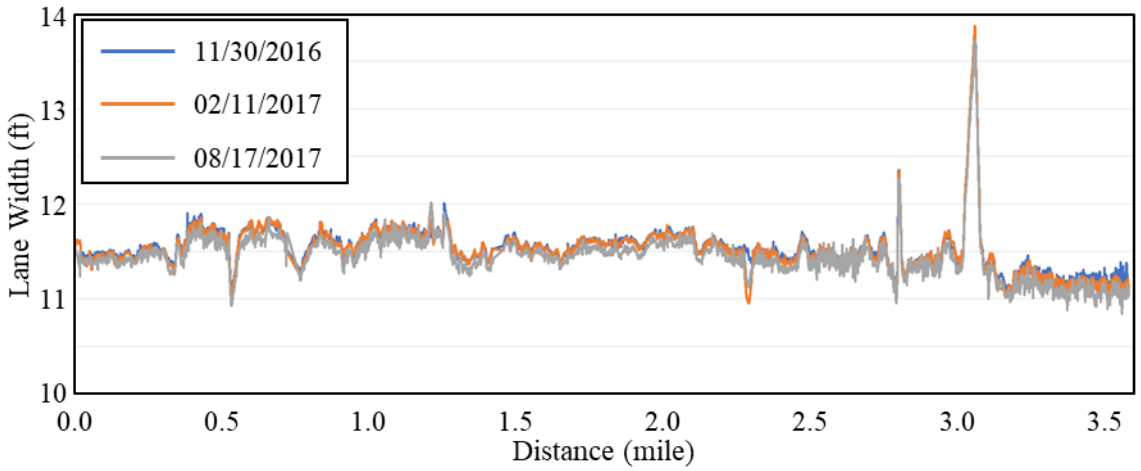

(a) US-231 S

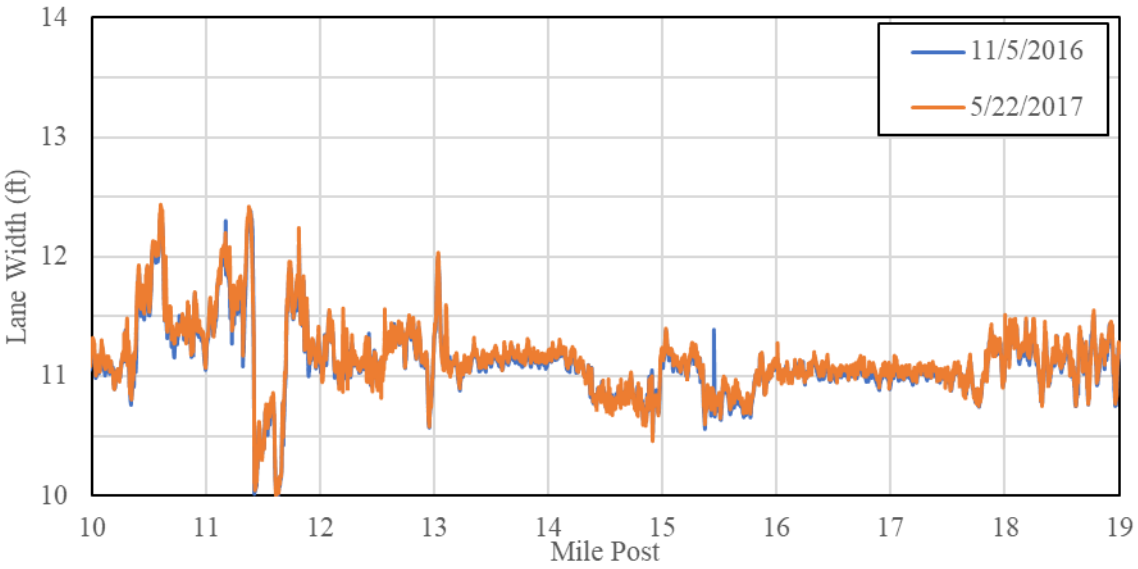

(b) I-70 W

Figure 55 Comparison lane width measurements from different data collection dates

7.3 Case Studies

The following case studies detail the use and results of the mobile LiDAR system work zone inspection. Discussion will include the reasoning behind the data collection and the results of the analysis of the point cloud. In some cases, mitigating actions were taken.

7.3.1 Reverse Curve

Beginning in the week of July 4, 2016, the magnitude of congestion and frequency of crashes increased on I-65 S in Tippecanoe County, in the C2 work zone. The congestion and crashes were concentrated in the area of mile post 173 to 176 (Figure 56). The frequency of crashes within the work zone increased by 2.9 times, from an average 1.75 crashes per week to 5 crashes per week.

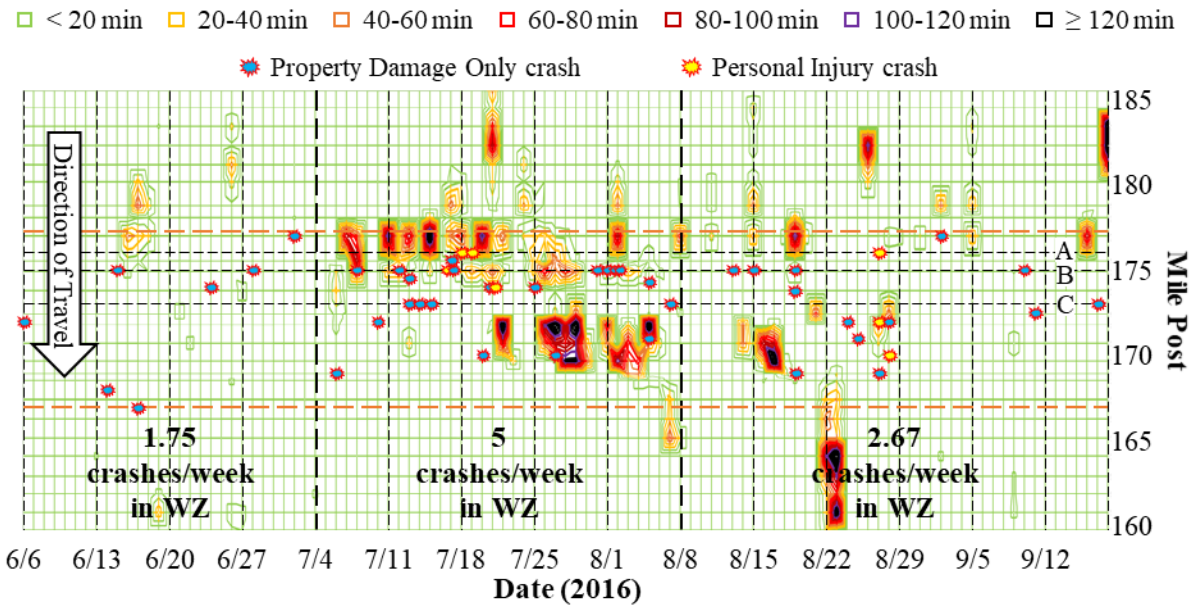

Figure 56 Crashes and frequency of speeddelta ≥ 15 MPH on I-65 S (C2)

In response to the increase in congestion and crashes, initially observed in the weekly work zone report, a visual inspection of the work zone was conducted. It was determined that during the week of July 4, 2016, there had been a construction phase change, resulting in a change in the maintenance of traffic. Three locations of interest were identified (A, B, and C) and are labelled in Figure 56. The southbound lanes split at Location A (mile post 176) (Figure 58a), with the left lane crossing over the median and the right lane shifting onto the left shoulder. Both lanes were shifted with a reverse curve. At Location B (mile post 175), traffic from the southbound entrance ramp from IN-25 merged with the right lane (Figure 58b). At Location C (mile post 173), the left lane crossed over the median again and the right lane shifted back to its original position (Figure 58c and Figure 58d). Both lanes were shifted with a reverse curve.

Figure 57 Map of C2S (I-65 S) work zone for July-August, 2016

(a) Location A (mile post 176)

(b) Location B (mile post 175)

Figure 58 Photos from C2S (I-65 S) work zone on July 28, 2016

Figure 58 continued

(c) Location C – right lane (mile post 173)

(d) Location C – left lane (mile post 173)

Based on the gathered traffic, crash, and photographic data, the following conclusions were drawn. First, drivers were slowing down upon arriving at the north reverse curve (Location A), causing recurring congestion. Second, there was an increase in traffic conflicts and crashes at the IN-25 entrance ramp (Location B) due to a shortened acceleration lane and distracting construction activity. Vehicles traveling in the right lane were unable to shift lanes to allow for the entrance ramp traffic to merge. Third, vehicles were shifting lanes too early or unintentionally at the south reverse curve (Location C). The navigation of reverse curves can be a complex task for drivers and can be difficult at high speeds.

During the week of August 8, 2016, the solid line between the lanes at Location C was extended by 300 ft, a “LANE ENDS MERGE LEFT” (W9-2) sign was added to the entrance ramp at Location B, and a trailer camera was deployed to Location C. On August 12, 2016, the mobile LiDAR system was deployed for the first time in an interstate work zone. Figure 59 shows the LiDAR point clouds at Location A and Location C. After the changes were implemented the crash frequency decreased by 0.5 times, from 5 crashes per week to 2.67 crashes per week.

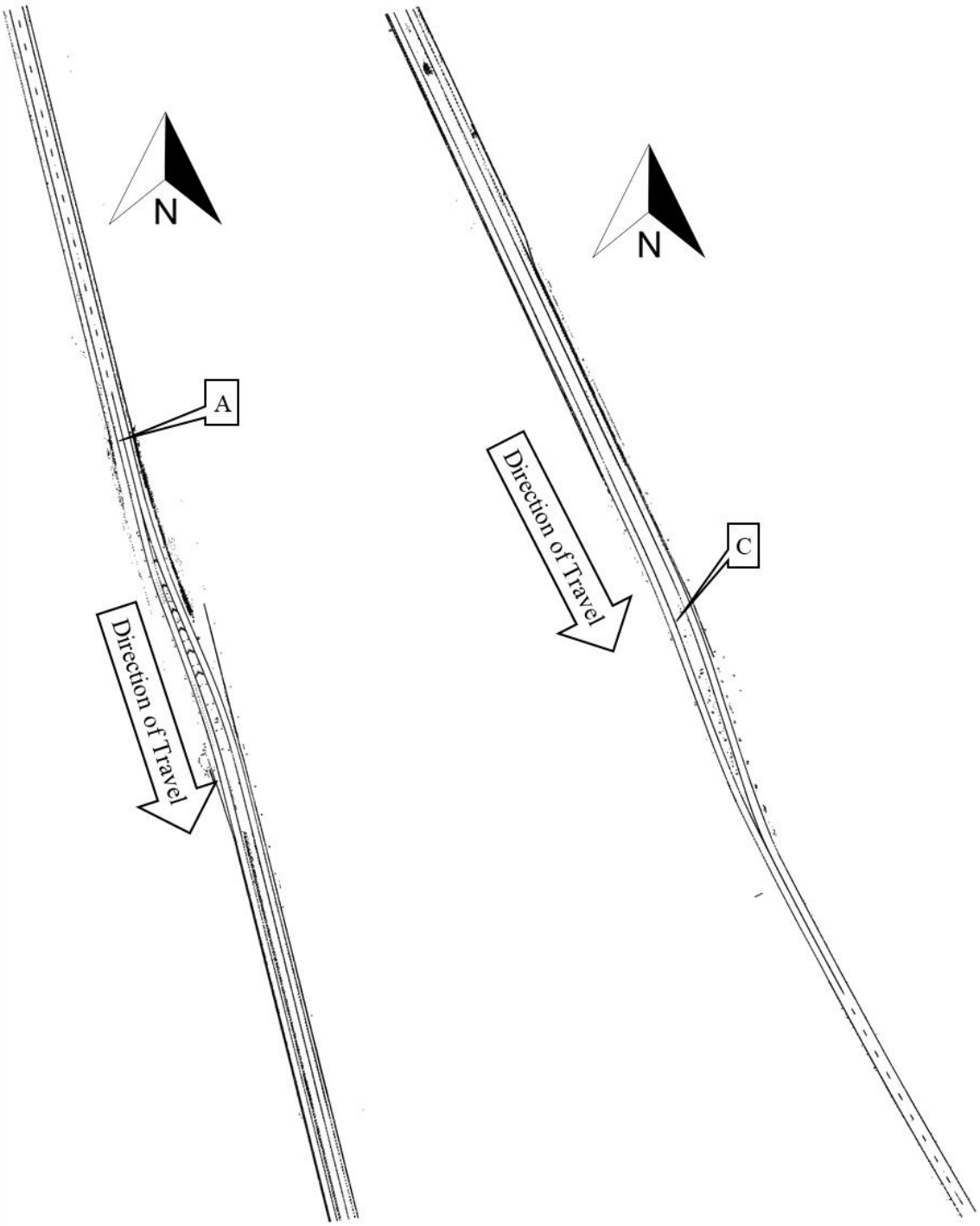

(a) Location A (mile post 176) (b) Location C (mile post 173)

Figure 59 LiDAR point cloud at reverse curve locations

7.3.2 Lane Width

During April and May of 2017, there was recurring congestion on I-70 W in Vigo County (C4 work zone). From mile post 12 to 10, the two lanes of travel were shifted towards the left shoulder with a concrete barrier on the right shoulder. In this location, commercial vehicles make up about 40% of traffic volumes. Vehicles consistently slowed down in the area of mile post 11.5 to 11 (Figure 60a). In Figure 60a, the dashed orange lines represent the work zone boundaries. The mobile LiDAR system was deployed to the work zone on May 22, 2017. From LiDAR point cloud, the lane width of the right lane by longitudinal location was extracted (Figure 60b). At approximately mile post 11.62, the lane width briefly narrows to 10 ft (callout 'i' in Figure 60). For this work zone, the minimum lane width allowed by INDOT is 11 ft.

Figure 61 shows photos of this location taken from the mobile LiDAR vehicle. During this phase of construction, the left lane would sometimes be closed during the day (Figure 61b) and all vehicles were required to drive in the narrow right lane. On days with lane closures, such as April 19, 2017 (Figure 60a), there is a greater impact on traffic. This data shows that the short narrow lane section has a recurring impact on traffic. Queues extended upstream of the work zone on 4 days within this time period.

The LiDAR point cloud at this location can be seen in Figure 62. Measured from the point cloud, the distance between the drum and the center, dashed lane marking, S_L, was 1.41 ft. The distance between the center lane marking and the right lane marking, or the lane width, W, was 10.01 ft. The distance between the right lane marking and the concrete barrier, S_R, was 1.48 ft. In nearby locations, the distance to the barrier decreased to less than 1 ft.

It would have been time-consuming and unsafe for an inspector or contractor to manually measure the lane widths in this 12-mile section at regular intervals. It is also difficult to identify the narrow lane section visually without the presence of a wide vehicle, such as in Figure 61a. The data collection process took only 20 minutes once the mobile LiDAR system was set up and calibrated and the work zone was reached. With the automation of data processing, the lane widths measurements can be obtained within a few days of the data collection.

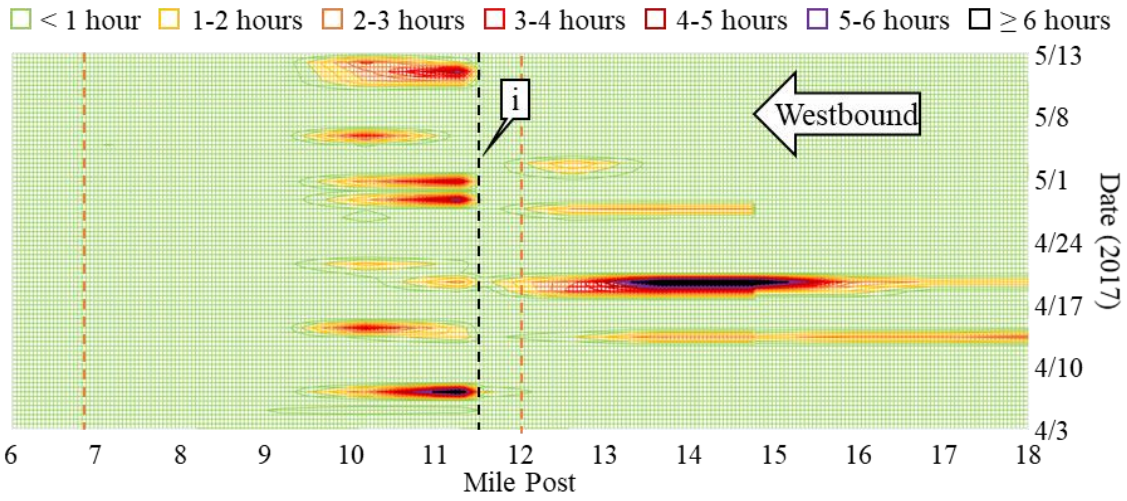

(a) Frequency of speeddelta ≥ 15 MPH

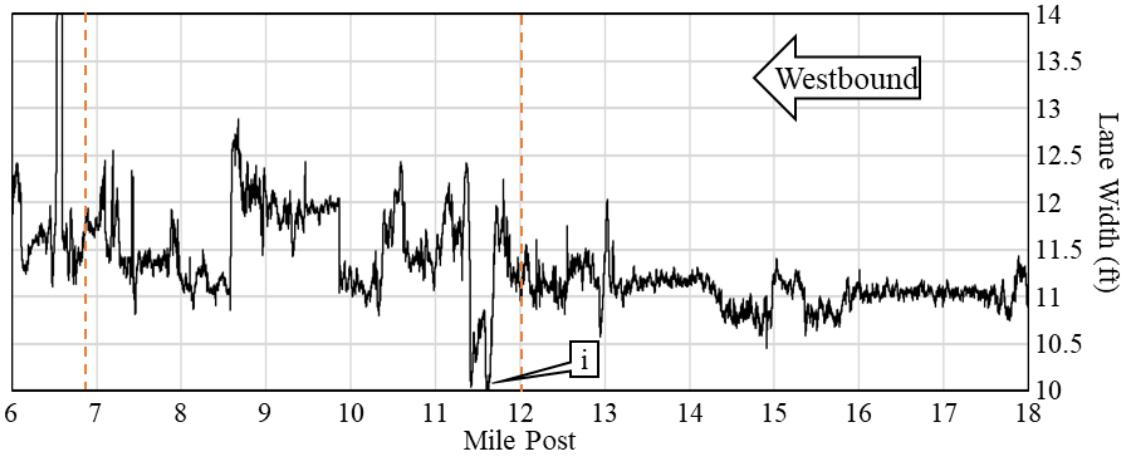

(b) Lane width by mile post

Figure 60 Comparison of lane width to frequency of speeddelta on I-70 W (C4)

(a) No lane closure (November 5, 2016)

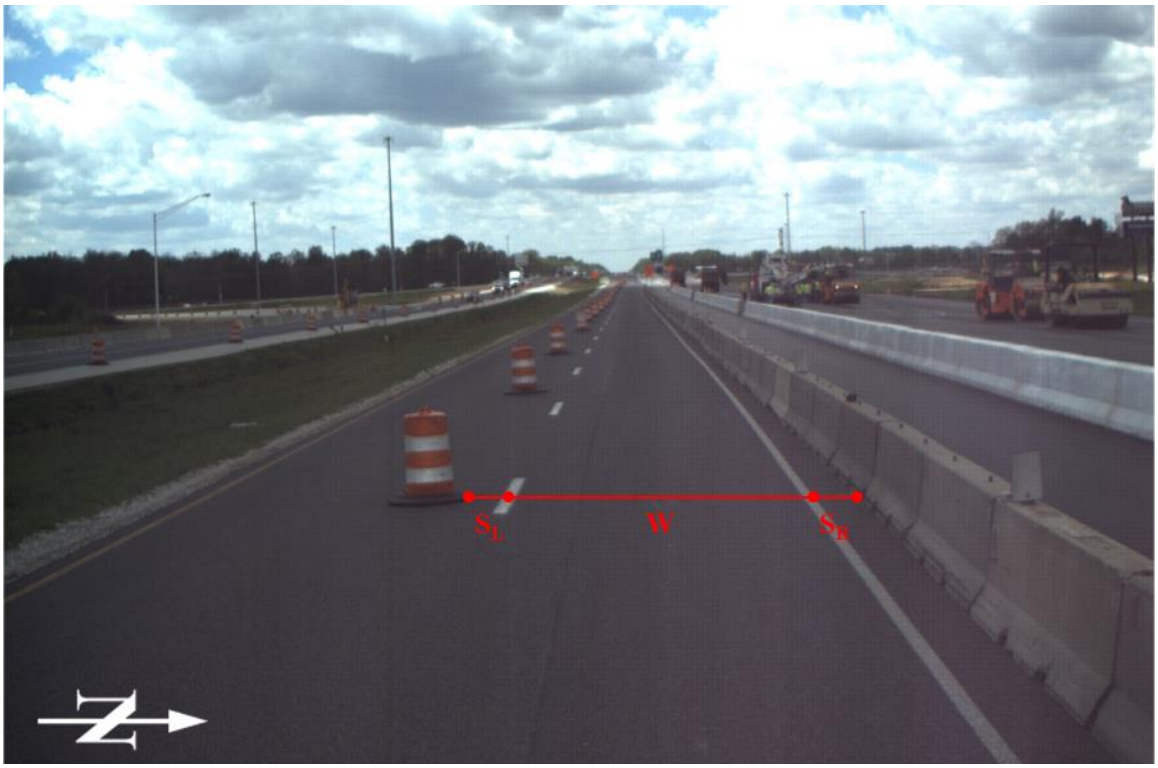

(b) Lane closure (May 22, 2017)

Figure 61 Camera images from mobile LiDAR vehicle at MP 11.62, I-70 W (C4)

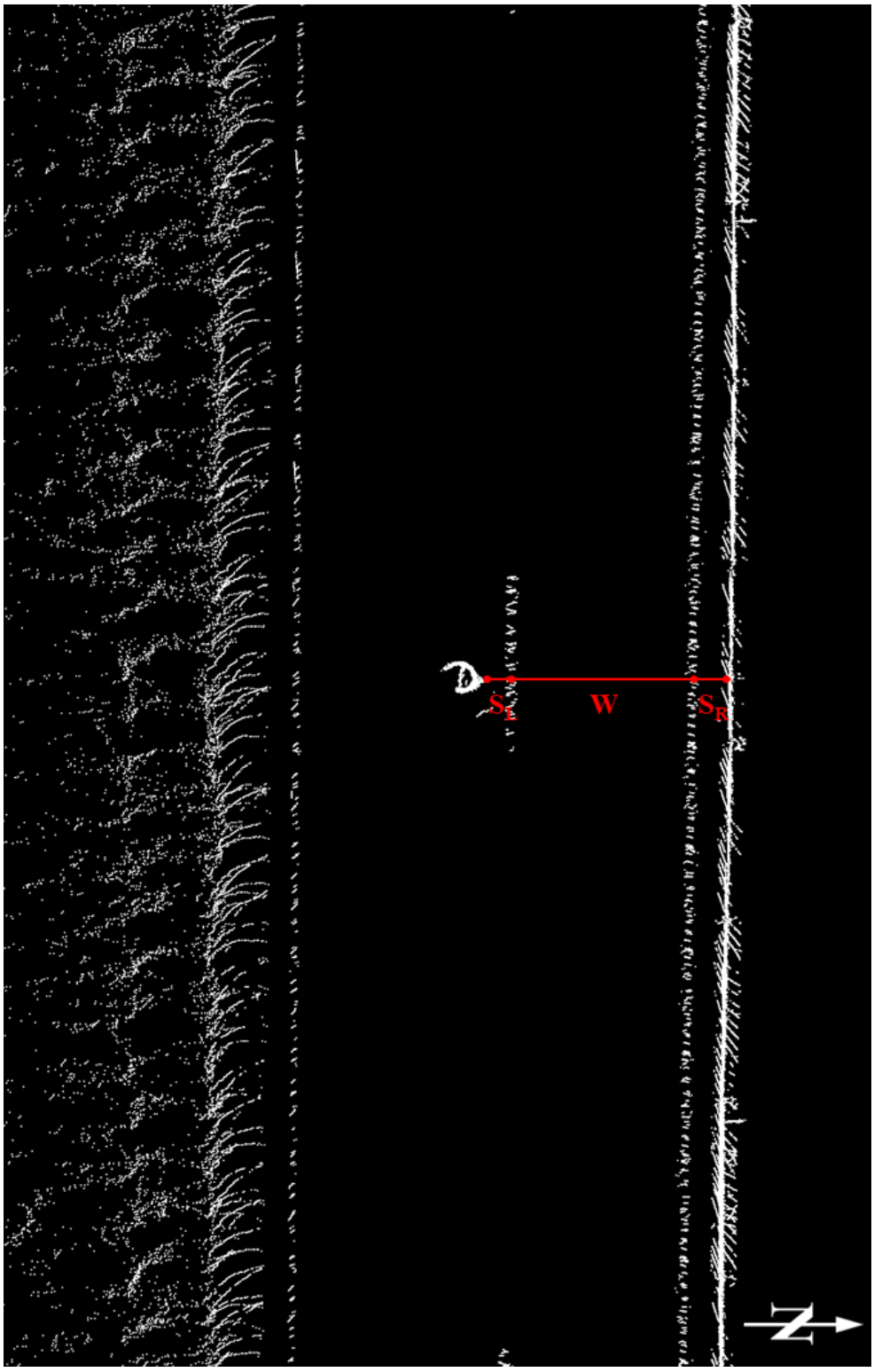

Figure 62 LiDAR point cloud at MP 11.62 on I-70 W (C4)

7.3.3 Taper Length

The third case study is from a work zone on I-65 N in northern Indiana (L2N), near Chicago. This area has high traffic volumes and recurring congestion under non-work zone conditions. Figure 63 is the frequency of speeddelta ≥ 15 MPH for mile post 259 to 261 during the week of May 8, 2017, with 30-minutes bins instead of 1-day bins. There is a congregation of hot spots between mile post 259 and 260 over the course of the week of May 8, 2017. The mobile LiDAR system was deployed to this work zone on May 11, 2017.

At mile post 259.8, there was a lane closure with a merging taper (Figure 64). The posted work zone speed limit was 55 MPH. According to the *INDOT Work Zone Traffic Control Guidelines* [28], the minimum required taper length is 680 ft. The *Manual on Uniform Traffic Control Devices* [27] recommended a taper length of 660 ft. Figure 65 depicts the lane markings and drums in the LiDAR point cloud. Callouts ‘i’, ‘ii’, ‘iii’, and ‘iv’ refer to the same objects in both Figure 64 and Figure 65. Callouts ‘i’ and ‘ii’ correspond to the first and last drum in the merging taper, respectively. Callout ‘iii’ corresponds to the arrow board on the left shoulder. Callout ‘iv’ refers to the 12 ft offset of the merging taper, or the width of the left lane. As measured in the LiDAR data, the actual merging taper length is only 471 ft, which is over 200 ft shorter than the INDOT minimum requirement.

This location has high traffic volumes and densely spaced, high-volume interchanges. In addition, this route became part of a detour for traffic heading to I-80 E. The typical route from I-65 N to I-80 E includes a ramp from I-94 E to I-80/I-90 E, which was closed during the implementation of the lane closure in the work zone. This likely caused an unanticipated increase in traffic volume, which would have contributed to the magnitude of congestion caused by the lane closure.

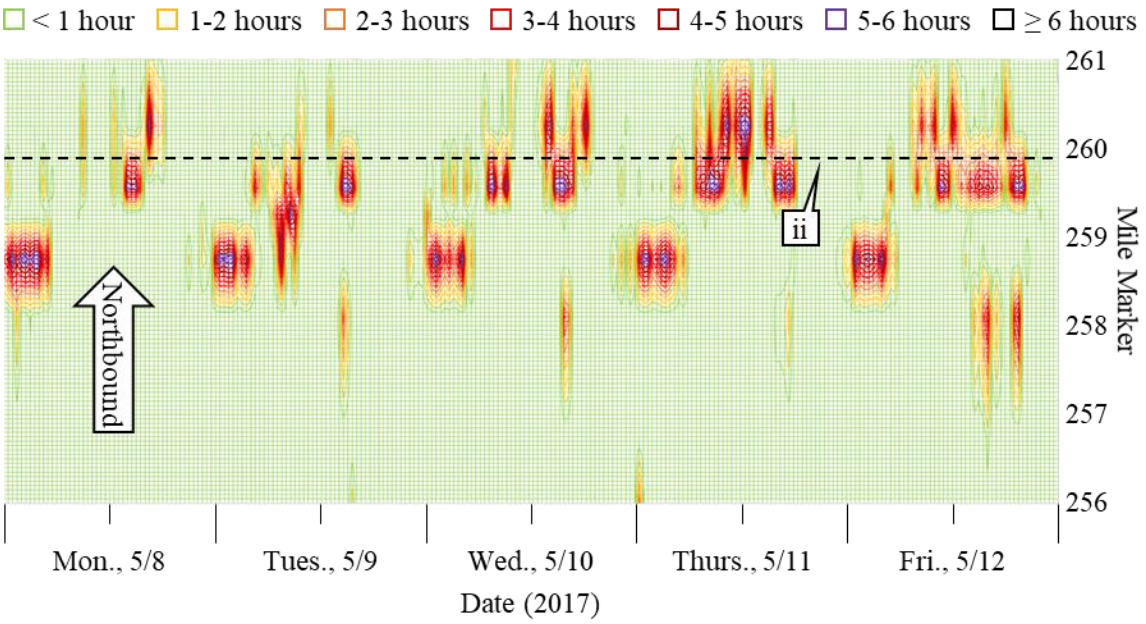

Figure 63 Frequency of speeddelta ≥ 15 MPH on I-65 N (L2)

Figure 64 Camera image from mobile LiDAR vehicle at MP 259.8, I-65 N (L2)

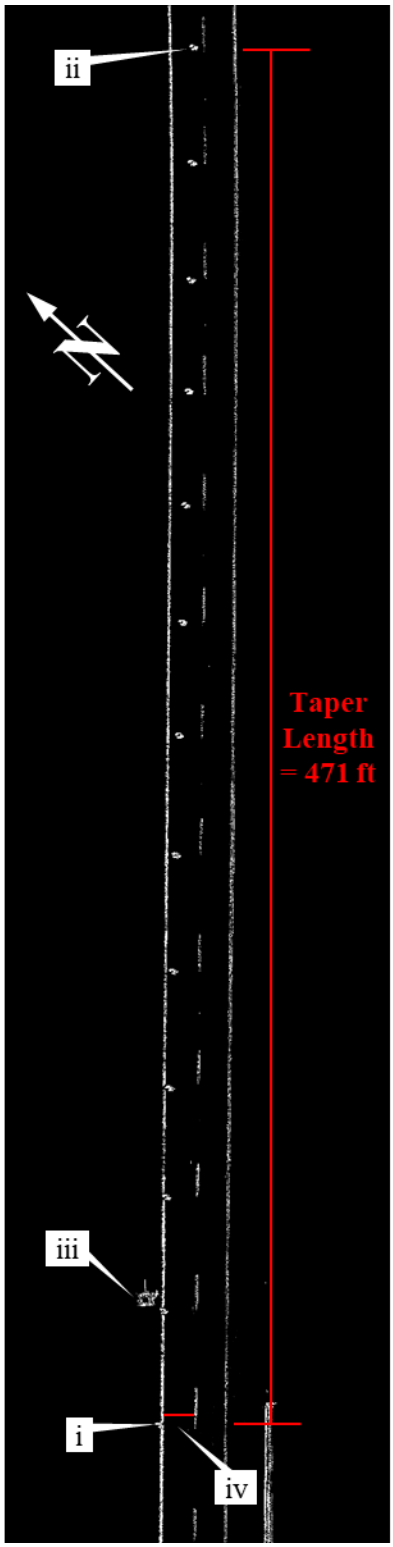

Figure 65 LiDAR point cloud at MP 259.8 on I-65 N (L2)

7.3.4 Nighttime Operation

On evening of June 1, 2017, construction workers closed the right lane of I-65 S at mile post 156 in Clinton County, IN (C1S). For several weeks in June and July of 2017, the primary construction activities in this work zone occurred at night due to restrictions by INDOT's *Interstate Highways Congestion Policy* [6]. In this area, a lane closure could occur only between 21:00 and 06:00. Construction activities moved to a different location each night. Figure 66 shows the queue heat map for mile post 155 to 160 on I-65 S for the evening of June 1, 2017. A queue formed at 21:00 at mile post 156 and dissipated at approximately 01:00. The maximum queue length during this time period was approximately 3 miles.

The mobile LiDAR system was deployed and reach mile post 156 on I-65 S at approximately 00:05. Figure 67 is a photo taken from the shadow vehicle. Callout 'i' is a construction drum. Callout 'ii' is a construction worker standing on the dashed, center lane marking and flagging vehicles to slow down. At this location, vehicle speeds were 15- 24 MPH. The posted speed limit was 55 MPH. Callout 'iii' refers to a group of construction workers on the right shoulder. All construction personnel were wearing appropriate reflective garments. Callout 'iv' refers to a floodlight attached to the top of a construction vehicle.

For drivers, it was difficult to see the construction workers past the glare of the floodlight. The flagger (callout 'ii') was not visible to the researchers until their vehicles reached the construction drum at Callout 'i'. Figure 68a shows the LiDAR point cloud at this location colored by reflective intensity on a blue background. The construction workers (callouts 'ii' and 'iii') and drums (callout 'i') are more clearly visible to the LiDAR system than to the human driver. However, the lane markings and edge of pavement at this location are not visible in the LiDAR point cloud. Figure 68b shows the LiDAR point cloud at this location colored by elevation on a white background. In this view, the construction vehicle with the floodlight (callout 'iv') are clearly visible.

This case study demonstrates some key advantages and disadvantages of LiDAR. Taking measurements based on lane markings is dependent on the quality (and existence) of the lane markings. For future consideration, autonomous vehicles that rely on LiDAR

technology would likely experience navigational difficulties in a work zone such as this. However, LiDAR can compensate for the lack of night vision in humans and standard cameras. Reflective materials stand out like beacons in the LiDAR point cloud, which is not affected by environmental lighting.

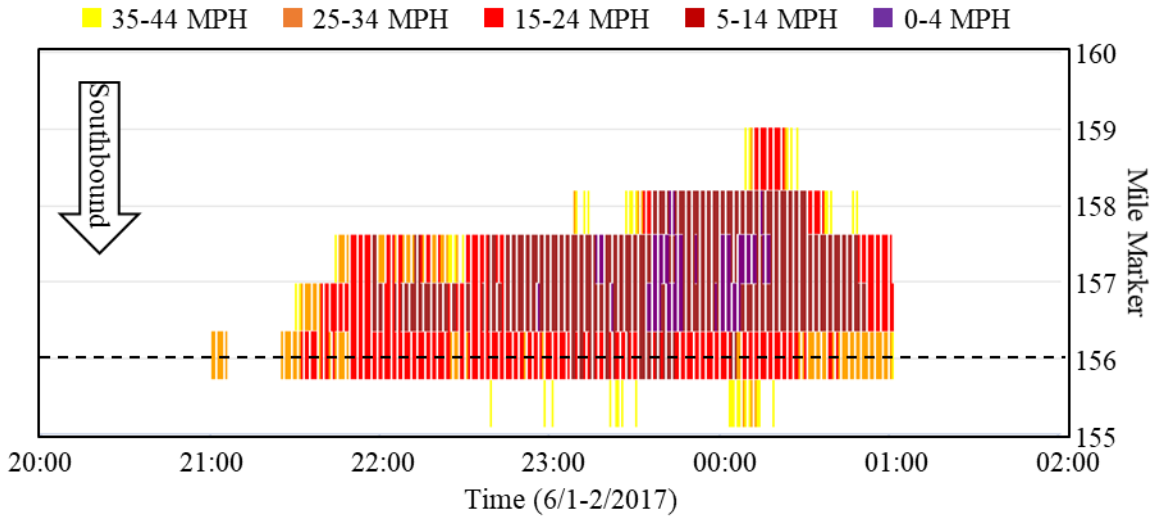

Figure 66 Queue heat map on I-65 S (C1)

Figure 67 Camera image from shadow vehicle at MP 156, I-65 S (C1)

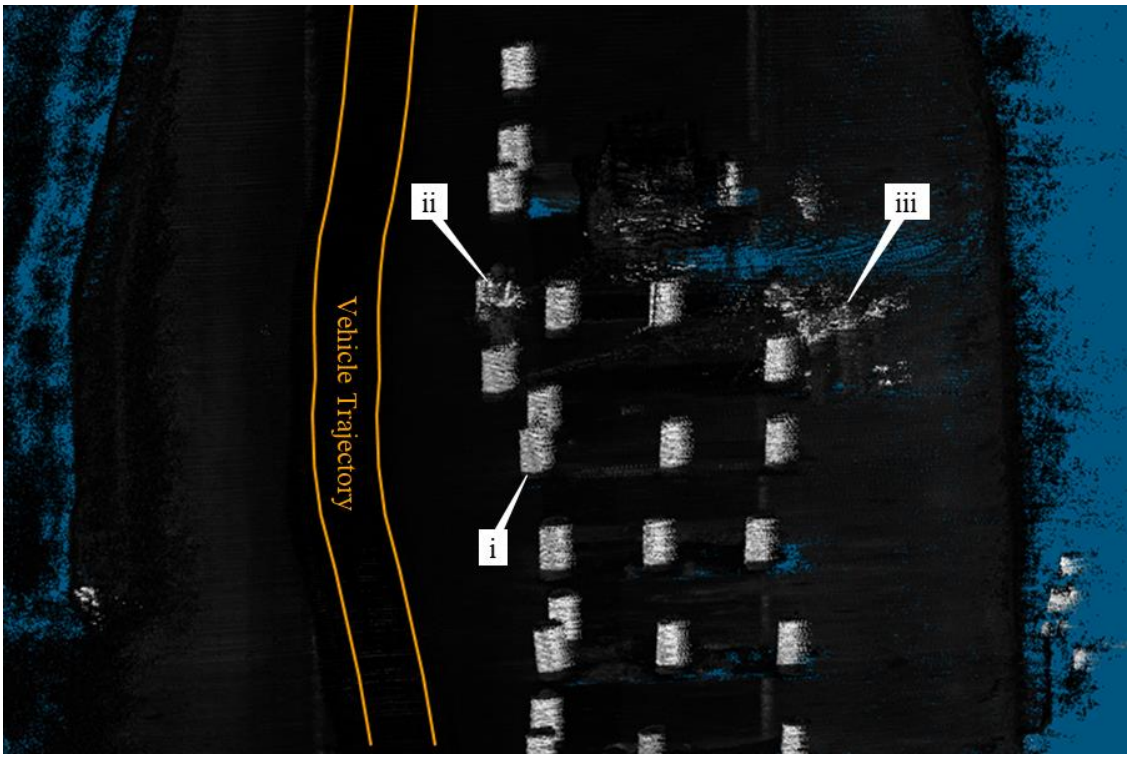

(a) Colored by reflective intensity

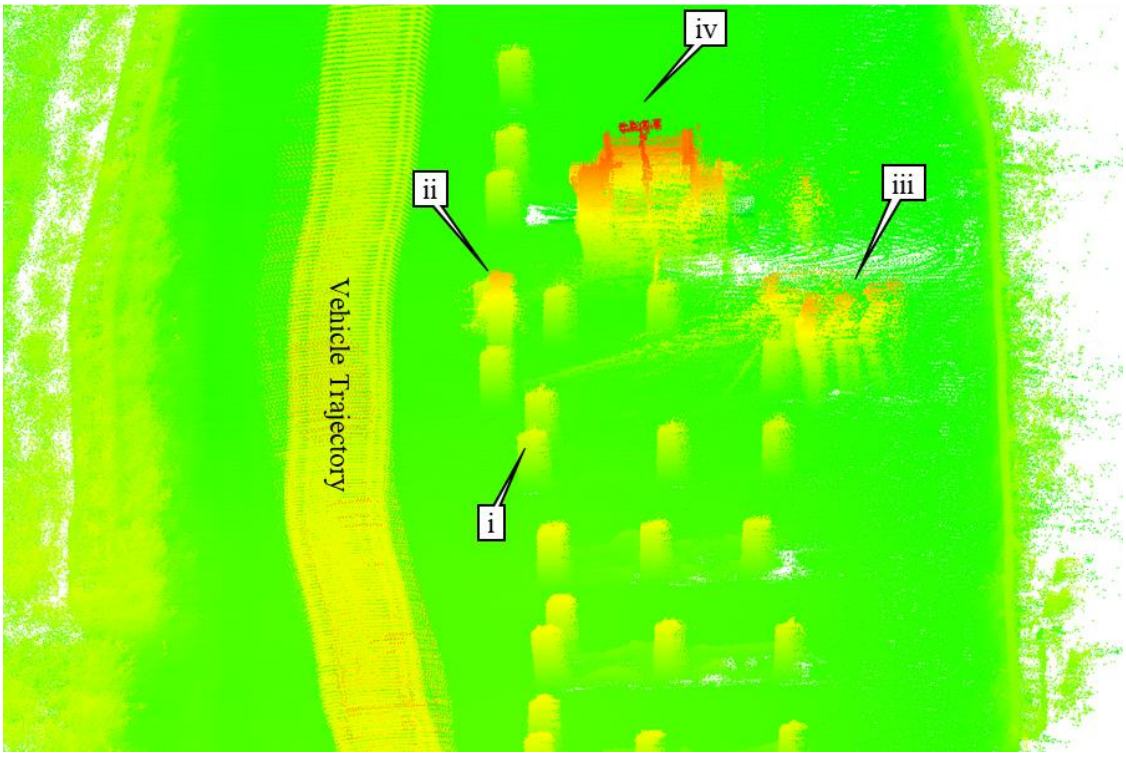

(b) Colored by elevation

Figure 68 LiDAR point cloud at MP 156 on I-65 S (C1)

7.3.5 Painting Operation

On the evening of October 2, 2017, the dashed, center lane markings on I-65 S near mile post 147 (C1S) were repainted. The mobile LiDAR system had been deployed on this evening to collect data for a lane closure in the C1S work zone. Figure 69a is a photo from the mobile LiDAR vehicle of an older, worn lane marking at mile post 153 in the work zone. Callout ‘i’ refers to a specific dash used in this analysis. Figure 69b is a photo from the mobile LiDAR vehicle of the fresh lane marking at mile post 147. Callout ‘ii’ refers to a specific dash used in this analysis. Callout ‘iii’ refers to the INDOT paint truck. Both lane markings are on asphalt pavement, though the fresh lane marking is on newer asphalt.

Figure 70 shows the LiDAR point clouds at both locations. Callouts ‘i’, ‘ii’, and ‘iii’ refer to the same objects in Figure 69 and Figure 70. Both point clouds include only data points with reflective intensities greater than or equal to 30. Figure 70a has more noise due to the aged pavement.

To compare the reflective intensity of the old and fresh paint, only the data points from the selected dashes (callouts ‘i’ and ‘ii’) where considered. Figure 71 is a cumulative frequency diagram of the reflective intensity of the data points within the old and new paint dashes. There is a significant difference between the reflectivity of the new paint and the old paint. Of particular interest are the shapes of the two curves. In both curves, there is a clear elbow at a reflective intensity of 100. A hypothesis to explain this phenomenon is that reflective intensities greater than 100 are due mostly to the presence of the glass beads found in the paint. It is expected that there is a greater amount of the glass beads in the fresh paint than in the old paint. This would result in a greater percentage of higher reflective points in the fresh lane marking. Future research into the application of LiDAR technology to retro-reflectivity measurements could be useful to agencies. In Indiana, retro-reflectivity is typically measured by an individual with a dedicated measurement device outside of a vehicle. Correlating LiDAR point cloud reflective intensity to standard retro-reflectivity measurements could potential save agencies money and time and increase the safety of their workers.

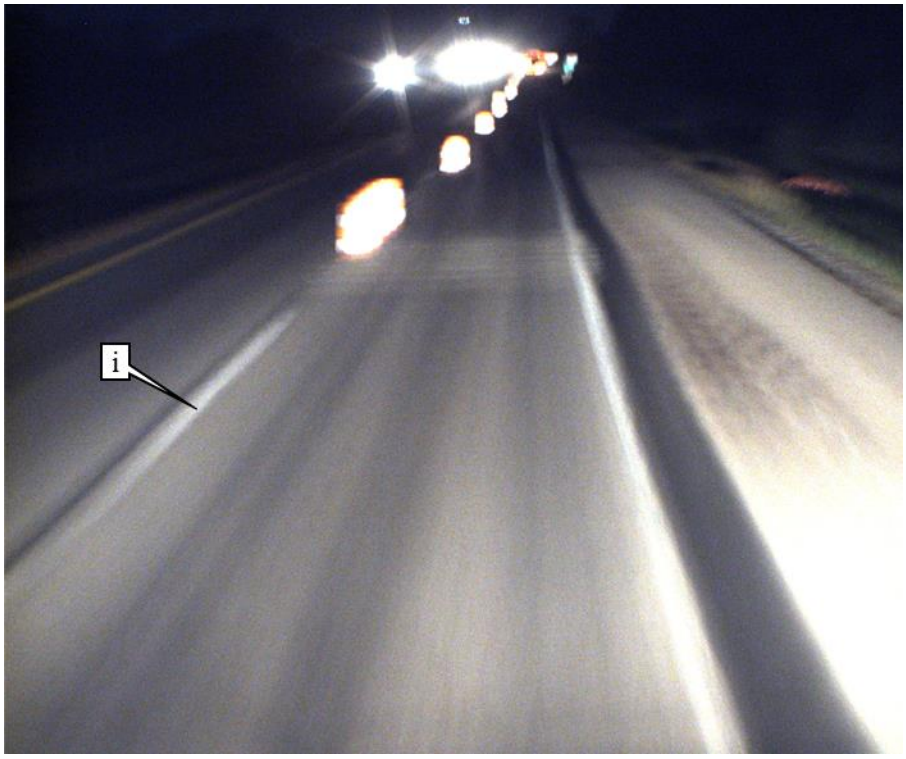

(a) Old paint (MP 153)

(b) Fresh paint (MP 147)

Figure 69 Camera images of lane markings on I-65 S (C1S), on October 2, 2017

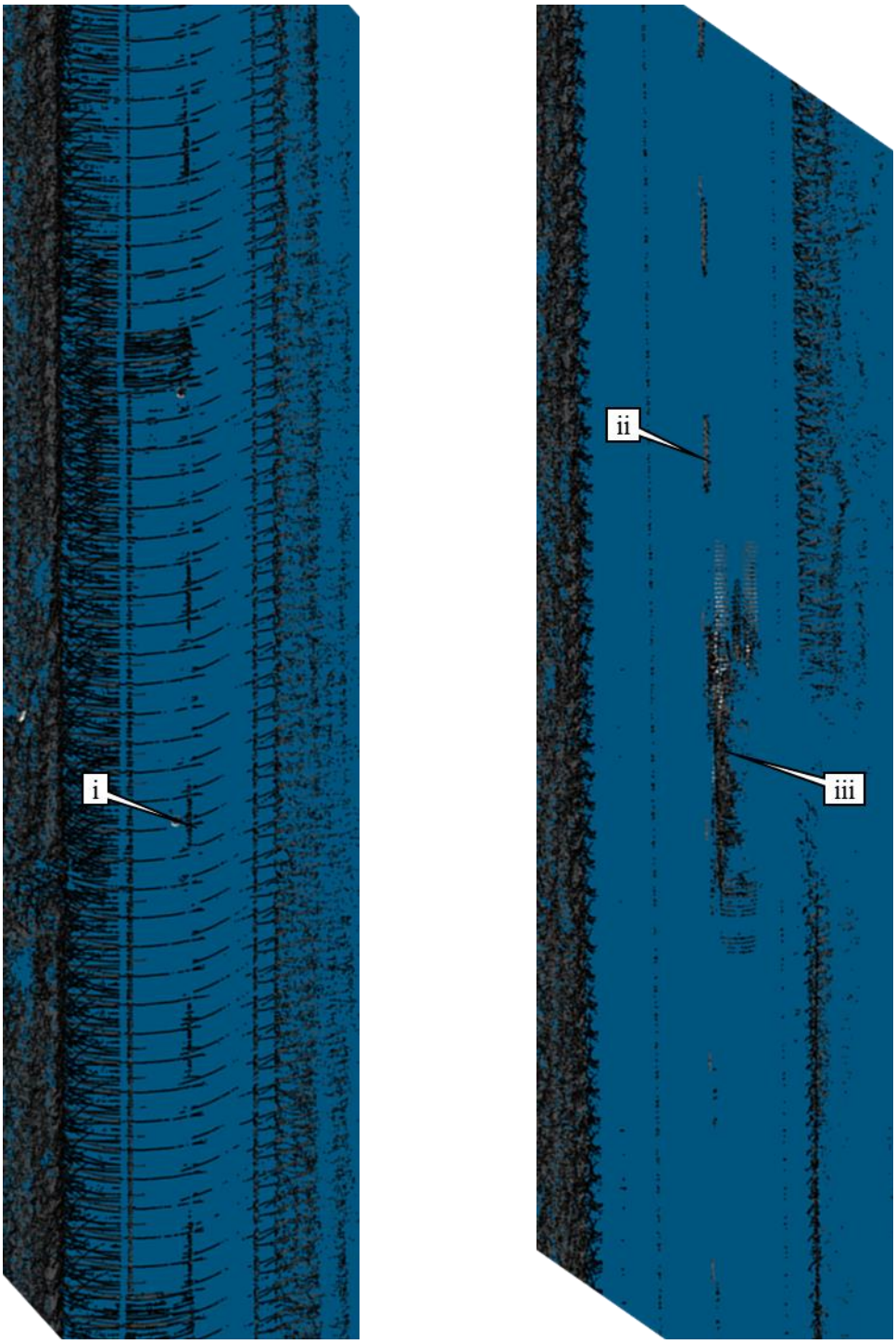

(a) Old paint (MP 153) (b) Fresh paint (MP 147)

Figure 70 LiDAR point clouds on I-65 S (C1)

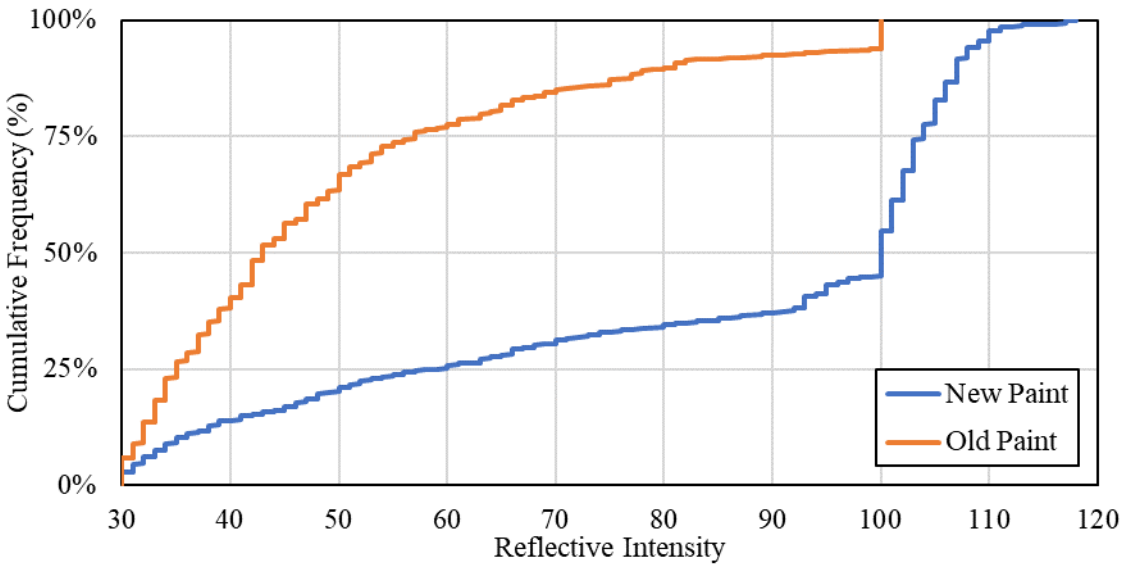

Figure 71 Comparison of reflective intensity of lane markings

7.3.6 Maintenance of Traffic Plans

The mobile LiDAR system was deployed to I-65 S between mile posts 253 and 234 (L1S) on September 19, 2017. There were negligible congestion and crashes in the weekly report for this work zone at this time. The decision to deploy was based on anecdotal evidence of a severe lane shift and a damaged guardrail by individuals that had driven through the work zone. The results of that deployment are focused on a 1500 ft section of the work zone near mile post 247 on I-65 S.

Figure 72 is a combined aerial view (courtesy of Google Maps), MOT plan overlay, and LiDAR point cloud overlay for the 1500 ft section from Station 1170+00 to Station 1155+00. The MOT plans consist of the black and gray overlay. The LiDAR point cloud (colored by elevation) overlay ranges from blue to bright red and is the topmost layer. Only the southbound lanes are shown in the point cloud. Callouts ‘i’, ‘ii’, and ‘iii’, ‘iv’ refer to the locations of photos in Figure 73 and Figure 74. The figure is split into 3 sections for a more detailed view. The MOT plan for this section of the work zone involved shifting the two southbound lanes onto the newly widened right shoulder, which is depicted as the solid light gray rectangle in Figure 72. The lane shift would be delineated with construction drums for the length of the shift (840 ft).

However, the actual, or implemented, start of the lane shift was about 180 ft further downstream than planned (Figure 72a). The implemented lane shift was split into two distinct segments. In Figure 73a, the degree of change between the existing lane markings and the start of the first segment of the lane shift was 3.90° to the right. In Figure 73b, the degree of change between the first and second segments of the lane shift was 2.11° to the right.

The actual end of the lane shift was about 60 ft further upstream of the planned end of the lane shift (Figure 72b). In Figure 73c, the degree of change between the second segment and the end of the lane shift was 1.21° to the left. The actual lane shift was 600 ft long, 240 ft shorter than planned. The planned ratio of longitudinal distance to lateral shift was 30:1. The implemented ratio was 26.1:1.

As there was negligible impact in terms of congestion, the difference between the plan and implementation may not have been a concern to INDOT or the project manager. However, due to an oversight in the plans, a guardrail was installed on the right shoulder at Station 1157+50 (Figure 72c) earlier than planned for in the MOT plan. While there were no reported crashes, the project manager confirmed that the guardrail had been hit by vehicles at least 4 times since the implementation of the lane shift. The distance between the right lane marking and the guardrail was 2 ft (Figure 73d).

During October of 2017, the contractor repaired the damaged guardrail and altered the maintenance of traffic implementation at this location to minimize future collisions. The mobile LiDAR system was redeployed to the location on October 31, 2017. The first segment of the lane shift was unchanged (Figure 74a). However, the second segment of the lane shift was removed (Figure 74b and Figure 74c) so that traffic no longer traveled on the new shoulder. This new configuration provided for 9 ft of space between the edge of the right lane and the guardrail (Figure 74d).

This case study demonstrates how inconsistencies in MOT plan implementation may not always be evident in the weekly work zone report. While the crashes in this case study went unreported, many agencies want to take proactive steps to prevent severe crashes before they occur. Using LiDAR technology could potentially help agencies identify deficiencies in work zone MOT plan implementation before problems arise.

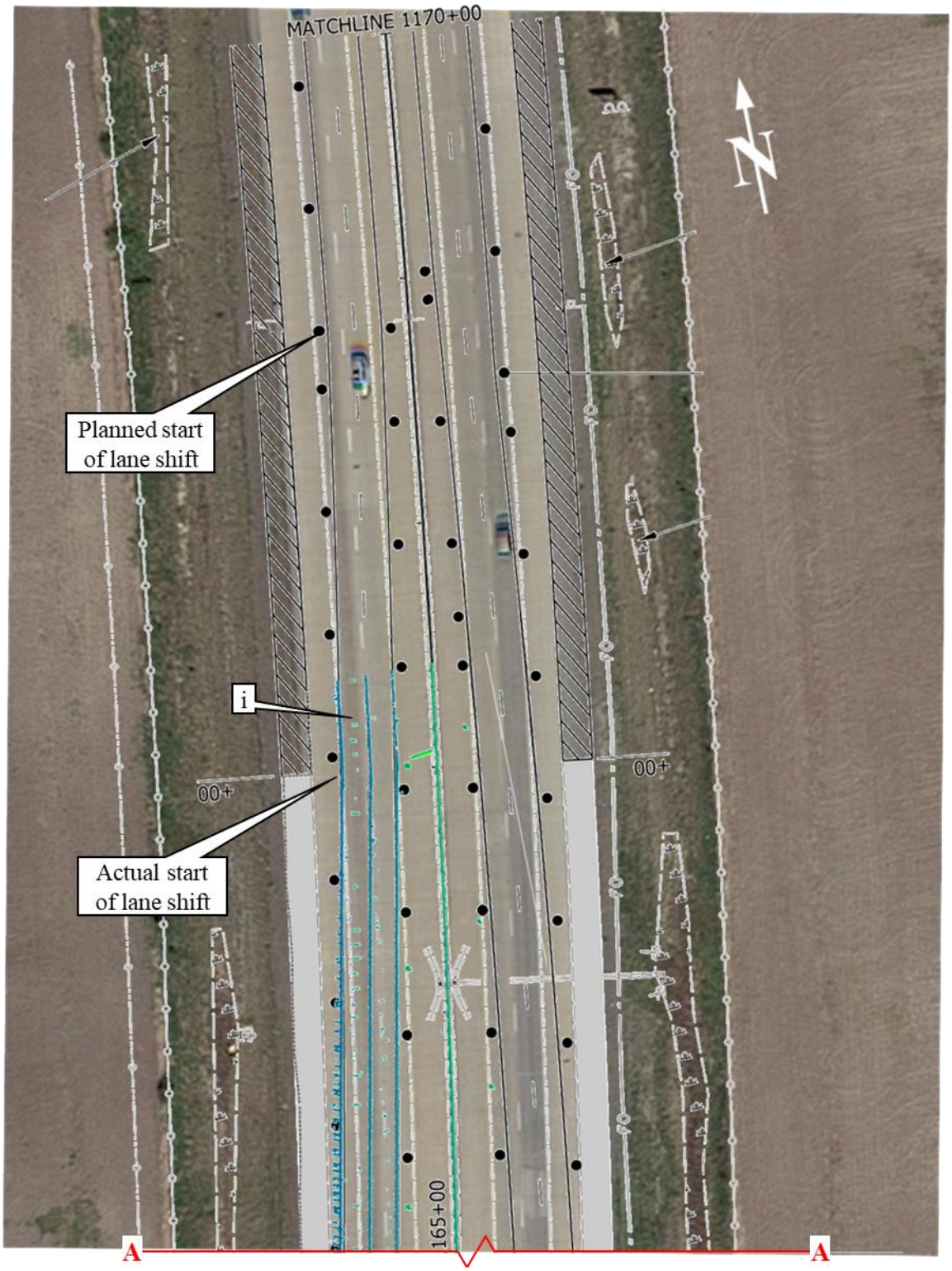

(a) STA 1170+00 to STA 1165+00

Figure 72 LiDAR point cloud at MP 247 on I-65 S (L1S)

Figure 72 continued

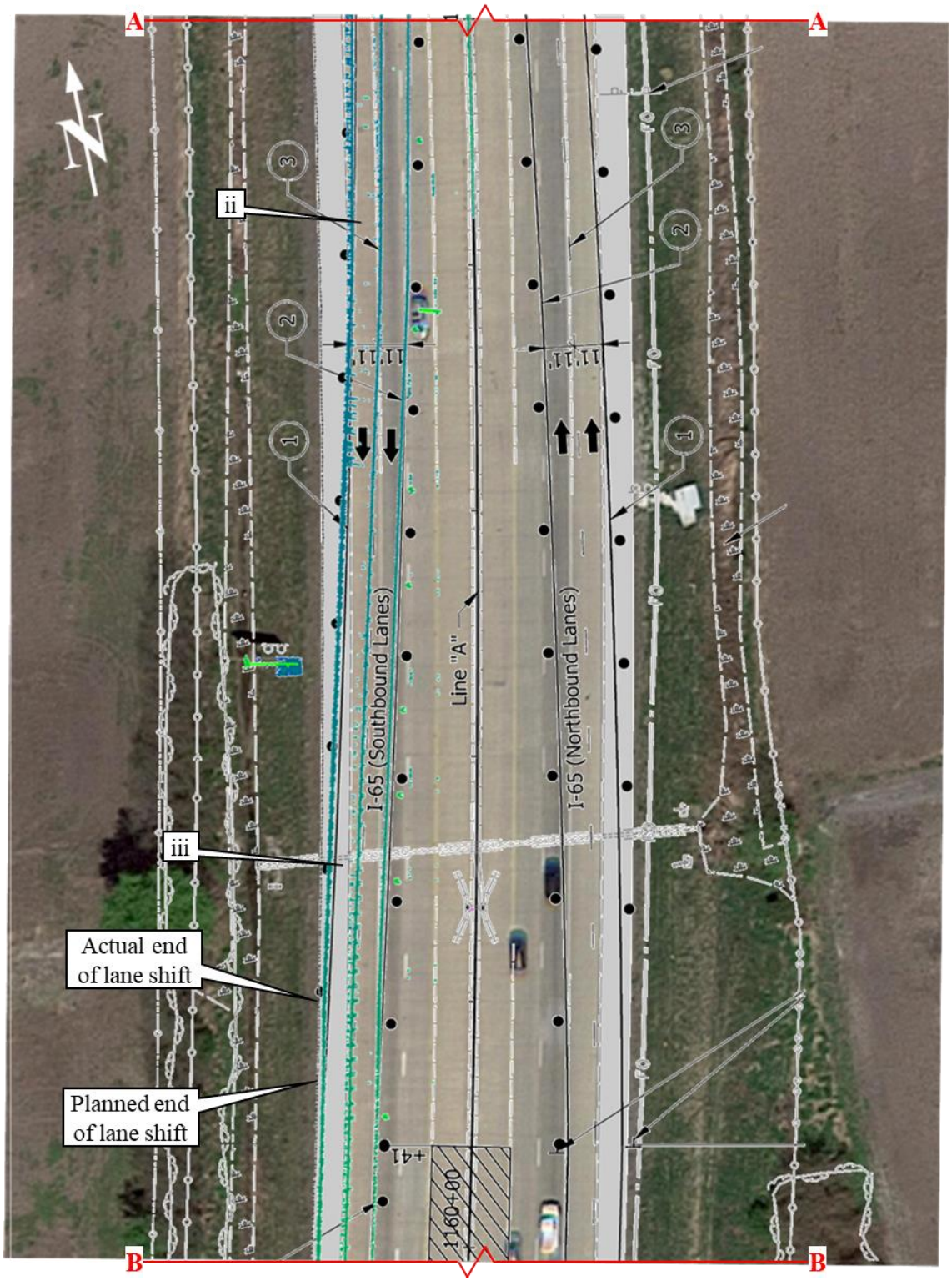

(b) STA 1165+00 to STA 1160+00

Figure 72 continued

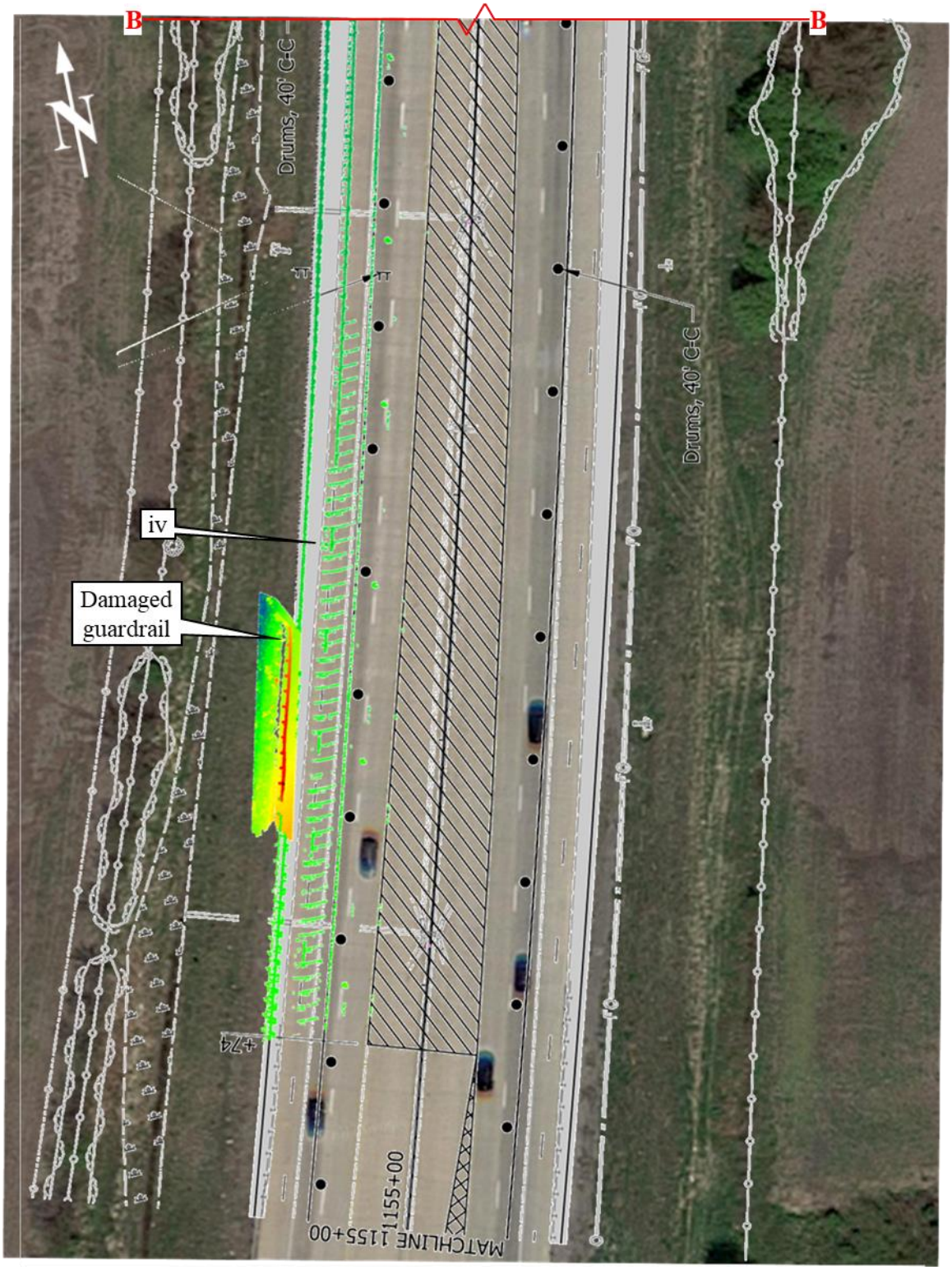

(c) STA 1160+00 to STA 1155+00

(a) Location ‘i’

(b) Location ‘ii’

Figure 73 Camera images at MP 247, I-65 S (L1) on September 19, 2017

Figure 73 continued

(c) Location ‘iii’

(d) Location ‘iv’

(a) Location ‘i’

(b) Location ‘ii’

Figure 74 Camera images at MP 247, I-65 S (L1) on October 31, 2017

Figure 74 continued

(c) Location ‘iii’

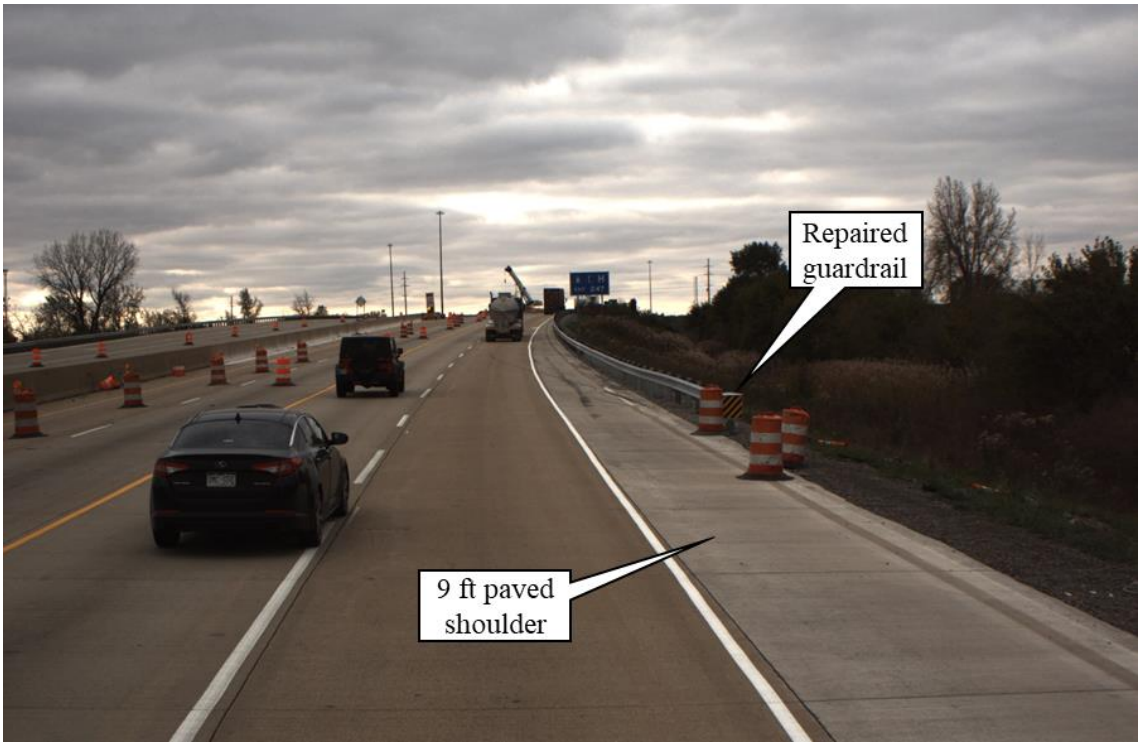

(d) Location ‘iv’

7.4 Contribution

Connected vehicle speed data can be used at both the statewide and segment level to identify bottleneck locations (recurring and in work zones), localized incidents (crashes), and regional incidents (holidays and weather events). Integration of LiDAR geometric data with the connected vehicle speed data enables the diagnosis of non-conforming geometric conditions in work zones. Collection of geometric data using LiDAR can occur at highway speeds, does not require lane closures, and dramatically reduces the exposure of inspectors to traffic. This study demonstrated that the integration of connected vehicle data and LiDAR data can be used to effectively identify unexpected congestion locations in a workzone and trace the cause of that congestion to a section of road. Results from the mobile LiDAR system used in this study were found to be repeatable and accurate. The variety of different case studies discussed demonstrate the versatile uses of the system as well as potential future uses. The work zone features assessed would be difficult to be assessed safely by an inspector in the field due to the high volume and speed of traffic. In conclusion, it is recommended to identify low-performing highway work zones using connected vehicle data and to use LiDAR to assess geometrics in those work zones.

8. CONCLUSIONS

This dissertation demonstrates that there is a clear need and opportunity for continued improvement of work zone performance and mitigation of queueing. The impact of congestion on safety was analyzed. Connected vehicle data was used in the development of a queue alert system and a work zone report. Mobile LiDAR was demonstrated as an emerging technology that can help improve work zone safety for both workers, inspectors, and the traveling public.

With the information provided by the tools discussed in this dissertation, traffic managers will be able to make more informed decisions regarding necessary countermeasures, improvements, and policy changes. If the real-time queue alert system is used to mitigate queueing or alert drivers within 30 minutes of initial queue formation, crash frequency on freeways could potentially be reduced by about 10%. The economic impact of work zones could be decreased by using the work zone reports to determine where and when countermeasures should be employed. Shifting the allotted time period for lane closures or deploying additional warning signs are changes that could cause measurable improvements in mobility and safety. Specific contributions to the transportation engineering profession are discussed in detail in the following sections.

8.1 Quantification of the Impact of Congestion on Safety

The impact of congestion on crashes is quite evident from the data presented in this dissertation. The integration of connected vehicle data with crash data uncovered a number of findings in the context of Indiana interstates. Of 456 fatal crashes in six years, 53 were back-of-queue crashes. Of these 53 fatal BOQ crashes, 90.6% involved at least one commercial vehicle. Of all interstate crashes in 2 years, 18.5% had congestion observable in the connected vehicle data at least 1 minute prior to the crash occurrence. Congestion was observable for at least 33 minutes prior to 10% of all crashes. When the interstate is congested, the crash rate increased by 20.6-24.0 times. There is a clear opportunity for safety improvement by minimizing congestion on the interstate.

8.2 Queue Alert System

A queue alert system was developed for INDOT to notify relevant personnel, such as work zone managers, of queues that exceed prescribed thresholds. The system uses real-time connected vehicle data and was validated with case studies. This tool can be used to identify queues in real-time, regardless of cause or prevalence of existing physical infrastructure at the location. This study has shown that it is feasible to deploy a system that sends targeted alerts that can potentially help public safety and traffic management personnel make more informed decisions during incidents. This model is also ready for integration into connected passenger cars to provide in-vehicle warning.

8.3 Work Zone Report

Connected vehicle data and crash data was utilized to develop a weekly work zone report and dashboards. The integration of these data provides project managers with quantitative information about traffic mobility and performance of work zones that can help them make informed decisions. With the material presented in this dissertation, agencies can generate and interpret the weekly work zone reports using connected vehicle data and online dashboards. The reports allow traffic managers to monitor queue lengths to determine if work zone congestion exceeded policy limits. In a five-month period, queueing greater than the congestion policy limit of 1.5 miles was observed for a total of 1923 hours. The maximum observed queue length was 22.5 miles in the C4W work zone. With these data, informed decisions can be made regarding necessary action, such as recalibration of queue models, changes to policy, or alteration of the work zone layout. The operational performance of work zones can be monitored to identify when changes, such as drum placement, have an adverse impact on queueing and safety. The reports also provide factual information to public information officers to communicate to the media regarding queue lengths, peak periods, and recovery after crashes. An economic analysis of two work zones showed that the economic impact of the work zones was 3.23 times greater than equivalent non-work zone segments.

8.4 Mobile LiDAR Deployment

Integration of LiDAR geometric data with the connected vehicle speed data enables the diagnosis of non-conforming geometric conditions in work zones. Collection of geometric data using LiDAR can occur at highways speeds, does not require lane closures, and dramatically reduces the exposure of inspectors to traffic. This paper demonstrated that the integration of probe data and LiDAR data could be used to effectively identify unexpected congestion locations in a work zone and trace the cause of that congestion to a section of road. A number of case studies demonstrated both the versatility and limitations of this technology for work zone inspection. For example, crash frequency in a work zone increased by 2.9 times, from an average 1.75 crashes per week to 5 crashes per week times, after a lane split with reverse curves was implemented. The increase in congestion and crashes was noted in the work zone report, the mobile LiDAR system was deployed, and recommendations were made to the project manager. After changes were implemented the crash frequency decreased by 0.5 times, from 5 crashes per week to 2.67 crashes per week. It is recommended to use LiDAR to assess geometrics in work zones with recurring congestion.

8.5 Evidence of Contributions

Sections of this dissertation have been accepted for publication in peer-reviewed journals and for presentation at national conferences. The work zone report is currently being used by INDOT traffic management personnel, project managers, and Indiana State Police for work zone traffic management. There has also been interest in these tools by other state agencies. The application of mobile LiDAR for work zone traffic management has been recognized by INDOT and has garnered significant interest from construction companies and consultants.

8.6 Future Work

There is opportunity for these work zone traffic management tools to be further automated and expanded in the future. There is interest to further expand the pool of

recipients of the queue alert system to include dispatchers, consultants, contractors, and individual drivers. There is potential for the work zone report to be fully developed as an online dashboard with greater versatility for individual users. Future work should also include the collection of feedback. Finally, the use and application of mobile LiDAR can be greatly expanded. As the technology matures, the economic viability of such a system will increase. In the future, consultants and contractors may employ their own systems for work zone inspection. Further study into the impact of this technology on work zone performance will be important.

APPENDIX A. MILE-HOURS OF CONGESTION

Written for Microsoft SQL Server Management Studio:

```
CREATE TABLE #MileHours
(
	day varchar(255),
	less45 decimal(28,5),
	less30 decimal(28,5),
	less15 decimal(28,5)
)

DECLARE @DateStart DateTime;
-- Set date of Monday of week of interest:
	SET @DateStart = '2018-02-05';
DECLARE @DateEnd DateTime;
-- Set date of Monday immediately after week of interest:
	SET @DateEnd = '2018-02-12';
DECLARE @toUTC int;
-- Set number of hours behind UTC. Consider time zone and daylight savings:
	SET @toUTC = '5';
DECLARE @Road varchar(10);
-- Set route/direction of interest:
	SET @Road = 'I-65 S';
DECLARE @StartMP decimal(4,1);
-- Set starting mile post of work zone:
	SET @StartMP = '141';
DECLARE @EndMP decimal(4,1);
-- Set ending mile post of work zone (must be larger than @StartMP):
	SET @EndMP = '165';
DECLARE @version DateTime;
-- Set appropriate version date (see [__version] table):
	SET @version = '2017-10-24';
DECLARE @CurrDateStart DateTime;
SET @CurrDateStart = @DateStart;
DECLARE @CurrDateEnd DateTime;
SET @CurrDateEnd = DATEADD(day,1,@DateStart);

WHILE @CurrDateStart < @DateEnd

BEGIN

INSERT INTO #MileHours
```

```
SELECT
        DATEFROMPARTS(YEAR(@CurrDateStart),MONTH(@CurrDateStart),
                DAY(@CurrDateStart)) AS [day]
        ,SUM(CASE WHEN [xdspeeds].[speed] < 45 AND [xdspeeds].[speed] >= 30
                Then [__xd].[Miles] Else 0 END)/60 AS less45
        ,SUM(CASE WHEN [xdspeeds].[speed] < 30 AND [xdspeeds].[speed] >= 15
                Then [__xd].[Miles] Else 0 END)/60 AS less30
        ,SUM(CASE WHEN xdspeeds].[speed] < 15 AND [xdspeeds].[speed] >= 0
                Then [__xd].[Miles] Else 0 END)/60 AS less15
FROM [xdspeeds]
        INNER JOIN [__xd] ON [xdspeeds].[xdid] = [__xd].[XDSegID]
        INNER JOIN [xdmm] ON [xdspeeds].[xdid] = [xdmm].[xdid]
        INNER JOIN [xdpaths] ON [xdspeeds].[xdid] = [xdpaths].[xdid]
WHERE
        [xdspeeds].[tstamp] >= DATEADD(hour,@toUTC,@CurrDateStart)
        AND [xdspeeds].[tstamp] < DATEADD(hour,@toUTC,@CurrDateEnd)
        AND [__xd].[version] = @version
        AND [xdpaths].[version] = @version
        AND [xdmm].[version] = @version
        AND [xdspeeds].[score] = '30'
        AND [xdpaths].[name] = @Road
        AND (([xdmm].[startmm] < @EndMP AND [xdmm].[endmm] > @StartMP)
                OR ([xdmm].[startmm]>@StartMP AND [xdmm].[endmm]<@EndMP))

SET @CurrDateStart = DATEADD(day, 1, @CurrDateStart);
SET @CurrDateEnd = DATEADD(day, 1, @CurrDateEnd);

END

SELECT * FROM #MileHours;

DROP TABLE #MileHours;
```

APPENDIX B. FREQUENCY OF SPEEDDELTA

Written for Microsoft SQL Server Management Studio:

```
CREATE TABLE #DeltaHeat
(
	startmm decimal(9,2),
	day date,
	frequency int
)

DECLARE @DateStart DateTime;
-- Set date of Monday of week of interest:
	SET @DateStart = '2018-03-05';
DECLARE @DateEnd DateTime;
-- Set date of Monday immediately after week of interest:
	SET @DateEnd = '2018-03-12';
DECLARE @toUTC int;
-- Set number of hours behind UTC. Consider time zone and daylight savings:
	SET @toUTC = '5';
DECLARE @Road varchar(10);
-- Set route/direction of interest:
	SET @Road = 'I-65 N';
DECLARE @StartMP decimal(4,1);
-- Set starting mile post of work zone:
	SET @StartMP = '141';
DECLARE @EndMP decimal(4,1);
-- Set ending mile post of work zone (must be larger than @StartMP):
	SET @EndMP = '165';
DECLARE @Delta int;
-- Set desired deltaspeed threshold (in MPH):
	SET @Delta = '15';
DECLARE @CurrDateStart DateTime;
SET @CurrDateStart = DATEADD(day,-28,@DateStart);
DECLARE @CurrDateEnd DateTime;
SET @CurrDateEnd = DATEADD(day,1,@CurrDateStart);

WHILE @CurrDateStart < @DateEnd

BEGIN

INSERT INTO #DeltaHeat
```

```
SELECT
	[startmm]
	,DATEFROMPARTS(YEAR(@CurrDateStart),MONTH(@CurrDateStart),
		DAY(@CurrDateStart)) AS [day]
	,COUNT(tstamp) AS frequency
FROM(
	SELECT
		DATEADD(hour,-@toUTC,[tstamp]) AS tstamp
		,[startmm]
		,[speeddelta]
	FROM [xdqueues]
	WHERE
		roadname = @Road
		AND startmm >= @StartMP AND startmm <= @EndMP
		AND tstamp >= DATEADD(hour,@toUTC,@CurrDateStart)
		AND tstamp < DATEADD(hour,@toUTC,@CurrDateEnd)
		AND speeddelta >= @Delta
	GROUP BY tstamp, startmm, speeddelta
	) AS stuff
GROUP BY startmm

SET @CurrDateStart = DATEADD(day, 1, @CurrDateStart);
SET @CurrDateEnd = DATEADD(day, 1, @CurrDateEnd);

END

SELECT * FROM #DeltaHeat ORDER BY [day], [startmm];

DROP TABLE #DeltaHeat;
```

APPENDIX C. HOURS OF QUEUEING

Written for Microsoft SQL Server Management Studio:

```
CREATE TABLE #QueueHours
(
	day date,
	hours_5 decimal(28,2),
	hours_past decimal(28,2)
)

DECLARE @DateStart DateTime;
-- Set date of Monday of week of interest:
	SET @DateStart = '2018-03-05';
DECLARE @DateEnd DateTime;
-- Set date of Monday immediately after week of interest:
	SET @DateEnd = '2018-03-12';
DECLARE @toUTC int;
-- Set number of hours behind UTC. Consider time zone and daylight savings:
	SET @toUTC = '5';
DECLARE @Road varchar(10);
-- Set route/direction of interest:
	SET @Road = 'I-65 N';
DECLARE @StartMP decimal(4,1);
-- Set starting mile post of work zone:
	SET @StartMP = '141';
DECLARE @EndMP decimal(4,1);
-- Set ending mile post of work zone (must be larger than @StartMP):
	SET @EndMP = '165';
DECLARE @Threshold int;
-- Set desired congestion threshold as '5', '15', '25', '35', or '45' (in MPH):
	SET @Threshold = '45';
DECLARE @CurrDateStart DateTime;
SET @CurrDateStart = @DateStart;
DECLARE @CurrDateEnd DateTime;
SET @CurrDateEnd = DATEADD(day,1,@DateStart);

WHILE @CurrDateStart < @DateEnd

BEGIN

INSERT INTO #QueueHours
```

```
SELECT
	DATEFROMPARTS(YEAR(@CurrDateStart),MONTH(@CurrDateStart),
		DAY(@CurrDateStart)) AS [day]
	,SUM(CASE WHEN max_length >= '5' Then 1.0000 Else 0 END)/60 AS hours_5
	,SUM(CASE WHEN (min_startmm < @Startmm) OR (max_startmm > @Endmm)
		Then 1.0000 Else 0 END)/60 AS hours_past
FROM(
	SELECT
		DATEADD(HOUR,-@toUTC,[tstamp]) AS tstamp
		,MAX(length) AS max_length
		,MIN(startmm) AS min_startmm
		,MAX(startmm) AS max_startmm
	FROM [xdqueues]
	WHERE
		tstamp >= DATEADD(hour,@toUTC,@CurrDateStart)
		AND tstamp < DATEADD(hour,@toUTC,@CurrDateEnd)
		AND threshold = @Threshold
		AND roadname = @Road
		AND endmm >= @StartMP
		AND endmm <= @EndMP
	GROUP BY tstamp
	)AS stuff

SET @CurrDateStart = DATEADD(day, 1, @CurrDateStart);
SET @CurrDateEnd = DATEADD(day, 1, @CurrDateEnd);

END

SELECT * FROM #QueueHours;

DROP TABLE #QueueHours;
```

REFERENCES

[1] Federal Highway Administration, "Final Rule on Work Zone Mobility and Safety," Washington, DC, 2004.

[2] L. B. Andrew and J. E. Bryden, "Managing construction safety and health: Experience of New York State Department of Transportation," *Transportation Research Record,* no. 1585, pp. 9-18, 1997.

[3] Virginia Department of Transportation, "Transportation management plan requirements," Richmond, VA, 2009.

[4] B. Cottrell, "Guidelines for developing transportation management plans in Virginia," Charlotsville, VA, 2005.

[5] C. L. Dickerson, J. Wang, J. Witherspoon and S. C. Crumley, "Work zone management in the District of Columbia: Deploying a citywide transportation management plan and work zone project management system," *Transportation Research Record,* no. 2554, pp. 37-45, 2016.

[6] Indiana Department of Transportation, Interstate Highways Congestion Policy, Indianapolis, IN, 2017.

[7] N. M. Rouphail, Z. S. Yang and J. Fazio, "Comparative study of short- and long-term urban work zones," *Transportation Research Record,* no. 1163, pp. 4-14, 1988.

[8] J. Gambatese and M. Johnson, "Impact of design and construction on quality, consistency, and safety of traffic control plans," *Transportation Research Record,* no. 2458, pp. 47-55, 2014.

[9] J. E. Bryden and L. B. Andrew, "Quality assurance program for work zone traffic control," *Transportation Research Record,* no. 1745, pp. 1-9, 2001.

[10] J. Collura, K. Heaslip, K. Moriarty, F. Wu, R. Khanta and A. Berthaume, "Simulation models for assessment of the impacts of strategies for highway work

zones: Eight case studies along interstate highways and state routes in New England," *Transportation Research Record,* no. 2169, pp. 62-69, 2010.

[11] T. Schnell, J. Mohror and F. Aktan, "Evaluation of traffic flow analysis tools applied to work zones based on flow data collected in the field," *Transportation Research Record,* no. 1811, pp. 57-66, 2002.

[12] M. Chitturi and R. Benekohal, "Work zone queue length & delay methodology," *Transportation Letters: The International Journal of Transportation Research,* vol. 2, no. 4, pp. 273-283, 2013.

[13] G. Pesti and R. Brydia, "Work zone impact assessment methods and applications," *Transportation Research Record,* no. 2617, pp. 52-59, 2017.

[14] J. Bourne, C. Eng, G. Ullman, D. Gomez, B. Zimmerman, T. Scriba, R. Lipps, D. Markow, K. Matthews, D. Holstein and R. Stargell, "Best practices in work zone assessment, data collection, and performance evaluation," Washington, DC, 2010.

[15] A. Gallo, L. Dougald and M. Demetsky, "Formalized process for performance assessment of work zone transportation management plans in Virginia," *Transportation Research Record,* no. 2337, pp. 50-58, 2013.

[16] T. Hartmann and H. Hawkins Jr., "Revised process for work zone decision making based on quantitative performance measures," *Transportation Research Record,* no. 2107, pp. 14-23, 2009.

[17] R. Haseman, J. Wasson and D. Bullock, "Real-time measurement of travel time delay in work zones and evaluation metrics using bluetooth probe tracking," *Transportation Research Record,* no. 2169, pp. 40-53, 2010.

[18] Transportation Research Board, Highway capacity manual, Washington, DC, 1985.

[19] Transportation Research Board, Highway capacity manual, Washington, DC, 1994.

[20] Transportation Research Board, Highway capacity manual, Washington, DC, 2000.

[21] Transportation Research Board, Highway capacity manual, Washington, DC, 2010.

[22] Y. Jiang, "Traffic capacity, speed, and queue-discharge rate of Indiana's four-lane freeway work zones," *Transportation Research Record,* no. 1657, pp. 10-17, 1999.

[23] J. Weng and Q. Meng, "Decision tree-based model for estimation of work zone capacity," *Transportation Research Record,* no. 2257, pp. 40-50, 2011.

[24] C. Yeom, A. Hajbabaie, B. J. Schroeder, C. Vaughan, X. Xuan and N. Rouphail, "Innovative work zone capacity models from nationwide field and archival sources," *Transportation Research Record,* no. 2485, pp. 51-60, 2015.

[25] M. C. Sharp and D. W. Harwood, "Effects of taper length on traffic operations in construction work zones," *Transportation Research Record,* no. 703, pp. 19-24, 1979.

[26] L. Theiss, M. D. Finley and G. L. Ullman, "Merging taper lengths for lane closures of short duration," *Transportation Research Record,* no. 2258, pp. 64-70, 2011.

[27] Federal Highway Administration, Manual on uniform traffic control devices, Washington, DC: US Department of Transportation, 2009, pp. 555-557.

[28] Indiana Department of Transportation, "Taper Length Criteria for Work Zones," in *Work Zone Traffic Control Quidelines,* Indianapolis, IN, 2013, p. 13.

[29] American Association of State Highway and Transportation Officials, Highway safety manual, Washington, DC: AASHTO, 2010.

[30] A. Mensah and E. Hauer, "Two problems of averaging arising in the estimation of the relationship between accidents and traffic flow," *Transportation Research Record,* no. 1635, pp. 37-43, 1998.

[31] J. Martin, "Relationship between crash rate and hourly traffic flow on interurban motorways," *Accident Analysis and Prevention,* vol. 34, no. 5, pp. 619-629, 2002.

[32] R. Elvik, A. Erke and P. Christensen, "Elementary units of exposure," *Transportation Research Record,* no. 2103, pp. 25-32, 2009.

[33] M. A. Quddus, C. Wang and S. G. Ison, "Road traffic congestion and crash severity: Econometric analysis using ordered response models," *ASCE Journal of Transportation Engineering,* vol. 136, pp. 424-435, 2010.

[34] P. P. Jovanis and H. Chang, "Modeling the relationship of accidents to miles traveled," *Transportation Research Record,* no. 1068, pp. 42-51, 1986.

[35] R. Pal and S. K. C., "Analysis of crash rates at interstate work zones in Indiana," *Transportation Research Record,* no. 1529, pp. 45-53, 1996.

[36] I. B. Potts, D. W. Harwood, C. A. Fees, K. M. Bauer and C. S. Kinzel, "Further development of the safety and congestion relationship for urban freeway," Washington, DC, 2015.

[37] H. Yeo, J. K. and A. Skabardonis, "Impact of traffic states on freeway collision frequency," Berkeley, CA, 2010.

[38] S. Song and H. Yeo, "Method for estimating highway collision rate that considers state of traffic flow," *Transportation Research Record,* no. 2318, pp. 52-62, 2012.

[39] H. Brodsky and A. S. Hakkert, "Highway accident rates and rural travel densities," *Accident Analysis and Prevention,* vol. 15, no. 1, pp. 73-84, 1983.

[40] D. Shefer and P. Rietveld, "Congestion and safety on highways: Towards and analytical model," *Urban Studies,* vol. 34, no. 4, pp. 679-692, 1997.

[41] J. Kononov, D. Reeves, C. Durso and A. B. K., "Relationship between freeway flow parameters and safety and its implications for adding lanes," *Transportation Research Record,* no. 2279, pp. 118-123, 2012.

[42] D. W. Harwood, K. M. Bauer and I. B. Potts, "Development of relationships between safety and congestion for urban freeways," *Transportation Research Record,* no. 2398, pp. 28-36, 2013.

[43] N. J. Garber and A. A. Ehrhart, "The effect of speed, flow, and geometric characteristics on crash rates for different types of Virginia highways," Charlottesville, VA, 2000.

[44] M. Zhou and V. Sisiopiku, "Relationship between volume-to-capacity ratios and accident rates," *Transportation Research Record,* no. 1581, pp. 47-52, 1997.

[45] S. Venugopal and A. Tarko, "Safety models for rural freeway work zones," *Transportation Research Record,* vol. 1715, pp. 1-9, 2000.

[46] E. Chen and A. P. Tarko, "Analysis of crash frequency in work zones with focus on police enforcement," *Transportation Research Record,* no. 2280, pp. 127-134, 2012.

[47] E. Chen and A. Tarko, "Modeling safety of highway work zones with random parameters and random effects models," *Analytical Methods in Accident Research,* vol. 1, no. 1, pp. 86-95, January 2014.

[48] E. Rista, T. Barrette, R. Hamzeie, P. Savolainen and T. J. Gates, "Work zone safety performance: Comparison of alternative traffic control strategies," *Transportation Research Record,* no. 2617, pp. 87-93, 2017.

[49] M. Osman, R. Paleti and S. Mishra, "Analysis of passenger-car crash severity in different work zone configurations," *Accident Analysis and Prevention,* vol. 111, pp. 161-172, 2018.

[50] Q. Meng and J. Weng, "Evaluation of rear-end crash risk at work zone using work zone traffic data," *Accident Analysis and Prevention,* vol. 43, pp. 1291-1300, 2011.

[51] A. D. May, Traffic flow fundamentals, Englewood Cliffs, NJ: Prentice Hall, 1990.

[52] J. N. Hourdos, V. Garg, P. G. Michalopoulos and G. A. Davis, "Real-time detection of crash-prone conditions at freeway high-crash locations," *Transportation Research Record,* no. 1968, pp. 83-91, 2006.

[53] D. Yang, Y. Chen and L. Xin, "Real-time detection and tracking of traffic shock waves by conjugated low-angle cameras," *Transportation Research Record,* no. 2380, pp. 36-47, 2013.

[54] K. Tiaprasert, K. Zhang, X. B. Wang and X. Zeng, "Queue length estimation using connected vehicle technology for adaptive signal control," *IEEE Transactions on Intelligent Transportation Systems,* vol. 16, no. 4, pp. 2129-2140, August 2016.

[55] A. J. Khattak, X. Wang and H. Zhang, "Incident management integration tool: Dynamically predicting incident durations, secondary incident occurence, and incident delays," *IET Intelligent Transport Systems,* vol. 6, no. 2, pp. 202-214, 2012.

[56] H. Li, S. Remias, C. Day, M. Mekker, J. Sturdevant and D. Bullock, "Shockwave boundary identification using cloud-based probe data," *Transportation Research Record,* no. 2526, pp. 51-60, 2015.

[57] T. Dinh, R. Billot, E. Pillet and N. El Faouzi, "Real-time queue-end detection on freeways with floating car data: Practice-ready algorithm," *Transportation Research Record,* no. 2470, pp. 46-56, 2014.

[58] P. B. Wiles, S. A. Cooner, C. H. Walters and E. J. Pultorak, "Advance warning of stopped traffic on freeways: Current practices and field studies of queue propagation speeds," College Station, TX, 2003.

[59] G. Ullman, V. Iragavarapu and R. Brydia, "Safety effects of portable end-of-queue warning system deployments at Texas work zones," *Transportation Research Record,* no. 2555, pp. 46-52, 2016.

[60] C. Nowakowski, D. Vizzini, S. Gupta and R. Sengupta, "Evaluation of real-time freeway end-of-queue alerting system to promote driver situational awareness," *Transportation Research Record,* no. 2324, pp. 37-43, 2012.

[61] C. M. J. Tampere, S. P. Hoogendoorn and B. v. Arem, "Continuous traffic flow modeling of driver support systems in multiclass traffic with intervehicle communication and drivers in the loop," *IEEE Transactions on Intelligent Transportation Systems,* vol. 10, no. 4, pp. 649-657, December 2009.

[62] N. El-Sheimy, C. Valeo and A. Habib, Digital terrain modeling: Acquisition, manipulation, and applications, Norwood, MA: Artech House, 2005.

[63] J. Shan and C. K. Toth, Eds., Topographic laser ranging and scanning: Principles and processing, Boca Raton, FL: CRC Press - Taylor & Francis Group, 2009.

[64] M. J. Olsen, G. V. Roe, C. Glennie, F. Persi, M. Reedy, D. Hurwitz, K. Williams, H. Tuss, A. Squellati and M. Knodler, "Guidelines for the use of mobile LIDAR in transportation applications," Washington, DC, 2013.

[65] J. C. Chang, D. J. Findley, C. M. Cunningham and M. K. Tsai, "Considerations for effective LiDAR deployment by transportation agencies," *Transportation Research Record,* no. 2440, pp. 1-8, 2014.

[66] Y. Yu, J. Li, H. Guan, F. Jia and C. Wang, "Learning hierarchical features for automated extraction of road markings from 3-D mobile LiDAR point clouds," *IEEE Journal of Selected Topics in Applied Earth Observations and Remote Sensing,* vol. 8, no. 2, pp. 709-726, 2015.

[67] B. Riviero, L. Diaz-Vilarino, B. Conde-Carnero, M. Soilan and P. Arias, "Automatic segmentation and shape-based classification of retro-reflective traffic signs from mobile LiDAR data," *IEEE Journal of Selected Topics in Applied Earth Observations and Remote Sensing,* vol. 9, no. 1, pp. 295-303, 2016.

[68] S. Pu, M. Rutzinger, G. Vosselman and S. O. Elberink, "Recognizing basic structures from mobile laser scanning data for road inventory studies," *ISPRS Journal of Photogrammetry and Remote Sensing,* vol. 66, no. 6, pp. S28-S39, 2011.

[69] A. Geiger, P. Lenz and R. Urtasan, "Are we ready for autonomous driving? The Kitti vision benchmark suite," in *2012 IEEE Conference on Computer Vision and Pattern Recognition*, Providence, RI, 2012.

[70] M. J. Lato, M. S. Diederichs, D. J. Hitchinson and R. Harrap, "Evaluating roadside rockmasses for rockfall hazards using LiDAR data: Optimizing data collecion and processing protocols," *Natural Hazards,* vol. 60, no. 3, pp. 831-864, 2012.

[71] S. Remias, T. Brennan, G. Grimmer, E. Cox, D. Horton and D. Bullock, "2011 Indiana interstate mobility report - Full version," West Lafayette, IN, 2012.

[72] S. Remias, T. Brennan, G. Grimmer, E. Cox, D. Horton and D. Bullock, "2012 Indiana mobility report: Full version," West Lafayette, IN, 2013.

[73] C. Day, S. Remias, H. Li, M. Mekker, M. McNamara, E. Cox, D. Horton and D. Bullock, "2013-2014 Indiana mobility report: Full version," West Lafayette, IN, 2014.

[74] C. M. Day, M. L. McNamara, H. Li, R. S. Sakhare, J. Desai, E. D. Cox, D. K. Horton and D. M. Bullock, "2015 Indiana Mobility Report and Performance Measure Dashboards," West Lafayette, IN, 2016.

[75] D. Schrank, B. Eisele, T. Lomax and J. Bak, "2015 Urban Mobility Scorecard," The Texas A&M Transportation Institute and INRIX, College Station, TX, 2015.

[76] T. M. Brennan, S. M. Remias, G. M. Grimmer, D. K. Horton, E. D. Cox and D. M. Bullock, "Probe vehicle-based statewide mobility performance measures for decision makers," *Transportation Research Record,* no. 2338, pp. 78-90, 2013.

[77] S. M. Remias, T. M. Brennan, C. M. Day, H. T. Summer, D. K. Horton, E. D. Cox and D. M. Bullock, "Spatially referenced probe data performance measures for infratructure investment decision makers," *Transportation Research Record,* no. 2420, pp. 33-44, 2013.

[78] A. F. Habib, A. P. Kersting, K. I. Bang, R. Zhai and M. Al-Durgham, "A strip adjustment procedure to mitigate the impact of inaccurate mounting parameters in parallel LiDAR strips," *The Photogrammetric Record,* vol. 24, no. 126, pp. 171-195, 2009.

[79] A. Habib, K. I. Bang, A. P. Kersting and J. Chow, "Alternative methodologies for LiDAR system calibration," *Remote Sensing,* vol. 2, no. 3, pp. 874-907, 2010.

[80] Y. J. Lin, R. Ravi, T. Shamseldin, M. Elbahnasawy, D. Bullock and A. Habib, "Comparative analysis of potential calibration alternatives for a multi-unit LiDAR system," in *Proceedings of the 10th International Symposium on Mobile Mapping Technology*, Cairo, Egypt, 2017.

[81] Joint Transportation Research Program, Purdue University, "Congestion Profile," 2015. [Online]. Available: http://its.ecn.purdue.edu/mobility/dashboards/volcano/index.html.

[82] Joint Transportation Research Program, Purdue University, "Queue MOT," 2016. [Online]. Available: http://its.ecn.purdue.edu/mobility/dashboards/queue_mot/.

[83] Joint Transportation Research Program, Purdue University, "Route Builder," 2017. [Online]. Available: http://itsdev1.ecn.purdue.edu/routebuilder/#!/home#graphs.

[84] Indiana Department of Transportation, "Traffic Count Database System," 2018. [Online]. Available: http://indot.ms2soft.com/tcds/tsearch.asp?loc=Indot&mod=.

[85] A. Hooper and D. Murray, "An analysis of the operational costs of trucking: 2017 update," American Transportation Research Institute, Arlington, VA, 2017.

[86] Bureau of Labor Statistics, "Occupational Employment Statistics," 2018. [Online]. Available: https://www.bls.gov/oes/tables.htm.

[87] F. Council, E. Zaloshnja, T. Miller and B. Persaud, "Crash cost estimates by maximum police-reported injury severity within selected crash geometries," Federal Highway Administration, McLean, VA, 2005.

[88] L. Blincoe, T. Miller, E. Zaloshnja and B. Lawrence, "The economic and societal impact of motor vehicle crashes, 2010 (revised)," US Department of Transportation, Washington, DC, 2015.

[89] R. Chapman, "The concept of exposure," *Accident Analysis and Prevention,* vol. 5, pp. 95-110, 1973.

[90] A. Kirk and N. Stamatiadis, "Crash rates and traffic maneuvers of younger drivers," *Transportation Research Record,* no. 1779, pp. 68-75, 2001.

[91] D. Stamatiadis and J. A. Deacon, "Quasi-induced exposure: Methodology and insight," *Accident Analysis and Prevention,* vol. 29, no. 1, pp. 37-52, 1997.

[92] J. D. Thorpe, "Calculating relative involvement rates in accidents without determining exposure," *Australian Road Research,* vol. 2, no. 1, pp. 25-36, 1964.

[93] A. Tarko, D. Shamo and J. Wasson, "Indiana lane merge system for work zones on rural freeways," *ASCE Journal of Transportation Engineering,* vol. 125, no. 5, pp. 415-420, 1999.

[94] A. P. Tarko, S. R. Kanipakapatnam and J. S. Wasson, "Modeling and optimization of the Indiana lane merge control system on approaches to freeway work zones,

Part I: Implementation report; Part II: Manual of the Indiana lane merge control system (2 volumes)," West Lafayette, IN, 1998.

[95] A. P. Tarko, S. R. Kanipakapatnam and J. S. Wasson, "Indiana lane merge system - Warrants for use," West Lafayette, IN, 2000.

[96] A. P. Tarko, M. Islam and J. E. Thomaz, "Improving safety in high-speed work zones: A super 70 study," West Lafayette, IN, 2011.

[97] B. R. Carr, "A statistical analysis of rural Ontario traffic accidents using induced exposure data," *Accident Analysis and Prevention,* vol. 1, pp. 343-357, 1969.